

QFS2018 Tokyo



# International Symposium on Quantum Fluids and Solids



*Ito International Research Center, the University of Tokyo*

July 25–31, 2018

# QFS2018

## International Symposium on Quantum Fluids and Solids

*Ito International Research Center,  
The University of Tokyo*

July 25-31, 2018

### **Committees**

#### **Organizing Committee**

Hiroshi Fukuyama (Univ. of Tokyo), *symposium chair*

Makoto Tsubota (Osaka City Univ.), *symposium vice chair*

Seiji Higashitani (Hiroshima Univ.)

Keiya Shirahama (Keio Univ.)

Koichi Matsumoto (Kanazawa Univ.)

Masaru Suzuki

Shin-ichi Ohkoshi (Univ. of Tokyo)

(Univ. of Electro-Communications)

Yutaka Sasaki (Kyoto Univ.)

Takeo Takagi (Univ. of Fukui)

#### **Program Committee**

Makoto Tsubota, *chair*

Takeshi Mizushima (Osaka Univ.)

Hiroki Ikegami (RIKEN)

#### **Publication Committee**

Takeo Takagi, *chair*

Hyoungsoon Choi (KAIST, Korea)

#### **Local Organizing Committee**

Hiroshi Fukuyama, *chair*

Satoshi Murakawa (Univ. of Tokyo)

Tomohiro Matsui (Univ. of Tokyo)

Sachiko Nakamura (Univ. of Tokyo)

Masashi Morishita (Univ. of Tsukuba)

## **QFS Steering Committee**

|  |                            |
|--|----------------------------|
| Ladislav Skrbek (Czech Republic), <i>chair</i> | Eckhard Krotscheck (USA)   |
| Robert Hallock (USA)                           | Dmitrii Tayurskii (Russia) |
| William P. Halperin (C5)                       | Makoto Tsubota (Japan)     |

## **International Program Advisory Committee**

|                               |                               |
|-------------------------------|-------------------------------|
| Vanderlei S. Bagnato (Brazil) | Susana Hernandez (Argentina)  |
| John R. Beamish (Canada)      | Yuki Kawaguchi (Japan)        |
| Natalia Berloff (UK)          | Wolfgang Ketterle (USA)       |
| Jordi Boronat (Spain)         | Eunseong Kim (Korea)          |
| Moses H. W. Chan (USA)        | Yoonseok Lee (USA)            |
| Franco Dalfovo (Italy)        | Anthony J. Leggett (USA)      |
| Vladimir Dmitriev (Russia)    | Paul Leiderer (Germany)       |
| Vladimir Eltsov (Finland)     | Jeevak Parpia (USA)           |
| Christian Enss (Germany)      | Jukka Pekola (Finland)        |
| Henri Godfrin (France)        | James A. Sauls (USA)          |
| Andrei Golov (UK)             | John Saunders (UK)            |
| Richard Haley (UK)            | Ladik Skrbek (Czech Republic) |
| William P. Halperin (USA)     | Dmitrii Tayurskii (Russia)    |
| Tetsuo Hatsuda (Japan)        | Grigorii Volovik (Finland)    |

# Program

## July 26 (Thursday)

|  |          |                         |   |
|--|----------|-------------------------|---|
| <b>08:50</b>                             |          | <b>Opening</b>          |   |
| <b>Session 1:</b>                        |          |                         | <i>Chair: John Saunders (Royal Holloway, Univ. of London)</i>   |
| <b>09:20</b>                             | O26.1    | Anthony J. Leggett      | p+ip Fermi superfluids: old results and new questions   |
| <b>10:00</b>                             |          | <i>coffee break</i>     |   |
| <b>Session 2: Topological Matters 1</b>  |          |                         | <i>Chair: Yutaka Sasaki (Kyoto Univ.)</i>   |
| <b>10:30</b>                             | O26.2    | James A. Sauls          | Frontiers in Quantum Matter: Symmetry, Topology & Strong Correlation Physics  |
| <b>11:10</b>                             | O26.3    | Richard P. Haley        | The orbitropic effect in superfluid helium-3 B-phase boundaries   |
| <b>11:40</b>                             | O26.4    | Kun Zuo                 | Towards Measurement based Majorana qubits   |
| <b>12:00</b>                             |          | <i>lunch</i>            |   |
| <b>Session 3: Low Dimensional Helium</b> |          |                         | <i>Chair: Paul Leiderer (Univ. of Konstanz)</i>   |
| <b>13:30</b>                             | O26.5    | Keiya Shirahama         | Elastic Anomalies in Adsorbed Films of Helium, Hydrogen and Neon  |
| <b>13:50</b>                             | O26.6    | Masashi Morishita       | QCM Measurements on Submonolayer $^4\text{He}$ Films on Graphite  |
| <b>14:10</b>                             | O26.7    | Junko Taniguchi         | Competition between thermodynamical and dynamical superfluid of $^4\text{He}$ confined in a nanometer-size channel                            |
| <b>14:30</b>                             | O26.8    | Yury Bunkov             | Spin superfluidity from ultralow to room temperature  |
| <b>14:50</b>                             |          | <i>coffee break</i>     |   |
| <b>Session 4: Quantum Solids</b>         |          |                         | <i>Chair: Izumi Iwasa (Kanagawa Univ.)</i>  |
| <b>15:20</b>                             | O26.9    | Jaeho Shin              | Mass flow through bulk solid helium and solid helium confined in Aerogel  |
| <b>15:50</b>                             | O26.10   | Zhigang Cheng           | Mass flow in quantum solids: $^4\text{He}$ and $^3\text{He}$  |
| <b>16:10</b>                             | O26.11   | Andrei Golov            | Characterization of vibrating dislocations in solid $^4\text{He}$ by their interaction with AC shear deformation and $^3\text{He}$ impurities |
| <b>16:30</b>                             | P26.1–36 | <b>Poster Session 1</b> |   |

## July 27 (Friday)

|   |                     |                         |   |
|---|---------------------|-------------------------|---|
| <b>Session 5: KT Transition and He Films</b> <i>Chair: Moses Chan (Penn State Univ.)</i>                  |                     |                         |   |
| <b>08:30</b>  | O27.1               | J. Michael Kosterlitz   | Topological Defects and Phase Transitions   |
| <b>09:15</b>  | O27.2               | John D. Reppy           | The Road to the KT Transition; Experiments with Thin $^4\text{He}$ Films  |
| <b>10:00</b>  | <i>coffee break</i> |                         |   |
| <b>Session 6: Spin Liquids</b> <i>Chair: Christian Enss (Heidelberg Univ.)</i>                            |                     |                         |   |
| <b>10:30</b>  | O27.3               | Kazushi Kanoda          | Spin liquid, Mott transition and BEC-BCS crossover exhibited by interacting electrons on triangular lattices                    |
| <b>11:10</b>  | O27.4               | Hikaru Kawamura         | Randomness-Induced Quantum Spin Liquids in Frustrated Magnets: Application to 2D $^3\text{He}$ and Organic Salts                |
| <b>11:40</b>  | O27.5               | Masahiro Kamada         | New Quantum Spin Liquids in $^3\text{He}$ Monolayer on Hydrogen Plated Graphite   |
| <b>12:00</b>  | <i>lunch</i>        |                         |   |
| <b>Session 7: 2D Helium Systems</b> <i>Chair: Keiya Shirahama (Keio Univ.)</i>                            |                     |                         |   |
| <b>13:30</b>  | O27.6               | John Saunders           | Helium in two dimensions and under nano-scale confinement: realizing quantum materials and topological mesoscopic superfluidity |
| <b>14:10</b>  | O27.7               | Aron Beekman            | The solid-to-hexatic quantum melting phase transition   |
| <b>14:30</b>  | O27.8               | Eunseong Kim            | Anomalous superfluid response in the second layer $^4\text{He}$ films adsorbed on graphite                                      |
| <b>14:50</b>  | <i>coffee break</i> |                         |   |
| <b>Session 8: Liquid and Solid <math>^4\text{He}</math></b> <i>Chair: John Beamish (Univ. of Alberta)</i> |                     |                         |   |
| <b>15:20</b>  | O27.9               | Eckhard Krotscheck      | Multimode-excitations in liquid $^4\text{He}$ above the phonon-roton spectrum: Experiments and Theory                           |
| <b>15:50</b>  | O27.10              | Luciano Reatto          | Quantum turbulence in $^4\text{He}$ as a source of non-thermal rotons and of quantum evaporation                                |
| <b>16:10</b>  | O27.11              | Ryuji Nomura            | Inchworm Driving of $^4\text{He}$ Crystals in Superfluid  |
| <b>16:30</b>  | P27.1–34            | <b>Poster Session 2</b> |   |

## July 28 (Saturday)

|  |                     |   |  |
|--|---------------------|---|--|
| <b>Session 9: Quantum Matters</b>                        |                     | <i>Chair: William Halperin (Northwestern Univ.)</i> |  |
| <b>08:30</b>   | O28.1               | Grigorii E. Volovik                                 | Topological matter: Weyl fermions, Higgs bosons, quantum gravity and room- $T$ superconductivity                             |
| <b>09:10</b>   | O28.2               | Ryo Shimano   | Higgs mode in conventional and unconventional superconductors  |
| <b>09:40</b>   | O28.3               | Jacques Tempere                                     | Collective excitations of a superfluid Fermi gas in the BEC-BCS crossover  |
| <b>10:00</b>   | <i>coffee break</i> |   |  |
| <b>Session 10: Neutron Star</b>                          |                     | <i>Chair: James Sauls (Northwestern Univ.)</i>      |  |
| <b>10:30</b>   | O28.4               | Tetsuo Hatsuda                                      | Neutron Star Core: Densest State of Matter   |
| <b>11:10</b>   | O28.5               | Kei Iida  | Neutron star crusts as low temperature laboratories  |
| <b>11:40</b>   | O28.6               | Takeshi Mizushima                                   | Anomaly-Induced Transport in Weyl Superconductors and Neutron Stars  |
| <b>12:00</b>   | <i>lunch</i>        |   |  |
| <b>Session 11: Superfluid <math>^3\text{He}</math> 1</b> |                     | <i>Chair: Seiji Higashitani (Hiroshima Univ.)</i>   |  |
| <b>13:30</b>   | O28.7               | Vladimir Eltsov                                     | Exploring superfluid $^3\text{He}$ universe with coherent bosons   |
| <b>14:10</b>   | O28.8               | Petri J. Heikkinen                                  | Phase diagram of superfluid $^3\text{He}$ in quasi-two-dimensional limit   |
| <b>14:30</b>   | O28.9               | Dmitry Zmeev  | Superfluidity beyond the Landau Velocity in $^3\text{He-B}$ and Dynamics of Surface States                                   |
| <b>14:50</b>   | <i>coffee break</i> |   |  |
| <b>Session 12: Topological Matters 2</b>                 |                     | <i>Chair: Takeshi Mizushima (Osaka Univ.)</i>       |  |
| <b>15:20</b>   | O28.10              | Dirk Manske   | Novel Josephson and Proximity Effect using Triplet Superconductors   |
| <b>15:50</b>   | O28.11              | V. Ngampruetikorn                                   | Impurity Induced Anomalous Thermal Hall Effect in Chiral Superconductors   |
| <b>16:10</b>   | O28.12              | Franco Nori   | Parity-Time-Symmetric Optics, extraordinary momentum and spin in evanescent waves, and the quantum spin Hall effect of light |
| <b>16:30</b>   | P28.1–39            | <b>Poster Session 3</b>                             |  |

## July 30 (Monday)

|  |   |  |   |
|--|---|--|---|
| <b>Session 13: Quantum Turbulence 1</b>                  |   | <i>Chair: Ladik Skrbek (Charles Univ.)</i>       |   |
| <b>08:30</b>   | O30.1   | Wei Guo  | Visualization study of quantum turbulence in superfluid helium-4: progress and future development |
| <b>09:10</b>   | O30.2   | Viktor Tsepelin                                  | Probing quantum turbulence using mechanical oscillators   |
| <b>09:40</b>   | O30.3   | Satoshi Yui                                      | Numerical Study of Coupled Dynamics in the Two-Fluid Model for Superfluid $^4\text{He}$           |
| <b>10:00</b>   | <i>coffee break</i>   |  |   |
| <b>Session 14: Superfluid <math>^3\text{He}</math> 2</b> |   | <i>Chair: Jeevak Parpia (Cornell Univ.)</i>      |   |
| <b>10:30</b>   | O30.4   | Vladimir Dmitriev                                | Superfluid $^3\text{He}$ in Planar Aerogel  |
| <b>11:00</b>   | O30.5   | Vladimir P. Mineev                               | Influence of Exchange Scattering on Superfluid $^3\text{He}$ states in Nematic Aerogel            |
| <b>11:20</b>   | O30.6   | Ryusuke Ikeda                                    | Stability of Half-Quantum Vortices in Polar Phase in Anisotropic Aerogel                          |
| <b>11:40</b>   | O30.7   | Jere Mäkinen                                     | Rotating superfluid wave turbulence   |
| <b>12:00</b>   | <i>lunch</i>  |  |   |
| <b>Session 15: Quantum Turbulence 2</b>                  |   | <i>Chair: Andrei Golov (Univ. of Manchester)</i> |   |
| <b>13:30</b>   | O30.8   | Yong-il Shin                                     | Quantum vortex shedding in atomic superfluid gases  |
| <b>14:10</b>   | O30.9   | Nir Navon  | Turbulence in a Quantum Gas   |
| <b>14:40</b>   | O30.10  | Davide Proment                                   | Quantum turbulence cascades in the Gross-Pitaevskii model   |
| <b>15:00</b>   | O30.11  | Emil Varga                                       | Vortex line density dynamics and temperature profile in thermal counterflow                       |
| <b>15:20</b>   | P30.1–38  | <b>Poster Session 4</b>                          |   |
| <b>18:00</b>   | <i>bus departure</i>  |  |   |
| <b>18:30</b>   | <i>welcome drink</i>  |  |   |
| <b>19:00</b>   | <i>Banquet (H<math>\bar{O}</math> room, Hotel New Ohtani)</i> |  |   |

## July 31 (Tuesday)

|   |                     |   |   |
|---|---------------------|---|---|
| <b>Session 16: Cold Atoms and Molecules</b> |                     | <i>Chair: Makoto Tsubota (Osaka City Univ.)</i> |   |
| <b>08:30</b>                                | O31.1               | Takamasa Momose                                 | Spectroscopy and dynamics of molecules in quantum fluids and solids: <i>Towards molecular superfluidity and ultracold chemistry</i> |
| <b>09:10</b>                                | O31.2               | Shin Inouye                                     | Efimov resonances in an ultracold mixture   |
| <b>09:40</b>                                | O31.3               | Pierbiagio Pieri                                | Screening corrections on the critical temperature and gap parameter throughout the BCS-BEC crossover                                |
| <b>10:00</b>                                | <i>coffee break</i> |   |   |
| <b>Session 17: Novel Techniques</b>         |                     | <i>Chair: Yoonseok Lee (Univ. of Florida)</i>   |   |
| <b>10:30</b>                                | O31.4               | Kimitoshi Kono                                  | Nano structures and Devices to Study Quantum Fluids and Solids  |
| <b>11:00</b>                                | O31.5               | John P. Davis                                   | Microfabricated Fourth-Sound Resonators for Confined Quantum Liquids  |
| <b>11:20</b>                                | O31.6               | Aleksei Shkarin                                 | Quantum Optomechanics with Superfluid Helium Density Waves  |
| <b>11:40</b>                                | O31.7               | Christian Enss                                  | A New Spin of Non-equilibrium Disordered Quantum Systems  |
| <b>12:00</b>                                |                     | William P. Halperin                             | <i>Summary Talk</i>   |
| <b>12:20</b>                                | <b>Closing</b>      |   |   |



# Posters

## July 26 (Thursday)

- P26.1 Yoshii, R. Casimir Effect for Interacting Fermion system and Boson system
- P26.2 Yamashita, K. Elasticity measurement of hydrogen films adsorbed on a porous glass
- P26.3 Matsushita, T. Singlet Dimer Bound State of  $^3\text{He}$  in Nanopore Suggested by NMR
- P26.4 Spathis, P. Confined fluids in alumina nanoporous membranes
- P26.5 Wada, N. Superfluid Transitions of  $^4\text{He}$  Films under Marginal Conditions among 1-, 2- and 3-Dimensions
- P26.6 Taniguchi, J. Slippage and localized-unlocalized transition in a  $^4\text{He}$  solid film system
- P26.7 Makiuchi, T. Quantum Phase Transition of Thin He Films on a Disordered Substrate
- P26.8 Kuwahara, K. Toward the direct observation of chiral edge mass current in quasi-2D  $^3\text{He-A}$
- P26.9 Huan, C. Nuclear spin relaxometry of  $^3\text{He}$  atoms confined in mesoporous MCM-41
- P26.10 Kim, E. Observation of unexpected extended relaxation in dislocation pinning dynamics of solid  $^4\text{He}$  with ultra-low  $^3\text{He}$  concentrations
- P26.11 Amrit, J. Thermal resistance of solid  $^4\text{He}$  to a classical solid
- P26.12 Vasiliev, S. Evidence for a solid-to-liquid transition of molecular hydrogen inside pores of solid neon below 1 K.
- P26.13 Beamish, J. R. Plastic Deformation in a Quantum Solid: Dislocation Avalanches and Creep in Helium
- P26.14 Iwasa, I. Critical Force for Unpinning  $^3\text{He}$  from Dislocations in Solid  $^4\text{He}$
- P26.15 Masaki-Kato, A. The superfluid transition in quasi one-dimensional hardcore Bosons: Effect of phase slippage
- P26.16 Wiman, J. J. Is Superfluid  $^3\text{He-A}$  the Precursor to Magnetically Ordered Solid  $^3\text{He}$ ?
- P26.17 Lotnyk, D. Size limited fountain effect in superfluid  $^3\text{He}$

- P26.18 Zavjalov, V. V. Stability and dynamics of HPD in superfluid  $^3\text{He-B}$
- P26.19 Tsutsumi, Y. Generation of spin current in liquid helium-3
- P26.20 Yoshida, K. Development of Equipment to Observe Majorana Cone at the Surface of Superfluid Helium Three B phase
- P26.21 Vasinovich, E. Superconductivity in model cuprate as an  $S = 1$  pseudomagnon condensation
- P26.22 Tada, Y. Orbital angular momentum in chiral superfluids
- P26.23 Masaki, Y. Charging effects around single vortex in chiral p-wave superconductor
- P26.24 Konno, R. Theory of thermal expansion of chiral p-wave superconductors
- P26.25 Yamaguchi, A. Influence of Magnetic Domain Structure on the Ferromagnetic Superconductivity of  $\text{UGe}_2$
- P26.26 Strydom, A. M. Multiband superconductivity in  $\text{PrPt}_4\text{Ge}_{12}$  probed by thermal transport
- P26.27 Liu, Y. Doping dependence of the local electronic structures around a nonmagnetic impurity in  $\text{BiS}_2$ -based superconductors
- P26.28 Fukui, K. Even- and Odd-Frequency Superconductivity in Q1D Organic Superconductors under Magnetic Field
- P26.29 Nissinen, J. Phase transition from Weyl to node-line superfluid: Antispace-time and novel effective electrodynamics
- P26.30 Gneiting, C. Disorder-dressed evolution in edge-mode transport and beyond
- P26.31 Kockum, A. F. Decoherence-free interaction between giant atoms in waveguide QED
- P26.32 Lee, Y.  $^3\text{He}$  Purification System with an Acoustic Cavity for Purity Monitoring
- P26.33 Autti, S. Chasing microkelvin electron temperatures in nanoelectronics
- P26.34 Jennings, A. Direct Measurement of Effectiveness of Silver Sinter with Different Boundary Conditions
- P26.35 Jeong, J. Developing high sensitive gyroscope to detect angular momentum of  $^3\text{He-A}$  in slab geometry
- P26.36 Kubota, M. Research Activity for New Types of Superfluidity by a NPO

## July 27 (Friday)

- P27.1 Miyakawa, K. Differential conductance anomalies in superconducting nanoconstrictions by hydrogen adsorption
- P27.2 Takata, H. Low-temperature hydrogen absorption in vanadium nanocontacts
- P27.3 Kawae, T. Collective Motion of Hydrogen Atoms via Quantum Tunneling in Niobium Nanocontacts
- P27.4 Badrutdinov, A. Non-ohmic currents of Wigner solid on helium in 3-terminal microchannel structure
- P27.5 Lin, J. -Y. Experiments on ac Driven Wigner Solid on Liquid Helium Confined in a Microchannel and Subjected to an External Periodic Potential
- P27.6 Leiderer, P. Critically charged superfluid  $^4\text{He}$  surfaces in inhomogeneous electric fields
- P27.7 Makiuchi, T. Elasticity Measurement of Neon Films on a Porous Glass Substrate
- P27.8 Hieda, M. Kosterlitz-Thouless Superfluid Transition of  $^4\text{He}$  Films on Planar Gold
- P27.9 Reatto, L. Prediction for two spatially modulated superfluids:  $^4\text{He}$  on fluorographene and on hexagonal BN
- P27.10 Kamada, M. Quantum Phase Diagram of  $^3\text{He}$  Monolayer on Hydrogen Plated Graphite
- P27.11 Uematsu, K. Randomness-induced quantum spin liquid behavior in the two-dimensional  $^3\text{He}$
- P27.12 Minoguchi, T. The Frank-Read mechanism in the crystalline bilayer of He-4
- P27.13 Ishibashi, K. Mass Decoupling and of  $^3\text{He}$ - $^4\text{He}$  Mixture Films and Its Relaxation
- P27.14 Nomura, R. Wetting Property of  $^4\text{He}$  Crystals on a Rough Wall
- P27.15 Bunkov, Yu. M. Conventional magnon BEC in antiferromagnets
- P27.16 Matsumoto, K. Propagation of heat pulse through superfluid  $^4\text{He}$  in 90% open aerogel
- P27.17 Zhang, G. M. Decoding quantum criticalities from the matrix product wave functions of one-dimensional topological states

- P27.18 Kanazawa, I. Localization of Chiral-like Spin Solitons with Carriers in the Layered Organic  $k\text{-(ET)}_2\text{Cu}_2(\text{CN})_3$
- P27.19 Yamaguchi, T. The optical conductivity for a spin-Peierls ground state of  $(\text{TMTTF})_2\text{PF}_6$  with tetramer formation
- P27.20 Koga, A. Quasiperiodicity and valence fluctuation in the spin-1/2 Falicov-Kimball model
- P27.21 Koga, A. Magnetic properties in the metallic magnets with large anisotropy
- P27.22 Ulitko, V. A. Thermodynamic properties of 2D spin-pseudospin model
- P27.23 Korovushkin, M. M. Diagram approach to the problem of the normal phase properties of the spin polaron ensemble in cuprate superconductors
- P27.24 Yamaguchi, A. Low Temperature Study of Superconducting Graphite Intercalation Compound  $\text{BaC}_6$
- P27.25 Strydom, A. M. Specific heat and magnetic susceptibility of single-crystal Pd
- P27.26 Chishko, K. A. Spin-spin interaction as a nature of microwave absorption in superfluid helium
- P27.27 Forstner, S. Superfluid Brillouin laser
- P27.28 Riekki, T. S. Cooling of  $^3\text{He}$  and  $^3\text{He}\text{-}^4\text{He}$  mixture beyond the Kapitza resistance bottleneck by adiabatic melting of solid  $^4\text{He}$  in liquid  $^3\text{He}$
- P27.29 Riekki, T. S. Effects of  $^4\text{He}$  film on quartz tuning forks in  $^3\text{He}$  at ultra-low temperatures
- P27.30 Tani, T. Fabrication of Micro-slit Structures for Studies of Topological Properties of Quasi-two Dimensional Superfluid  $^3\text{He}$
- P27.31 Schmoranzer, D. Development of a sub-mK Continuous Nuclear Demagnetization Refrigerator
- P27.32 Takimoto, S. Development of a Compact and Low Heat-dissipation Shielded Superconducting Magnet Usable at Sub-mK Temperature
- P27.33 Sebedash, A. Melting curve thermometry in  $^3\text{He}\text{-}^4\text{He}$  mixtures at ultra-low temperatures
- P27.34 Tanabe, H. Development of cryogenic C-MOS and pHEMT amplifiers

## July 28 (Saturday)

- P28.1 Soldatov, A. A. Superfluid  $^3\text{He}$  in ultra dense nematic aerogel
- P28.2 Rysti, J. Half-quantum vortices and Kibble walls in the polar-distorted phases of superfluid  $^3\text{He}$
- P28.3 Regan, R. C. The Vortex-Core Phase Transition in Rotating Superfluid  $^3\text{He-B}$
- P28.4 Coppens, F. Capture of Xe and Ar atoms by quantised vortices in  $^4\text{He}$  nanodroplets
- P28.5 Schmoranzner, D. Universal Drag Force Scaling in Oscillatory Flows of He II
- P28.6 Ancilotto, F. Spinning superfluid  $^4\text{He}$  nanodroplets
- P28.7 Moroshkin, P. Dynamics of the free surface of superfluid  $^4\text{He}$  probed by electrically charged tracer particles
- P28.8 Inui, S. Dynamics of fine particles due to quantized vortices on the surface of superfluid  $^4\text{He}$
- P28.9 Jackson, M. J. Characterization of Instabilities in Oscillatory Flows of Superfluid  $^4\text{He}$
- P28.10 Forstner, S. Real-time monitoring of vortex dynamics in a superfluid helium thin film
- P28.11 Noble, M. T. Looking for Quantum Vortex Production in Oscillatory Motion
- P28.12 Khomenko, D. Turbulent statistics and intermittency enhancement in coflowing superfluid  $^4\text{He}$
- P28.13 Lee, Y. The Effect of Remnant Vortices in He II on Multiple Modes of a Micro-electromechanical Resonator
- P28.14 Usami, J. The Role of Substrate Roughness on the Superfluid Film Flow Rate of  $^4\text{He}$
- P28.15 Nago, Y. Nanomechanical Wire Resonator for Probing Quantum Vortex in Superfluid He
- P28.16 Takeuchi, H. Instability of a Doubly Quantized Vortex in Uniform Superfluids at Zero Temperature
- P28.17 Pomyalov, A. A theory of energy spectra in superfluid He-4 counterflow turbulence
- P28.18 Švančara, P. Visualization study of thermal counterflow in the heater proximity
- P28.19 Kobayashi, H. Numerical Study on Entrance Length in Thermal Counterflow of Superfluid  $^4\text{He}$
- P28.20 Matsushita, T. Generation of  $^4\text{He}_2^*$  Clusters via Neutron- $^3\text{He}$  Absorption Reaction towards Visualization of Full Velocity Field in Quantum Turbulence

- P28.21 Varga, E. Peculiarities of a spherically symmetric thermal counterflow
- P28.22 Yano, H. Vortex Emission from Quantum Turbulence Generated in Superfluid  $^4\text{He}$
- P28.23 Matsumura, I. Vorticity of suction vortex observed by second sound in superfluid  $^4\text{He}$
- P28.24 Hamazaki, K. Vortex Emission from Turbulence Produced by Counterflow in Superfluid  $^4\text{He}$
- P28.25 Sato, K. Power dependence of vortex emission generated by vibrating wire in HeII
- P28.26 Kanazawa, I. Induced fractional electric charge in a boojum on the interface between superfluid  $^3\text{He-A}$  and  $^3\text{He-B}$
- P28.27 Krotscheck, E. Pairing Phenomena from Cold Gases to Neutron Stars
- P28.28 Tsuchiya, S. Hidden charge-conjugation, parity, time-reversal symmetries and Higgs modes in superconductors
- P28.29 Nakamura, S. Infrared-active Higgs mode in an s-wave superconductor NbN under DC current injection
- P28.30 Korovushkin, M. M. Influence of the intersite Coulomb repulsion on the superconducting gap of the spin-polaron quasiparticles in cuprate superconductors
- P28.31 Aikawa, Y. Magnetic Response of Critical Current in Junctions using Ion-gated  $\text{MoS}_2$  and Conventional Superconductor
- P28.32 Wang, D. Local electronic structure around a nonmagnetic impurity in multiband superconductor  $\text{CeCu}_2\text{Si}_2$
- P28.33 Liu, B. Impurity-induced resonance states and their spatial modulation in heavy-fermion superconductor  $\text{CeCoIn}_5$
- P28.34 Nori, F. Quantum Nonlinear Optics without Photons, how to excite two or more atoms simultaneously with a single photon, and other unusual properties of ultra-strongly-coupled QED systems including superconducting circuit QED
- P28.35 Guthrie, A. Probing Quantum Fluids with Nanomechanical Systems
- P28.36 Shkarin, A. B. Optomechanics with Acoustic Modes in Helium
- P28.37 Tsuji, Y. Statistical property of small particle trajectories in fully developed turbulent state of HeII
- P28.38 Tsuji, Y. Periodic Oscillation of Liquid Helium Boiling in Narrow Rectangular Duct
- P28.39 Shammah, N. Superradiant phase transition in the open Dicke model with local and collective driven-dissipative effects

## July 30 (Monday)

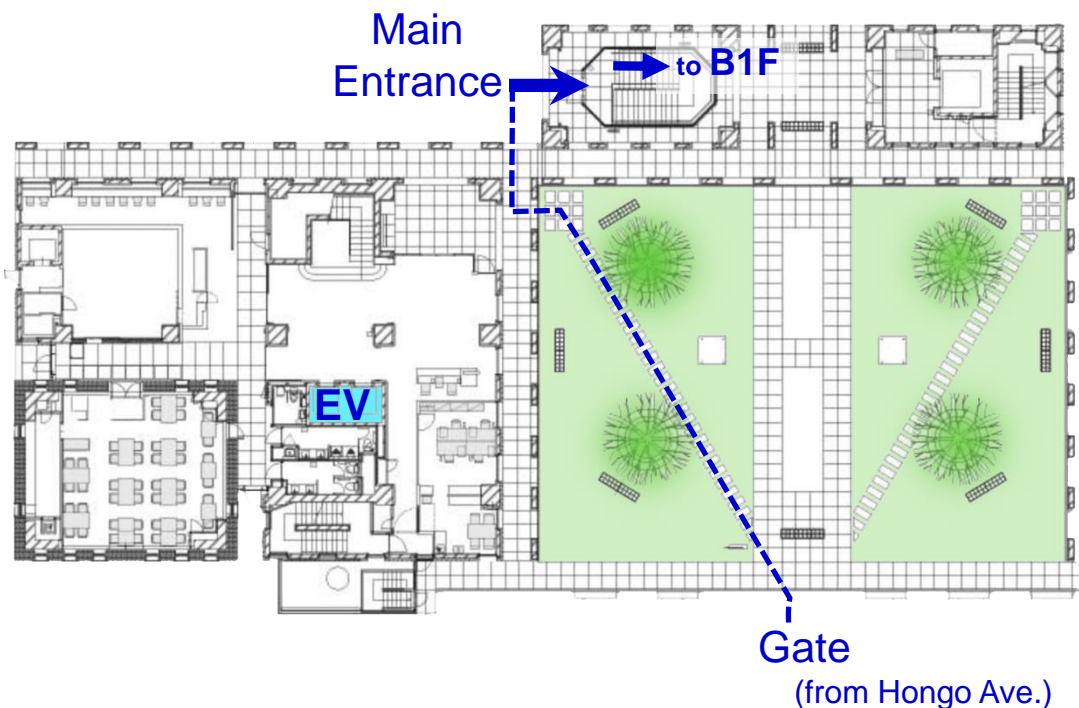
- P30.1 Soldatov, A. Spin diffusion in liquid  $^3\text{He}$  confined in planar aerogel
- P30.2 Rysti, J. Second-order Transition between the Polar and the Polar-distorted B Phases of Superfluid  $^3\text{He}$
- P30.3 Jennings, A. Anisotropic Aerogel on a Floppy Wire in  $^3\text{He}$
- P30.4 Zimmerman, A. M Spin Waves in Disordered Superfluid  $^3\text{He}$
- P30.5 Nguyen, M. D. The Polar-phase of Superfluid  $^3\text{He}$  Stabilized in Anisotropic Silica Aerogel
- P30.6 Surovtsev, E. Phase Diagram of Superfluid  $^3\text{He}$  in Nematic Aerogel in Strong Magnetic Field (Ginzburg-Landau Theory)
- P30.7 Yudin, A. N. NMR Shifts in Pure  $^3\text{He}$  in Anisotropic Aerogels Induced by Demagnetizing Fields
- P30.8 Yoshida, K. Spectrum in the strong turbulence region of Gross-Pitaevskii turbulence
- P30.9 Jackson, M. J. Visualization of a Coflow Jet in Superfluid  $^4\text{He}$  Using Tracer Particles
- P30.10 Kamppinen, T. T. Nanomechanical probes of the quantum fluids with single-vortex sensitivity
- P30.11 Noble, M. T. Picturing Quantum Turbulence with a Quasiparticle Camera
- P30.12 Proment, D. Vortex reconnections in superfluids: universal properties and sound emission
- P30.13 Han, J. Vortex phase separation in two-component Bose-Einstein condensates
- P30.14 Yoshino, T. Collective modes of vortex lattices in two-component Bose-Einstein condensates in synthetic gauge fields
- P30.15 Takeuchi, H. Anomalous hierarchy in domain coarsening dynamics of two-component Bose-Einstein condensates
- P30.16 Hsueh, C. Thermalization of a weakly interacting Bose gas in a disordered trap
- P30.17 Kunimi, M. Can the truncated-Wigner approximation correctly describe thermal and quantum phase slips in one-dimensional Bose gases?
- P30.18 Naidon, P. Impurities in a Bose-Einstein Condensate: from Yukawa to Efimov
- P30.19 Kagamihara, D. Minimum of the ratio of shear viscosity to entropy density in an ultracold Fermi gas

- P30.20 Sato, R. Isothermal Compressibility of an Ultracold Fermi Gas in the BCS-BEC Crossover
- P30.21 Inotani, D. Strong coupling effects on specific heat in the BCS-BEC crossover
- P30.22 Mondal, S. Photoemission Spectra in the BCS-BEC Crossover Regime of a Rare-Earth  $^{173}\text{Yb}$  Fermi Gas in a Harmonic Trap
- P30.23 Manabe, K. Photoemission Spectrum in the Normal State of a Strongly Interacting Bose-Fermi Mixture
- P30.24 Asano, Y. Collective excitations in Bose-Fermi mixtures
- P30.25 Tokimoto, J. Higgs mode in a superfluid Fermi gas in the BCS-BEC crossover
- P30.26 Pieri, P. Comparative study of many-body  $t$ -matrix theories for a Fermi gas through the BCS-BEC crossover
- P30.27 Tajima, H. Multi-body correlations in  $\text{SU}(3)$  Fermi gases
- P30.28 Edmonds, M. J. A mobile soliton-impurity system in an attractive binary quantum gas
- P30.29 Kohno, W.  $3/2$ -body correlations in the ground state of Bose-Einstein condensates
- P30.30 Kirikoshi, A. Many-Body Effects in the Bose-Einstein Condensates at Finite Temperature
- P30.31 Watabe, S. Decay of phase-imprinted dark soliton in Bose-Einstein condensate at non-zero temperature
- P30.32 Oh, B. Y. Transferring angular momentum of non-resonant lights onto exciton-polariton condensation
- P30.33 Ishizuka, H. Robustness of anomaly-related transport phenomena in Weyl semimetals
- P30.34 Ueki, H. Microscopic Theory for the Sign Change of the Hall Coefficient in Type-II Superconductors
- P30.35 Ishiguro, R. Development of superconducting electronic cooling with controlled Schottky barrier by using electric double layer transistor structure
- P30.36 Byun, H. S. Operating a MEMS Gyroscope on a Dilution Refrigerator
- P30.37 Človečko, M. Study of the non-linear dynamics of micro-resonators based on a Sn-whisker in vacuum and at mK temperatures
- P30.38 Fefferman, A. Thermal coupling of silicon oscillators in cryogen-free dilution refrigerators

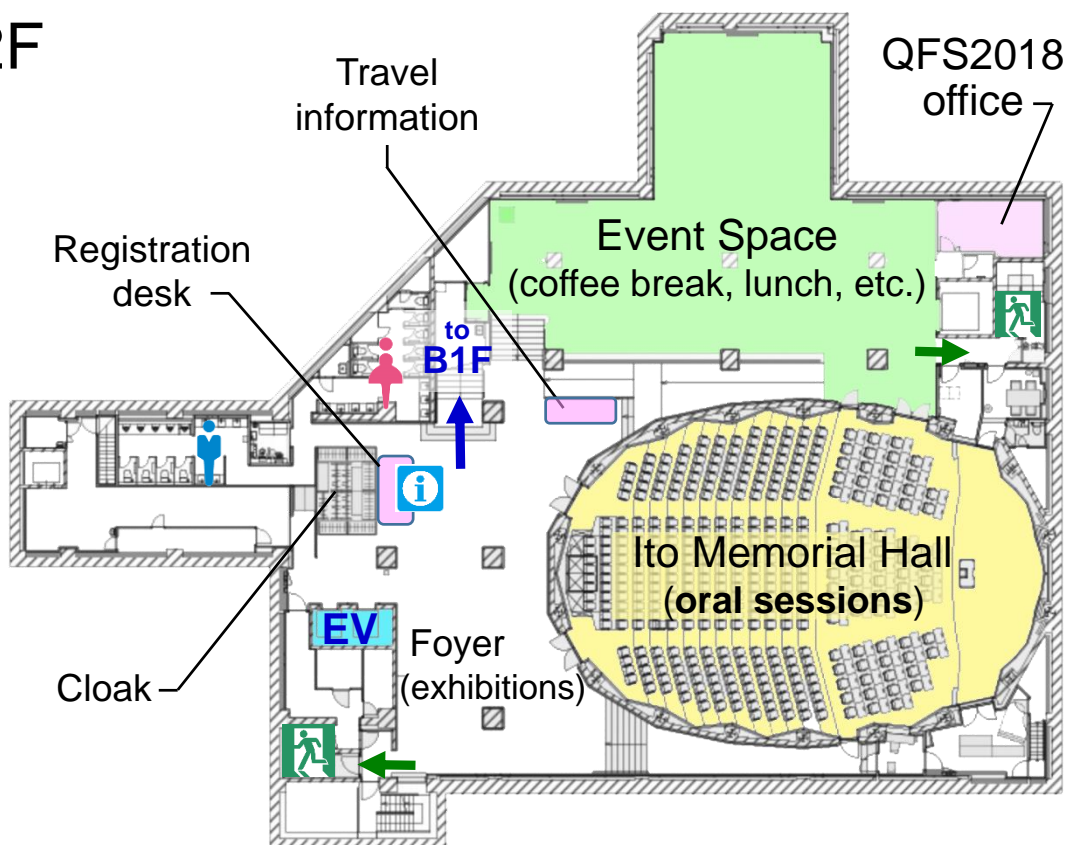


# Maps and General Arrangements

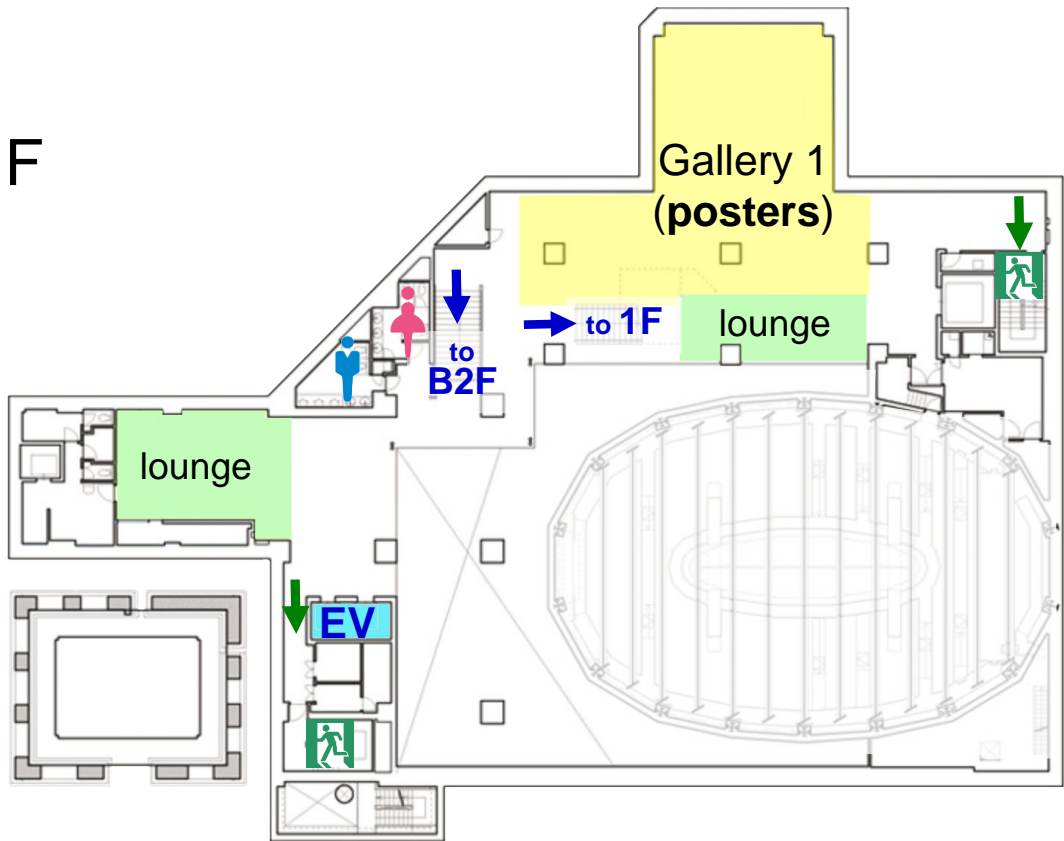
## 1F



## B2F



# B1F

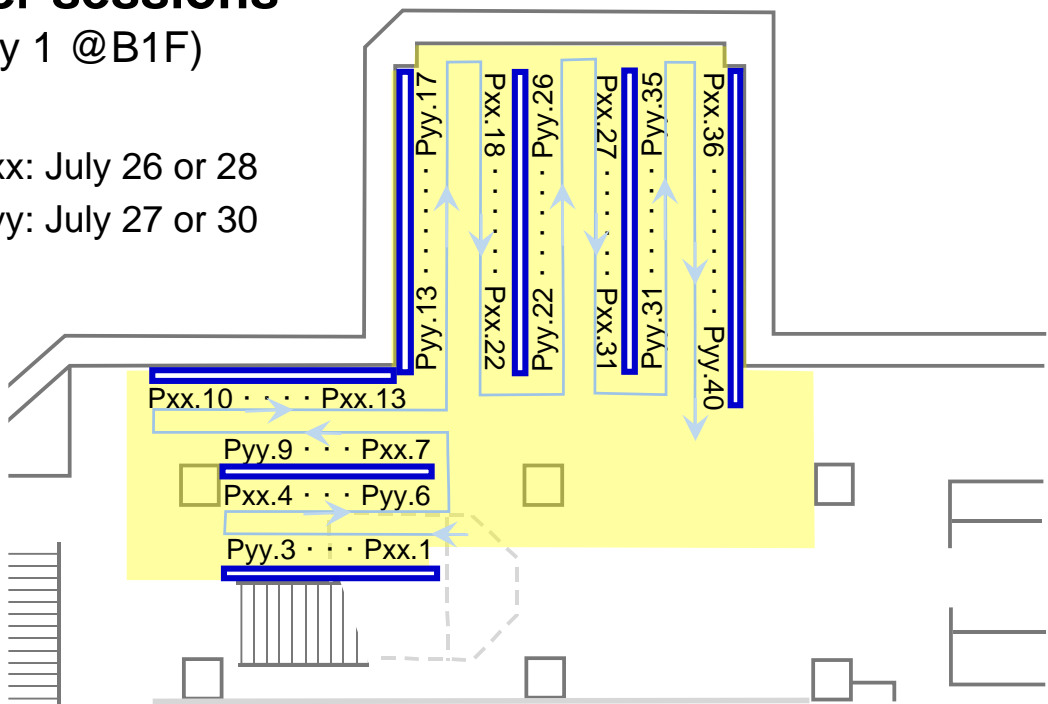


## Poster sessions

(Gallery 1 @B1F)

Pxx: July 26 or 28

Pyy: July 27 or 30





|   |  |  |   |  |
|---|--|--|---|--|
| 1 Yasuda Auditorium                                     | 44 Yayoi Auditorium Annex                              | 82 Faculty of Law Bldg.3                               | 116 Faculty of Engineering Bldg.4       | 234 Biotechnology Research Center  |
| 2 Sanjo Conference Hall                                 | 45 Ward A  | 83 Faculty of Law Bldg.4                               | 77 Faculty of Engineering Bldg.5        | 117 Food Science Bldg.   |
| 3 Ikutokuken (Sanshiro Pond)                            | 46 Ward B  | 84 General Research Bldg.                              | 78 Faculty of Engineering Bldg.6        | 118 Life Sciences Research Bldg.B  |
| 4 Chuo Refectory (Underground)                          | 47 Central Bldg. (East Wing)                           | 85 School of Law Bldg.                                 | 79 Faculty of Engineering Bldg.7        | 429 Protein Research Laboratory  |
| 5 Second Refectory                                      | 48 Central Bldg. (South Wing)                          | 86 Faculty of Letters Bldg.3                           | 80 Faculty of Engineering Bldg.8        | 24 Interfaculty Initiative in Information Studies & Graduate School of Interdisciplinary Information Studies |
| 6 Administration Bureau                                 | 49 Akamon General Research Bldg.                       | 87 Akamon General Research Bldg.                       | 81 Faculty of Engineering Bldg.9        | 122 In-Fukutake Hall   |
| 7 General Library                                       | 50 Faculty of Letters Annex                            | 88 Faculty of Letters Annex                            | 82 Institute of Engineering Innovation  | 123 In-Daiva Ubiquitous Computing Research Bldg.   |
| 8 Shichiboku (Japanese Sports Gymnasium)                | 51 Economics Research Bldg.                            | 89 East Clinical Research Bldg.                        | 83 Faculty of Engineering Bldg.10       | 124 Earthquake Research Institute Bldg.1   |
| 9 Administration Bureau Bldg.2                          | 52 International Center for Disability Services Office | 90 International Center for Disability Services Office | 84 Faculty of Engineering Bldg.11       | 125 Earthquake Research Institute Bldg.2   |
| 10 Kaitokukan   | 53 Hongo Office - IJSTEP                               | 91 Administration & Research Bldg.                     | 85 Faculty of Engineering Bldg.12       | 126 Earthquake Research Institute Bldg.3   |
| 11 Ikutokudo (Japanese Archery Range)                   | 54 UCH Plaza   | 92 Clinical Research Bldg.A                            | 86 Faculty of Engineering Bldg.13       | 127 Institute of Molecular and Cellular Biosciences  |
| 12 Student Counseling Center (In-Spin Resources) Office | 55 Faculty of Letters Bldg.3                           | 93 South Clinical Research Bldg.                       | 87 Faculty of Engineering Bldg.14       | 128 Institute for Advanced Studies on Asia   |
| 13 Communication Support Room                           | 56 Akamon Research Bldg.                               | 94 Clinical Research Ward                              | 88 Takeda Bldg.                         | 129 Institute of Social Science  |
| 14 Peer Support Room                                    | 57 Faculty of Letters Annex                            | 95 Advanced Clinical Research Center                   | 89 Takeda Hall                          | 130 Historiographical Institute  |
| 15 Career Support Office                                | 58 Faculty of Letters Annex                            | 96 Energy Station                                      | 90 VLSI Design and Education Center     | 131 Asian Natural Environment Science Center   |
| 16 Yayoi Auditorium                                     | 59 Economics Research Bldg.                            | 97 Pharmaceutical Sciences Research Library            | 91 Seakeeping Tank/Ship Model Basin     | 132 University Museum  |
|   | 60 International Center for Disability Services Office | 98 Faculty of Pharmaceutical Sciences Research Bldg.   | 92 Experimental Tank                    | 133 Micro Analysis Laboratory, Pandem Accelerator (PAL)  |
|   | 61 Faculty of Medicine Bldg.1                          | 99 Faculty of Medicine Annex of Bldg.3                 | 93 Cavitation Tunnel                    | 134 Environmental Science Center   |
|   | 62 Faculty of Medicine Bldg.2                          | 100 Bioscience Research Bldg.                          | 94 Monozukuri Lab.                      | 135 Environmental Science Center Annex   |
|   | 63 Faculty of Law & Letters Bldg.1                     | 101 Faculty of Medicine Bldg.4                         | 95 Power Dynamics Experiment Laboratory | 136 Isotope Science Center   |
|   | 64 Faculty of Law & Letters Bldg.2                     | 102 Faculty of Medicine Bldg.5                         | 96 Wind Engineering Lab.                | 137 Information Technology Center  |
|   | 65 Faculty of Law & Letters Bldg.3                     | 103 Faculty of Medicine International Research Center  | 97 High Voltage Electron Microscope     | 138 Agricultural and Life Sciences Museum  |
|   |  | 104 Faculty of Medicine International Research Center  |   | 139 Life Sciences Research Bldg.   |
|   |  | 105 Faculty of Medicine International Research Center  |   | 140 Veterinary Medical Center  |

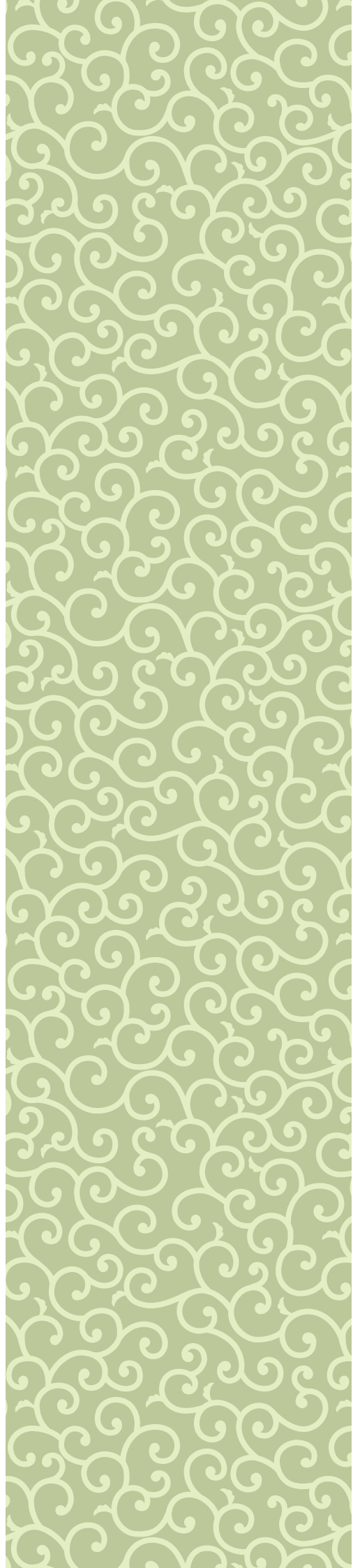
☆: Chartered bus

Getting to the Hongō Campus

- Hongō-sanchohme Station (Subway Marunouchi Line) 8 minutes' walk.
- Hongō-sanchohme Station (Subway Oedo Line) 6 minutes' walk.
- Yushima Station or Nezu Station (Subway Chiyoda Line) 8 minutes' walk.
- Todaimae Station (Subway Namboku Line) 1 minute's walk.
- Kasuga Station (Subway Mita Line) 10 minutes' walk.
- Ochanomizu Station (JR Chuo Line, JR Sobu Line) <Subway>Subway Marunouchi Line (for Ikebukuro) → get off at Hongō-sanchohme Station.
- <Subway>Subway Chiyoda Line (for Ioriide) → get off at Yushima Station or Nezu Station.
- Toei Bus>茶51 for Komagome Station South Exit or 茶43 for Arakawa-dote-soshajo → get off at Todai-Akamon-mae, Todai-Seimon-mae, Todai-Ngakukub-mae stops
- Toei Bus>茶07 for the University of Tokyo → get off at Tatsuokamon, Todai-Byoin-mae, Todai-Konai stops.
- Ueno Station (JR Yamanote Line, other lines) <Toei Bus>茶01 for the University of Tokyo → get off at Tatsuokamon, Todai-Byoin-mae, Todai-Konai stops.
- Okachimachi Station (JR Yamanote Line, other lines) <Toei Bus>茶02 for Otsuka Station or 茶69 for Otakibashi-shako-mae → get off at Yushima-yonchohme, Hongō-sanchohme Eki-mae stops.



**July 26 (Thursday)**



# Abstracts

## July 26 (Thursday) Oral Presentations

### O26.1 $p+ip$ Fermi superfluids: old results and new questions

A. J. Leggett<sup>ab</sup>

<sup>a</sup>Dept. of Physics, University of Illinois at Urbana-Champaign, USA

<sup>b</sup>Shanghai Center for Complex Physics, Shaanghai Jiaotong University, PRC

Liquid helium-3-A is the first laboratory system (along with its sister B state) confidently believed to undergo Cooper pairing in a non-s-wave state, and it has been widely used as an analog for certain metallic systems such as strontium ruthenate, with both falling into the class of “2D  $p + ip$ ” Fermi superfluids. One of the most fascinating predictions concerning this class of systems is that they may be able to sustain exotic quasi-fermionic excitations such as Majorana fermions, and that these may then be used to implement topological quantum computation (TQC). I review the current state of play regarding the  $p + ip$  Fermi superfluids, and call attention to some questions about them, particularly ones relevant to TQC, which I believe are currently unresolved.

PLENARY TALK

### O26.2 **Frontiers in Quantum Matter: Symmetry, Topology & Strong Correlation Physics**

J. A. Sauls

Department of Physics, Northwestern University, USA

I highlight some current and frontier directions in low-temperature physics and quantum matter, focusing on unsolved problems and open questions: (i) is superfluid  $^3\text{He-A}$  the precursor to magnetically ordered solid  $^3\text{He}$ ?, (ii) Majorana particles in superfluid  $^3\text{He}$  - where are they and should we care?, (iii) what do we *not* understand about the dynamics of mesoscopic objects in a quantum bath at ultra-low temperatures?, and (iv) does our understanding of quantum fluids and quantum turbulence provide any insight into the rotational dynamics of pulsars?

PLENARY TALK

### O26.3 The orbitropic effect in superfluid helium-3 B-phase boundaries

M. Arrayás<sup>a</sup>, R. P. Haley<sup>b</sup>, G. R. Pickett<sup>b</sup>, and D. Zmeev<sup>b</sup>

<sup>a</sup>Área de Electromagnetismo, Universidad Rey Juan Carlos, Tulipán s/n, 28933 Móstoles, Madrid, Spain

<sup>b</sup>Department of Physics, Lancaster University, Lancaster, LA1 4YB, UK

We have studied the influence of orbital viscosity on the dynamics of the order parameter texture in the superfluid B phase of helium-3 near a moving boundary. When the interface between the B phase and the boundary moves, the thermally-excited quasiparticles redistribute in response to changes in the texture of the orbital angular momentum. In our model this bestows a significant effective mass and gives a mechanism for friction impeding the motion of the boundary. The model has been tested quantitatively against previously unexplained measurements of the anomalously large and non-linear dissipation of a moving AB interface.

INVITED TALK

### O26.4 Towards Measurement based Majorana qubits

K. Zuo<sup>a</sup>, S. Heedt<sup>b</sup>, F. Borsoi<sup>b</sup>, K. van Hoogdalem<sup>b</sup>, M. de Moor<sup>b</sup>, N. de Jong<sup>b</sup>, M. Quintero Perez<sup>b</sup>, S. Gazibegovic<sup>d</sup>, R. op het Veld<sup>d</sup>, S. Balk<sup>d</sup>, E. Bakkers<sup>d</sup>, E. Uccelli<sup>b</sup>, M. Wimmer<sup>b</sup>, and L. Kouwenhoven<sup>bc</sup>

<sup>a</sup>Superconducting Quantum Electronics Research Team, CEMS, RIKEN

<sup>b</sup>QuTech, Delft University of Technology, 2600 GA Delft, Netherlands

<sup>c</sup>Station Q Delft, Microsoft Research, 2600 GA, Delft, Netherlands

<sup>d</sup>Department of Applied Physics, Eindhoven University of Technology, 5600 MB Eindhoven, Netherlands

Majorana bound states (MBS) spotted first in the hybrid semiconductor-superconductor nanowire system are among the best candidates to create Majorana qubits. These qubits are not only topologically protected due to the topological origin of MBS, but also the qubit operation by braiding the MBS are protected. However, achieving Majorana qubits and the gate operations requires physically shuffling MBS, which is extremely challenging both in material growth and in fabrication techniques. In consideration of these issues, we experimentally implement a more recent scheme, where braiding is achieved by utilizing specific transport measurements. This largely reduces the barrier for demonstrating the Majorana qubits.

In this talk, I will briefly discuss the requirements for realizing the measurement based Majorana qubit and the current status of the projects at Station-Q Delft. I will mainly focus on the conventional InSb nanowire network system which is more straightforward and makes the first Majorana qubit within reach. After that, I will introduce the so-called Selective Area Grown (SAG) InSb nanowires. The SAG InSb nanowires are even more patternable and, therefore, more suitable for addressing the advanced large-scale Majorana qubits. Initial results on these SAG InSb nanowires are very intriguing and promising.

INVITED TALK

## O26.5 Elastic Anomalies in Adsorbed Films of Helium, Hydrogen and Neon

K. Shirahama<sup>a</sup>, T. Makiuchi<sup>a</sup>, M. Tagai<sup>a</sup>, K. Yamashita<sup>a</sup>, Y. Nago<sup>a</sup>, and D. Takahashi<sup>b</sup>

<sup>a</sup>Department of Physics, Keio University, Japan

<sup>b</sup>Center for Liberal Arts and Sciences, Ashikaga University, Japan

<sup>4</sup>He films adsorbed on disordered substrates undergo a quantum phase transition (QPT) between localized solid and superfluid at a critical coverage  $n = n_c$ <sup>1</sup>. We have found that the localized states of <sup>4</sup>He and <sup>3</sup>He films adsorbed on a porous glass show anomalous elastic phenomena, which are well explained by a thermal activation model<sup>2</sup> with peculiar energy band structure near the QPT<sup>3</sup>. At low temperatures helium films under AC strain stiffens with an excess dissipation. The characteristic temperature of stiffening decreases as  $n$  approaches  $n_c$ . The elastic anomalies are quantitatively explained by thermal activation of helium atoms from the localized band to extended one with energy gap  $\Delta$  with distribution. The mean gap  $\Delta$  decreases to zero obeying a powerlaw  $\Delta \propto (n - n_c)^\alpha$  with  $\alpha \sim 1.3$  for <sup>4</sup>He and 1.8 for <sup>3</sup>He. It is concluded that the ground states are identically *gapped* and *compressible* for <sup>4</sup>He and <sup>3</sup>He films. We propose that the ground states are a Mott insulator or Mott glass<sup>4</sup>, both of which can be self-organized by strong correlation among helium adatoms. We have recently discovered same elastic anomalies in neon (<sup>20</sup>Ne) and hydrogen deuteride (HD) films as in helium. However, these "less quantum" films do not exhibit QPT, suggesting that the elastic anomalies are caused by gapped excitations in 2D solids. Our results suggest that the elastic anomalies are ubiquitous and can occur in physisorbed films of *any* atomic or molecular species, and molecules excited to possible extended states show superfluidity.

1. P. A. Crowell, *et al.*, PRB **55**, 12620 (1997).
2. R. H. Tait, and J. D. Reppy, PRB **20**, 997 (1979).
3. T. Makiuchi *et al.*, arXiv:1806.06624.
4. T. Giamarchi, *et al.*, PRB **64**, 245119 (2001).

INVITED TALK

## O26.6 QCM Measurements on Submonolayer <sup>4</sup>He Films on Graphite

Masashi Morishita<sup>a</sup>, Masatoshi Umemoto<sup>a</sup>, Junko Taniguchi<sup>b</sup>, and Masaru Suzuki<sup>b</sup>

<sup>a</sup>Faculty of Pure and Applied Sciences, University of Tsukuba, Japan

<sup>b</sup>Department of Engineering Sciences, University of Electro-Communications, Japan

Fluidity inside the domain walls of adsorption structure of submonolayer <sup>4</sup>He solid films on graphite has been proposed according to the results of heat capacity measurements of small amounts of <sup>3</sup>He dissolved in submonolayer <sup>4</sup>He films. The observed anomalous  $T^2$ -dependence of heat capacities is attributed to the Dirac fermion behavior of <sup>3</sup>He for the honeycomb domain walls. For a direct detection of the fluidity inside the domain walls, we have performed quartz-crystal microbalance measurements on submonolayer <sup>4</sup>He films on graphite. The results revealed that submonolayer <sup>4</sup>He films slip or decouple from the graphite substrate below at least 10 K. Only for higher areal densities than  $6.4 \text{ nm}^{-2}$ , which is the areal density of the  $\sqrt{3} \times \sqrt{3}$  phase, the resonant frequencies ( $f_0$ ) decrease around 0.4 K. This behavior can be attributed to the suppression in slippage by the counterflow of superfluid inside the domain walls against the slipping solids, and strongly suggests the fluidity inside the domain walls. By decreasing the temperature further,  $f_0$  increases rather suddenly for areal densities greater than  $6.4 \text{ nm}^{-2}$ . Although the origin of this observation has not been clarified, it indicates that the submonolayer <sup>4</sup>He films decouple from the substrate again. The increases in  $f_0$  are accompanied by precursors of dissipation ( $Q^{-1}$ ) peaks. The onset temperature of the increase in  $f_0$  and the  $Q^{-1}$  peak temperatures depend on the areal density in a rather complicated manner, and increase anomalously with an increase in the amplitude of oscillation. Furthermore, the peak height of  $Q^{-1}$  appears to be inversely proportional to the corresponding peak temperature.

INVITED TALK

## O26.7 Competition between thermodynamical and dynamical superfluid of $^4\text{He}$ confined in a nanometer-size channel

J. Taniguchi, K. Taniguchi, and M. Suzuki

Dept. Engineering Science, University of Electro-Communications, Japan

$^4\text{He}$  confined in a one-dimensional (1D) channel is one of the suitable systems to study the superfluid of Tomonaga-Luttinger (TL) liquid. Theorists predict that the coherence of superfluid of TL liquid is broken by phase slips, which are excited thermally<sup>1</sup> or dynamically<sup>2</sup>. In the former case, the superfluid shows a gradual temperature dependence, and in the latter, the superfluid onset becomes sharp. We have measured the superfluid of  $^4\text{He}$  confined in a 2.5-nm channel (FSM-14) and found that its temperature dependence is well fitted to the former (thermal) one. On the other hand,  $^4\text{He}$  in a 2.8-nm channel (FSM-16) shows a sharp superfluid onset at low pressure, in the same manner as the dynamical one.<sup>3</sup> With increasing pressure, the superfluid starts to show the gradual temperature dependence below the superfluid onset, and at last the sharp onset disappears. These results indicate that the phase slip is thermally excited at the lower temperature for the narrower channel, and that the dynamical superfluid onset may not be observed when the thermally excited phase slips break the superfluid at the lower temperature than the dynamical ones.

1. A. Del, Maestro et al. (2011). “ $^4\text{He}$  Luttinger Liquid in Nanopores”. PRL **106**, 105303.
2. T. Eggel et al. (2011). “Dynamical Theory of Superfluidity in One Dimension” PRL **107**, 275302.
3. J. Taniguchi et al. (2013). “Dynamical superfluid response of  $^4\text{He}$  confined in a nanometer-size channel”, PRB **88**, 014502.

INVITED TALK

## O26.8 Spin superfluidity from ultralow to room temperature

Yu. M. Bunkov

Kazan Federal University, Kazan, Russia

Supermagnonics and conventional Bose-Einstein condensation of magnon is a new branch of quantum physics of condensed matter. The subject is dealing with the formation, development and applications of coherent quantum liquid of magnons in magnetically ordered materials.<sup>1</sup> The quantum phenomena like spin supercurrent, Josephson effect, critical current, phase slippage, quantum vortex, Goldstone modes etc. was discovered for magnon liquid at low and ultralow temperatures. Recently the magnon BEC and spin supercurrent was observed at 1.5 K in antiferromagnets with Suhl-Nacamura interaction<sup>2</sup> and at room temperature in normally magnetized YIG film. The formation of magnon BEC in all these materials is described by the same mechanism of Bose Condensation of excited magnons with overcritical density.<sup>3</sup> For normally magnetized YIG film we have found the long lived induction decay signal (the main signature of magnon BEC) and Q-ball phenomena. The spatial transport between two YIG films, connected by a bridge, have also been observed. This discovery opens the door for a many applications of supermagnonics.

1. Yury Bunkov, (2016) “Magnon BEC Versus Atomic BEC”, J. Low Temp. Phys., 183, 399.
2. Yu. M. Bunkov, et.al. (2012) “High Tc spin superfluidity in antiferromagnets”, Phys. Rev. Lett. 108, 177002.
3. Yu. M. Bunkov, V. L. Safonov, (2018) “Magnon condensation and spin superfluidity”, Journal of Magnetism and Magnetic Materials, 452, 30.

INVITED TALK



## O26.9 Mass flow through bulk solid helium and solid helium confined in Aerogel

Jaeho Shin and Moses H. W. Chan

Department of Physics, The Pennsylvania State University, University Park, Pennsylvania 16802-6300, USA

We have made mass flow measurements through 2.5 mm thick solid  $^4\text{He}$  samples sandwiched between Vycor rods infused with superfluid. Bulk samples, samples where the flow path are partially blocked by a thin disk and samples confined in silica aerogel of 96% porosity were studied. The mass flow of the bulk samples showed superfluid-like properties similar to that found in 4 cm<sup>1</sup> and 8  $\mu\text{m}^2$  samples. While the flow rate varies from sample to sample, it decreases with increasing temperature up to 1 K and similar to that found in the 8  $\mu\text{m}$  samples decays exponentially with pressure from melting up to 30 bar. In samples intersected by the thin disks, the flow rate shows a correspondingly dramatic decrease. We found no evidence of mass flow in samples grown in silica aerogel. Since the mean separation of the silica strands in aerogel is on the order 100 nm, these strands prevent the formation of dislocations network in solid  $^4\text{He}$ . These results indicate dislocation network in the solid is essential for the observed mass flow. We will also report on the ongoing studies of solid helium samples nucleated on the surface of highly oriented pyrolytic graphite (HOPG). Single crystal helium samples with the c-axis grown perpendicular and parallel to the direction of the mass flow were studied.

This research is supported by NSF under grant DMR-1103159 and DMR-1707340

1. M. W. Ray and R. B. Hallock, PRL 100, 235301 (2008)
2. J. Shin, D. Kim, A. Haziot, and M.H.W Chan, PRL 118, 235301 (2017)

INVITED TALK

## O26.10 Mass flow in quantum solids: $^4\text{He}$ and $^3\text{He}$

Zhi Gang Cheng and John Beamish

University of Alberta, Canada

A series of experiments have observed low temperature mass transport through solid  $^4\text{He}$  sandwiched between superfluid reservoirs, generating broad interest in possible superflow in quantum solids. When the length scale for the solid flow was reduced from centimeters to micrometers, the flow occurred over broader temperature and pressure ranges, and  $^3\text{He}$  impurities were no longer effective in suppressing the flow at the lowest temperatures. However, the mechanism of mass transport and the effect of  $^3\text{He}$  remains unclear.

In contrast to the “liquid-solid-liquid” sandwich of these experiments, we have studied mass transport in  $^4\text{He}$  through a “solid-liquid-solid” junction and in a geometry with no liquid present. By comparing the effects of  $^3\text{He}$  impurities for these geometries, we conclude that the mass transport may be two-dimensional, e.g. along superfluid channels at cell walls and/or grain boundaries. To understand the nature of this phenomenon, we have conducted experiments to search for mass transport in solid  $^3\text{He}$ . Although mass flow was observed, it decreases monotonically with temperature, the opposite behavior to that that seen in solid  $^4\text{He}$ , supporting a superfluid interpretation of the mass flow in solid  $^4\text{He}$ . Above 100 mK, the mass flow in solid  $^3\text{He}$  is dominated by thermally activated vacancy motion, but at lower temperatures approaches a constant value that is a manifestation of the quantum nature of bcc  $^3\text{He}$ .

Note: Zhi Gang Cheng’s current address: Institute of Physics, Chinese Academy of Sciences, China

INVITED TALK

O26.11 **Characterization of vibrating dislocations in solid  $^4\text{He}$  by their interaction with AC shear deformation and  $^3\text{He}$  impurities**

A. I. Golov<sup>a</sup>, M. Yu. Brazhnikov<sup>b</sup>, and Yu. M. Mukharsky<sup>c</sup>

<sup>a</sup>School of Physics and Astronomy, The University of Manchester, Manchester M13 9PL, UK

<sup>b</sup>Institute of Solid State Physics, Chernogolovka, 142432 Russia

<sup>c</sup>Department of Condensed Matter Physics, CEA-Saclay/IRAMIS, 91191 Gif sur Yvette, Cedex, France

Mobile dislocations, especially the distribution of their lengths, in polycrystalline hcp  $^4\text{He}$  were investigated through their interaction with an oscillatory shear strain of various frequencies. In particular, the response of solid  $^4\text{He}$  to an oscillatory twisting at frequencies 161 Hz and 931 Hz was examined along with its thermal conductivity (i. e. scattering of thermal transverse phonons off dislocations). Polycrystalline samples of  $^4\text{He}$  with concentration of  $^3\text{He}$   $x_3 \sim 3 \times 10^{-7}$ , grown by the blocked capillary method at molar volume  $19.53 \text{ cm}^3 \text{ mol}^{-1}$ , have been studied at temperatures 0.1–1.0 K before and after annealing at temperatures 1.8–2.0 K, and also after cold working by high-amplitude twisting below 0.3 K and after the successive annealing at 0.6–0.7 K.

Monitoring temperature-dependent response to twisting at small amplitudes as well as the amplitude dependence at stronger forcing allowed to extract the distribution of lengths of mobile segments of dislocations in a wider range than previous authors, and to compare them after each treatment of the sample. Unlike measurements on single crystals, we observed no saturation at small lengths. Annealing always resulted in the reduction of the number of short dislocations (e. g. introduced by cold working) and in the proliferation of longer ones.

INVITED TALK

# July 26 (Thursday) Poster Presentations

## P26.1 Casimir Effect for Interacting Fermion system and Boson system

R. Yoshii<sup>a</sup>, S. Takada<sup>b</sup>, N. Flachi<sup>c</sup>, and M. Nitta<sup>d</sup>

<sup>a</sup>Department of Physics, Chuo University, Tokyo, Japan<sup>b</sup>Earthquake Research Institute, The University of Tokyo, Tokyo, Japan<sup>c</sup>Department of Physics, Keio University, Yokohama, Japan

<sup>d</sup>Department of Physics, Keio University, Yokohama, Japan

The Casimir effect refers to the appearance of a macroscopic force due to the deformations in the quantum vacuum induced by the presence of boundaries. The relevance of the Casimir effect is now recognized in many areas of science, e.g., applications to nanotechnology, string theory, or cosmology. In spite of the importance, the Casimir effect in the presence of the interaction has not been well understood.

We present the results of Casimir effect in both the interacting fermion system and the interacting boson system. We analyze the BCS model<sup>1</sup> and the nonlinear sigma models<sup>2</sup>. We explain the methods to obtain the exact solutions of those system in the presence of the boundaries within the mean-field approximation. We show the exact solutions and the tunability of the Casimir force in those systems by changing the interaction strength. We also show the non-trivial behavior of the Casimir force in the presence of the magnetic field.

1. A. Flachi, M. Nitta, S. Takada and R. Yoshii, "Sign Flip in the Casimir Force for Interacting Fermion Systems," *Phys. Rev. Lett.* **119**, 031601 (2017).
2. A. Flachi, M. Nitta, S. Takada and R. Yoshii, "Casimir Force for the  $CP^{N-1}$  Model," arXiv:1708.08807.

## P26.2 Elasticity Measurements of Hydrogen Films Adsorbed on a Porous Glass

K. Yamashita, T. Makiuchi, M. Tagai, Y. Nago, and K. Shirahama

Department of Physics, Keio University, Japan

<sup>4</sup>He film adsorbed on solid substrates undergoes superfluidity above a critical coverage  $n_c$ . We have recently found that <sup>4</sup>He and <sup>3</sup>He films stiffen at low temperatures at  $n < n_c$ <sup>1</sup>. Our results show that the ground state of helium films is the gapped many-body state such as Mott insulator or Mott glass. Hydrogen (H<sub>2</sub>, HD, D<sub>2</sub>) shows quantum effects following helium because of its large zero-point energy but its large intermolecular force. A heat capacity study suggested that the temperature-coverage phase diagram of H<sub>2</sub> film resembles that of <sup>4</sup>He film<sup>2</sup>. The heat capacity drops rapidly in the low coverage and low temperature phase, which is explained by the islands at the minimum potential of the surface. Therefore, it is expected to examine whether the gapped model can explain the ground state of hydrogen film. We have measured elastic constants of HD film adsorbed on a porous glass by torsional oscillator (TO) technique used in our previous helium-film studies<sup>1</sup>. HD was chosen as adatoms because of the absence of ortho-para conversion. We have found that HD film also shows stiffening behavior similar to helium films<sup>1</sup>, which is observed as an elasticity increase accompanied by a dissipation peak. Results of HD film will be discussed in comparison with helium films.

1. T. Makiuchi, *et al.*, another poster; T. Makiuchi, M. Tagai, Y. Nago, D. Takahashi, and K. Shirahama, in preparation.
2. R. H. Torii, H. J. Maris, and G. M. Seidel, *PRB* **41**, 7167 (1990).

### P26.3 Singlet Dimer Bound State of $^3\text{He}$ in Nanopore Suggested by NMR

Taku Matsushita<sup>a</sup>, Kazunori Amaike<sup>a</sup>, Mitsunori Hieda<sup>b</sup>, and Nobuo Wada<sup>a</sup>

<sup>a</sup>Department of Physics, Nagoya University, Nagoya, Japan

<sup>b</sup>College of Liberal Arts and Sciences, Tokyo Medical and Dental University, Ichikawa, Japan

On  $^4\text{He}$ -preplated walls of substrates,  $^3\text{He}$  atoms can move rather freely being bounded on the surface, and show a rich variety of gas-like behavior. Recently the heat capacity experiment for  $^3\text{He}$  in 3D-connected 3nm nanopore of HMM-2 have shown that they have various characters of 3D strongly-correlated Fermi fluid, depending on the  $^4\text{He}$  thickness and  $^3\text{He}$  density. Among them, one of the most interesting states is a bound state which appears at low temperatures on relatively thin  $^4\text{He}$  film, and at which the heat capacity decreases exponentially as  $T$  decreases. Although the temperature region of the bound state becomes lower with increasing  $^4\text{He}$  thickness, the state remains even on superfluid  $^4\text{He}$  film, which suggests that it is caused by interaction between  $^3\text{He}$  atoms rather than the substrate interaction. In order to study the nature of this bound state, we have conducted  $^3\text{He}$  NMR experiments for this system. On 1.6 layer  $^4\text{He}$  superfluid film, where the heat capacity peak indicating the bound state onset is observed at 60 mK, the susceptibility decreases from the Curie law below around 100 mK independently of the  $^3\text{He}$  density, and with characteristic decreases of the spin-spin relaxation time. The estimated spin-gap energy assuming the non-magnetic ground state is about 80 mK close to the bound state gap shown by the heat capacity, which strongly suggests that the bound state accompanies formation of spin-singlet  $^3\text{He}$  dimers. At high  $^3\text{He}$  densities where the bound state is not observed by the heat capacity, these characteristic features observed by NMR was confirmed to disappear. In addition, for  $^3\text{He}$  on 1.35 layer  $^4\text{He}$  film which is the superfluid onset thickness for  $^4\text{He}$ , deviation of the susceptibility from the Curie law has been observed from even higher temperatures, correspondingly to the higher onset temperature of the bound state.

### P26.4 Confined fluids in alumina nanoporous membranes

P. Spathis<sup>a</sup>, F. Souris<sup>a</sup>, V. Doebele<sup>a</sup>, H. Böttcher<sup>a</sup>, A. Grosman<sup>b</sup>, I. Trimaille<sup>b</sup>, E. Rolley<sup>c</sup>, L. Cagnon<sup>a</sup>, and P.E. Wolf<sup>a</sup>

<sup>a</sup>Institut Neel, CNRS/UGA, UPR2940, Grenoble, France

<sup>b</sup>INSP, CNRS/UPMC, UMR 7588, Paris

<sup>c</sup>LPS-ENS, CNRS/Univ. Paris Diderot/UPMC, UMR 8550, Paris

Condensation and evaporation of fluids in mesoporous materials are affected by confinement. In this context, the occurrence of cavitation at the nanoscale is highly debated. We use nanoporous alumina membranes as a model system to investigate the effect of confinement and different fluids to probe fluid-fluid and fluid-wall interactions. In particular, we use helium to vary the temperature over a large range and investigate the effect of thermal activation. The alumina membranes obtained through anodization techniques have monodisperse cylindrical pores of well-defined nanometric dimensions. To study cavitation, we have used additional fabrication steps to obtain cavities connected to the external vapor reservoir through a narrow constriction. This forces the fluid to large negative pressures, in a deep metastable state. We have measured isotherms with a combination of volumetric and optical techniques. The first results using hexane show that evaporation proceeds indeed through cavitation. Measurements currently underway with helium will also be presented.

This work is supported by the ANR through the project CAVCONF.

## P26.5 Superfluid Transitions of $^4\text{He}$ Films under Marginal Conditions among 1-, 2- and 3-Dimensions

Nobuo Wada<sup>a</sup>, Taku Matsushita<sup>b</sup>, Mitsunori Hieda<sup>c</sup>, and Ryo Toda<sup>d</sup>

<sup>a</sup>School of Science, Nagoya University, Nagoya 464-8602, Japan

<sup>b</sup>Department of Physics, Nagoya University, Nagoya 464-8602, Japan

<sup>c</sup>Col. of Lib. Arts & Sci., Tokyo Medical and Dental Univ., 2-8-30 Kounodai, Ichikawa, 272-0827, Japan

<sup>d</sup>Cryogenic Research Center, The University of Tokyo, Yayoi, Tokyo 113-0032, Japan

We found superfluid (SF) onset of the  $^4\text{He}$  film formed in nanopore depends on dimensional form of its pore connection, the pore diameter, and so on. In case of  $^4\text{He}$  nanotubes with diameter  $d'$  and length  $L$  formed in 1D channels, SF onset (crossover) depends on an effective 1D length  $L_{\text{eff}} = L/\pi d'$ . The onset temperature  $T_X$  for  $L_{\text{eff}} \gtrsim 50$  becomes lower than the 2D KT temperature. In this SF onset for the finite 1D length, an excitation of  $2\pi$ -phase winding in the length  $L_{\text{eff}}$  plays the most important role<sup>1</sup>.  $^4\text{He}$  film formed in 3D nanopores of HMM-2 shows both 3D SF and 2D degenerate states, depending on fluid film coverage. The phase diagram can be understood by relative lengths among a 2D mean atomic distance  $\langle r_{2D} \rangle$ , a 3D one  $\langle r_{3D} \rangle$  and a 3D connection length  $L_{3D}$  of the film<sup>2</sup>. At a very low coverage, the film directly causes the 3D transition from the normal fluid state to the long-range-ordered SF state, since  $\langle r_{3D} \rangle \lesssim \langle r_{2D} \rangle$ . Increasing the coverage, where  $\langle r_{3D} \rangle > \langle r_{2D} \rangle$ , the film sets into the 2D degenerate state followed by the 3D transition at a lower temperature. Superfluid density and heat capacity observed for the 3D SF have properties similar to BEC of the 3D Bose gas rather than those of the bulk  $^4\text{He}$  liquid.

1. T. Matsushita, *et al.*, J Low Temp Phys **183**, 273 (2016).
2. T. Matsushita, *et al.*, J. Phys. Soc. Jpn **86**, 103601 (2017).

## P26.6 Slippage and localized-unlocalized transition in a $^4\text{He}$ solid film system

J. Taniguchi, H. Ichida, and M. Suzuki

Dept. Engineering Science, University of Electro-Communications, Japan

We have performed the ultrasound measurements for  $^4\text{He}$  film adsorbed on a mesoporous material (FSM-16). In the coverage region where adsorbed  $^4\text{He}$  atoms form an inert solid layer, we observed an increase of sound velocity ( $v$ ) at low temperature accompanied by an attenuation peak. It seems that the amount of  $v$  increase ( $\Delta v$ ) is limited by the variation of  $v$  due to the mass loading of  $^4\text{He}$  film. As the coverage is increased, both  $\Delta v$  and the attenuation peak are suppressed, and disappear at the coverage where the inert solid layer is completed. The temperature dependence of  $v$  and attenuation can be explained by the relaxation of ultrasound stresses via a defect motion.

Our very recent heat capacity measurements confirm that in the same coverage region the localized-delocalized transition occurs. This coincidence indicates that the defects correspond to the unoccupied localized states and furthermore the defect motion may be a microscopic picture of the slippage of entire solid film.

## P26.7 Quantum Phase Transition of Thin He Films on a Disordered Substrate

T. Makiuchi<sup>a</sup>, M. Tagai<sup>a</sup>, K. Yamashita<sup>a</sup>, Y. Nago<sup>a</sup>, D. Takahashi<sup>b</sup>, and K. Shirahama<sup>a</sup>

<sup>a</sup>Department of Physics, Keio University, Japan

<sup>b</sup>Center for Liberal Arts and Sciences, Ashikaga University, Japan

Adsorbed He film is an ideal two-dimensional (2D) system which shows a variety of quantum phases depending on coverage (density) and substrate. <sup>4</sup>He film on atomically rough surface does not show superfluidity until the coverage  $n$  reaches a critical value  $n_c$ . Unveiling the nature of the non-superfluid phase is an important issue to understand the quantum phase transition (QPT) occurring at  $n_c$ . We report measurements of elasticity of He films adsorbed in a nanoporous Gelsil glass, which provides a disordered substrate. The elasticity was directly measured by using a torsional oscillator containing a porous glass in the torsion rod. We have found that both pure <sup>4</sup>He and <sup>3</sup>He films stiffen at low temperatures for  $n < n_c$ . The stiffening is quantitatively explained by thermal activation model<sup>1</sup> in which He atoms are localized with an  $n$ -dependent energy gap which closes as  $n \rightarrow n_c$ . The 2D compressibility diverges as  $n \rightarrow n_c$ , which means that He films are completely soft at  $n_c$ . We have also discovered that Ne films exhibit similar stiffening at about 5 K, without closing an energy gap, suggesting that Ne films are classical solid puddles in contrast to He. Our results reject the possibility of Bose glass as the ground state of <sup>4</sup>He film<sup>2</sup> but definitely shows that the ground states of both <sup>4</sup>He and <sup>3</sup>He films are the same gapped quantum many-body state such as Mott insulator or Mott glass<sup>3</sup>, which is originated from quantum nature of He films, while Ne film does not show QPT.

1. R. H. Tait and J. D. Reppy, PRB **20**, 997 (1979); P. A. Crowell, *et al.*, PRB **55**, 12620 (1997).
2. M. P. A. Fisher *et al.*, PRB **40**, 546 (1989).
3. T. Giamarchi *et al.*, PRB **64**, 245119 (2001).

## P26.8 Toward the direct observation of chiral edge mass current in quasi-2D <sup>3</sup>He-A

K. Kuwahara<sup>a</sup>, T. Shimoda<sup>a</sup>, T. Terabayashi<sup>b</sup>, M. Mukaida<sup>b</sup>, T. Makiuchi<sup>a</sup>, Y. Nago<sup>a</sup>, J. Yan<sup>b</sup>, and K. Shirahama<sup>a</sup>

<sup>a</sup>Department of Physics, Keio University, Yokohama 223-8522 Japan

<sup>b</sup>Department of Mechanical Engineering, Keio University, Yokohama 223-8522 Japan

Superfluid <sup>3</sup>He-A is known to exhibit topological properties in a thin slab with thickness of about 1  $\mu\text{m}$ . In such a microscale slab, a chiral symmetry is broken, and spontaneous superfluid mass current has been expected at the edge of the slab<sup>1</sup>. The purpose of our study is to detect the chiral edge current in the A-phase. The device for detecting edge current is a low-frequency torsional oscillator which consists of a OFHC cell with 1  $\mu\text{m}$  thick slab machined by a ultrahigh precision lathe, and two thin BeCu capillaries as torsion rods. The backaction torque produced by spontaneously generated mass current is measured by a SQUID-based displacement sensor. We have assembled the device and tested using liquid <sup>4</sup>He. Current problems and improvements of the device will be discussed.

1. Y. Tsutsumi, T. Mizushima, M. Ichioka, and K. Machida, J. Phys. Soc. Jpn. **79**, 034301 (2010).

## P26.9 Nuclear spin relaxometry of $^3\text{He}$ atoms confined in mesoporous MCM-41

C. Huan<sup>a</sup>, J. Adams<sup>a</sup>, M. Lewkowicz<sup>a</sup>, N. Masuhara<sup>a</sup>, D. Candela<sup>b</sup>, and N.S. Sullivan<sup>a</sup>

<sup>a</sup>Department of Physics and NHMFL, University of Florida, USA

<sup>b</sup>Department of Physics, University of Massachusetts, Amherst, USA

MCM-41 is a unique mesoporous material with cylindrical-like pores, which proves to be an ideal platform to study 1D properties of adsorbed atoms.<sup>1</sup> In this research, we use pulsed NMR technique to measure the nuclear spin-lattice relaxation times ( $T_1$ ) and the nuclear spin-spin relaxation times ( $T_2$ ) at various temperatures. Two different relaxation rates are identified in both  $T_1$  and  $T_2$  results, which suggests two different dynamics for atoms bound at the walls and fluid-like atoms at the cores. We also extend the measurements to dilute  $^3\text{He}$  adsorbed on a  $^4\text{He}$  preplated MCM-41 system in the temperature regime of 0.025-3.0 K, which shows a strong temperature dependence near the expected Fermi degeneracy temperature.

1. Yager, B., et al (2013). "NMR Signature of One-Dimensional Behavior of  $^3\text{He}$  in Nanopores". PRL, 111, 215303.

Work carried out at the National High Magnetic Field Laboratory supported by the NSF-DMR-1644779 and the State of Florida.

## P26.10 Observation of unexpected extended relaxation in dislocation pinning dynamics of solid $^4\text{He}$ with ultra-low $^3\text{He}$ concentrations

Jaeho Shin<sup>†</sup>, Jaewon Choi<sup>‡</sup>, and Eunseong Kim

Department of Physics, KAIST, Daejeon 34141, Republic of Korea

We have measured the shear modulus of hcp solid helium containing ultra-low  $^3\text{He}$  impurities at low temperatures where shear modulus increases significantly. Solid helium made with commercially available UHP  $^4\text{He}$  exhibits fast relaxation to a stiffened state during the cooling. As the  $^3\text{He}$  impurity concentration decreases down to 0.6 ppb, the relaxation time extends substantially. At this  $^3\text{He}$  concentration lower than 300ppb, nominal impurity concentration of UHP  $^4\text{He}$ , the critical strain for softening solid  $^4\text{He}$  shows much weaker  $^3\text{He}$  concentration dependence than predicted by the classical homogeneous pinning mechanisms by  $^3\text{He}$  impurities. We studied novel pinning mechanisms that can explain unexpected relaxation.

<sup>†</sup> present address: Department of Physics, the Pennsylvania State University, PA16802, USA

<sup>‡</sup> present address: Physik Institut, University of Zurich, Switzerland

## P26.11 Thermal resistance of solid $^4\text{He}$ to a classical solid

J. Amrit<sup>a</sup>, A. Ramiere<sup>b</sup>, and S. Volz<sup>c</sup>

<sup>a</sup>LIMSI-CNRS, University of Paris Sud, Rue John von Neumann, 91405, Orsay, France

<sup>b</sup>Dept. of Physics, South University of Science and Technology, Shenzhen 518055, China

<sup>c</sup>LIMMS-CNRS, Institute of Industrial Science, University of Tokyo, Tokyo 153-8505, Japan

Upon solidifying superfluid  $^4\text{He}$  in contact with a Si crystal, a shift in the thermal interface resistance  $R_K$  was observed at the minimum of the melting curve<sup>1</sup>. However, experiments performed at copper/solid  $^4\text{He}$  interfaces<sup>2</sup> did not display this feature. In this study we explain the behavior of  $R_K$  for solid  $^4\text{He}$  in contact with a classical solid. We show the predominance of two independent mechanisms which influence the thermal interface resistance, namely, the resonant scattering of phonons at the interface, as predicted by Adamenko and Fuks<sup>3</sup> for solid/superfluid interfaces, and the flutter mechanism of dislocations due to phonon interactions in solid  $^4\text{He}$ .

1. Ramiere, A., Volz, S. and Amrit, J. (2016). “Thermal resistance at a solid/superfluid helium interface”. *Nat. Mater.* 15, 512.
2. Folinsee, J. and Anderson, A. (1973). “Anomalous Kapitza resistance to Solid Helium”. *Phys. Rev. Lett.* 31, 1580 .
3. Adamenko I. N. and Fuks I. M. (1971). “Roughness and Thermal Resistance of the Boundary between a solid and liquid helium”. *Sov. Phys. JETP* 32, 1123.

## P26.12 Evidence for a solid-to-liquid transition of molecular hydrogen inside pores of solid neon below 1 K.

S. Vasiliev<sup>a</sup>, J. Ahokas<sup>a</sup>, J. Jarvinen<sup>a</sup>, L. Lehtonen<sup>a</sup>, S. Sheludiakov<sup>b</sup>, V. V. Khmelenko<sup>b</sup>, D. M. Lee<sup>b</sup>, and Yu. A. Dmitriev<sup>c</sup>

<sup>a</sup>Department of Physics and Astronomy, University of Turku, 20014 Turku, Finland

<sup>b</sup>Institute for Quantum Science and Engineering, Department of Physics and Astronomy, Texas A&M University, College Station, TX, 77843, USA

<sup>c</sup>Ioffe Institute RAS, 26 Politekhnicheskaya, St. Petersburg 194021, Russian Federation

We report on an electron spin resonance study of atomic hydrogen stabilized in a solid Ne matrices carried out at a high field of 4.6 T and temperatures below 1 K [1]. The films of Ne, slowly deposited on the substrate at the temperature  $\sim 1$  K, exhibited a high degree of porosity. We found that H atoms may be trapped in two different substitutional positions in the Ne lattice as well as inside clusters of pure molecular  $\text{H}_2$  in the pores of the Ne film. The latter type of atoms was very unstable against recombination at temperatures 0.3-0.6 K. Based on the observed nearly instant decays after rapid small increase of temperature, we evaluate the lower limit of the recombination rate constant  $k_r \geq 5 \cdot 10^{-20} \text{ cm}^3\text{s}^{-1}$  at 0.6 K, five orders of magnitude larger than that previously found in the thin films of pure  $\text{H}_2$  at the same temperature. Such behavior assumes a very high mobility of atoms and may indicate a solid-to-liquid transition for  $\text{H}_2$  clusters of certain sizes, similar to that observed in experiments with  $\text{H}_2$  clusters inside helium droplets [2].

1. S. Sheludiakov, *et. al*, *Phys. Rev. B.* **97**, 104108 (2018)
2. Kirill Kuyanov-Prozument and Andrey F. Vilesov, *Phys. Rev. Lett.* **101**, 205301 (2008)



## P26.13 Plastic Deformation in a Quantum Solid: Dislocation Avalanches and Creep in Helium

John Beamish and Zhi Gang Cheng

University of Alberta, Canada

Conventional solids deform elastically for small stresses - reversibly with a linear, rate-independent relationship between stress and strain. Beyond the yield point, plastic deformation begins - irreversible, nonlinear and time dependent. Plasticity involves the motion and multiplication of dislocations and here we report observations of such “metallurgical” phenomena in hcp  $^4\text{He}$ , a solid whose defect behaviour is dominated by quantum effects. Below 0.4 K, there is a strain threshold for elastic deformation above which sudden stress drops and acoustic emissions (AE) appear, the signatures of dislocation avalanches. The dimensions of these slip events range from mm to  $\mu\text{m}$ . At higher temperatures the avalanches are replaced by continuous creep involving dislocations and we observe steady flow at stresses as low as 400 Pa.

Note: Zhi Gang Cheng’s current address: Institute of Physics, Chinese Academy of Sciences, China

## P26.14 Critical Force for Unpinning $^3\text{He}$ from Dislocations in Solid $^4\text{He}$

I. Iwasa

Faculty of Science, Kanagawa University, Japan

Pinning of dislocations by  $^3\text{He}$  impurity atoms affects the mechanical properties of solid  $^4\text{He}$  at low temperatures. Dislocations can be unpinned from the impurities when sufficiently large shear stress is applied. The critical force for unpinning a  $^3\text{He}$  atom,  $F_c$ , has been estimated at first from the amplitude dependence of the torsional oscillator (TO) frequency to be  $F_c = 1.0 \times 10^{-16}$  N,<sup>1</sup> and then from the amplitude dependence of the shear modulus to be  $F_c = 6.8 \times 10^{-15}$  N.<sup>2</sup> The first estimation which was based on the shear stress in the TO cell body may not be correct because the shift of the TO frequency is mainly caused by the change in the shear modulus of solid  $^4\text{He}$  in the torsion rod.<sup>3</sup> We will report a new value of  $F_c$  assuming that the amplitude dependence of the TO frequency is originated from pinning of the dislocations in solid  $^4\text{He}$  in the torsion rod.

1. Iwasa, I., J. Low Temp. Phys. **171**, 30 (2013).
2. Fefferman, A.D. et al., Phys. Rev. **B 89**, 014105 (2014).
3. Beamish, J. et al., Phys. Rev. **B 85**, 180501 (2012).

## P26.15 The superfluid transition in quasi one-dimensional hardcore Bosons: Effect of phase slippage

A. Masaki-Kato<sup>a</sup>, D. Hirashima<sup>b</sup>, and S. Yunoki<sup>a</sup>

<sup>a</sup>Computational Condensed Matter Physics Laboratory, RIKEN, Wako, Saitama 351-0198, Japan

<sup>b</sup>Department of Natural Sciences, International Christian University, Mitaka, Tokyo 180-8585, Japan

In quasi-one dimension (q-1D), superfluidity is rapidly destroyed at finite temperatures with increasing  $L_z$  and the transition temperature also approaches to zero. One may then expect that no superfluid behavior is observed in quasi-1D systems except at extremely low temperatures. However, recent experiments on <sup>4</sup>He in nanopores using a torsional oscillator (TO) have found superfluid behavior at finite temperatures.<sup>1</sup>

We present results of the quantum Monte Carlo simulation of the hardcore Bosons on q-1D lattices under a special boundary condition which suppresses the phase slippage.<sup>2</sup> Actually, we perform simulations using 2D ( $L_x \times L_z$ ) and 3D ( $L_x \times L_x \times L_z$ ) lattice systems with  $L_x \ll L_z$ .

We show that the superfluid density survives up to around the Berezinskii-Kosterlitz-Thouless transition temperature in 2D or the  $\lambda$ -transition temperature in 3D, that is, once phase slippage is suppressed, superfluid density remains finite at finite temperatures. In experiments with a TO, finite superfluid density can then be observed as far as the relaxation time (caused by phase slippage) is longer than the inverse of the frequency of the TO.

1. For example, N. Wada *et al.*, Phys. Rev. Lett. **86**, 4322 (2001); J. Taniguchi *et al.*, Phys. Rev. Lett. **94**, 065301 (2005).

2. K. Yamashita and D. S. Hirashima, Phys. Rev. B **79**, 014501 (2009).

3. A. Masaki-Kato, S. Yunoki, and D. S. Hirashima, in preparation.

## P26.16 Is Superfluid <sup>3</sup>He-A the Precursor to Magnetically Ordered Solid <sup>3</sup>He?

J. J. Wiman and J. A. Sauls

Department of Physics and Astronomy, Northwestern University, USA

Despite our deep understanding of the properties of the phases of superfluid <sup>3</sup>He, we have lacked a quantitative theoretical understanding of the pairing mechanism, phase diagram and thermodynamics of the superfluid phases. Above the polycritical pressure of 21 bar, the A phase is stabilized near  $T_c$ , and separated from the B phase by a pressure and temperature dependent first-order transition. The existence of the A phase requires a pairing theory that goes beyond weak-coupling BCS theory. The “feedback” mechanism of spin-triplet pairing correlations on the spin-fluctuation-mediated pairing interaction provided a model for the stability of the equal-spin-pairing A phase, but does not provide quantitative predictions for the pressure-temperature phase diagram or thermodynamic potential. We present a strong-coupling theory of superfluid <sup>3</sup>He based on quasiparticle interactions that accurately describe the thermodynamic potentials for the A and B phases at all pressures and temperatures below  $T_c(p)$ . Our theory and analysis is based on the next-to-leading order expansion of the free-energy functional beyond weak-coupling BCS theory formulated by Rainer and Serene. We find that the interaction potentials exhibit a broad ferromagnetic spin-fluctuation peak near  $q = 0$ , the key feature of paramagnon theory. We also find resonances corresponding to antiferromagnetic spin-fluctuations and density fluctuations at wavevector  $Q/2k_f = 0.82$ . This wavevector corresponds to a reciprocal lattice vector of bcc solid <sup>3</sup>He at melting pressure. Our results provide both a quantitative strong-coupling theory for the stability of the A phase, and provide new theoretical evidence that liquid <sup>3</sup>He at high pressures is an almost localized Fermi liquid near a Mott transition, and suggest that the equal-spin pairing A phase is the precursor of the UDD phase of solid <sup>3</sup>He.

## P26.17 Size limited fountain effect in superfluid $^3\text{He}$

D. Lotnyk, A. Eyal, N. Zhelev, T.S. Abhilash, M. Terelli, E.N. Smith, and J.M. Parpia

Department of Physics, Cornell University, Ithaca NY 14853, USA

We study the conduction of heat through a rectangular channel (height  $1.1 \mu\text{m} \times 100 \mu\text{m}$  long  $\times 3 \text{mm}$  width) filled with liquid helium-3. The excitations' mean free path exceeds the channel height below a few mK in the normal state. We focus on the superfluid state where heat applied in a small-volume isolated chamber is rapidly coupled at low temperatures through the channel to a second outer chamber cooled by a sintered silver heat exchanger. No such rapid transport is observed in the normal state or at high pressure below the superfluid transition temperature,  $T_c$ , where the mean free path is relatively short. At 0 bar (longest mean free path), we observe rapid heat transport at all temperatures below  $T_c$ . At slightly elevated pressure, we observe the rapid transport near  $T_c$ , but the rapid response decreases sharply below  $T_c$ , reappearing well below  $T_c$ . We presently attribute the rapid transport to superflow toward the heated region (thus increasing the chemical potential and pressure in the isolated chamber) together with slip of the normal fluid fraction in the channel that transports heat to the outer chamber. In the normal state, the lack of superflow excludes the pressure increase and thus there is only diffusive heat flow. Slip only occurs when the mean free path,  $\lambda$ , is much larger than the channel height,  $D$ , so the counterflow is only observed at all temperatures at zero pressure.

## P26.18 Stability and dynamics of HPD in superfluid $^3\text{He-B}$

V. V. Zavjalov, A. M. Savin, and P. J. Hakonen

Low Temperature Laboratory, Aalto University, P.O. Box 15100, FI-00076 AALTO, Finland

Homogeneously precessing domain (HPD) is a coherent state observed in NMR experiments in superfluid  $^3\text{He-B}$ . It is characterized by coherent precession of magnetization with large tilting angle ( $\beta > 104^\circ$ ) stabilized by superfluid spin currents [1]. This state has proven to be a good instrument for studying  $^3\text{He}$  properties. In Ref. [2] two oscillation modes of the HPD have been found theoretically. One of them, a so-called  $\gamma$ -mode, is responsible for HPD parametric instability at low temperatures [3]. A third mode appears in the presence of a radio-frequency field when the HPD is created in continuous-wave NMR [4-5].

At present, we are preparing a precision NMR setup for using HPD as a probe of superfluid coherence across graphene immersed in  $^3\text{He}$ . In this preliminary work, we study HPD in a simple cylindrical cell by means of continuous-wave NMR. We found that under certain conditions the  $\gamma$ -mode directly observed. Its frequency is proportional to the difference between the rf-drive and Larmor frequencies (HPD frequency shift). The proportionality factor depends on the Leggett frequency and changes from  $3/8$  at  $T = T_c$  to  $\approx 0.42$  at high pressure and low temperatures where the Leggett frequency reaches its maximum. We also discuss a process of HPD decay which happens at large values of the frequency shift.

1. I. A. Fomin, *Sov. Phys. JETP*, **61**, 1207 (1985)
2. I. A. Fomin, *Sov. Phys. JETP*, **57**, 1227 (1983)
3. Yu. M. Bunkov, V. S. Lvov, G. E. Volovik, *JETP Lett.*, **83**, 530 (2006)
4. V. V. Dmitriev, V. V. Zavjalov, D. Ye. Zmeev, *J. Low Temp. Phys.*, **138**, 765 (2005)
5. M. Človečko, E. Gažo, M. Kupka, P. Skyba, *Phys. Rev. Lett.*, **100**, 155301 (2008)

## P26.19 Generation of spin current in liquid helium-3

Yasumasa Tsutsumi and Sadamichi Maekawa

RIKEN Center for Emergent Matter Science, Japan

In the field of spintronics, the generation of spin current of electron spins has been investigated extensively. Since effects of mechanical rotation on spin current has been formulated recently,<sup>1</sup> we can expect the generation of spin current in various systems. Indeed, spin current has been generated in a copper film, which has only a weak spin-orbital interaction, by using a surface acoustic wave.<sup>2,3</sup> The generation of spin current by hydrodynamic flows in liquid-metals, Hg and GaInSn, also has been demonstrated.<sup>4,5</sup> This spin hydrodynamic generation will be utilized for generating spin current of nuclear spins in the liquid helium-3. We will demonstrate that a hydrodynamic flow in the liquid helium-3 generates spin current by the vorticity gradient due to a fluid velocity distribution. Note that spin current generation efficiency against the vorticity gradient for nuclear spins is much higher than that for electron spins by three orders of magnitude. We will also discuss detection of the spin current by NMR measurement. Investigations of mechanical generation of spin current in the liquid helium-3, the most well-known Fermi liquid, will be helpful to understand coupling of quasiparticle spins and mechanical rotation microscopically.

1. M. Matsuo, *et al.*, Phys. Rev. Lett. **106**, 076601 (2011).
2. M. Matsuo, *et al.*, Phys. Rev. B **87**, 180402(R) (2013).
3. D. Kobayashi, *et al.*, Phys. Rev. Lett. **119**, 077202 (2017).
4. R. Takahashi, *et al.*, Nature Phys. **12**, 52 (2016).
5. M. Matsuo, *et al.*, Phys. Rev. B **96**, 020401(R) (2017).

## P26.20 Development of Equipment to Observe Majorana Cone at the Surface of Superfluid Helium Three B phase

K. Yoshida<sup>a,b</sup>, S. Yamazaki<sup>a,b</sup>, and S. Murakawa<sup>a,b</sup>

<sup>a</sup>Cryogenic Research Center, University of Tokyo, Japan

<sup>b</sup>Department of Physics, The University of Tokyo, Japan

Superfluid Helium 3-B phase is well known as one of the topological materials, and the surface state is described by Majorana quasi-particles. Also it is believed that such a surface state shows a linear dispersion named Majorana cone. At the surface of superfluid helium 3-B phase, a quantum phenomenon called a quantum Andreev reflection occurs when the excited quasi-particles are incident from the inside of the superfluid surface. The quasiparticle follows back the same path[1], and the reflection rate depends on Surface Density of State (SDOS)[2]. In the electron system, Angle-Resolved Photoemission Spectroscopy (ARPES) is used to measure the dispersion relation, we will measure the relation of the superfluid helium 3-B phase surface state based on the same principle. In order to inject quasi-particles at various angles, we prepare a hemispherical cell with a double shell structure using the principle of blackbody radiation[3]. The two shells, an inside one has a slit and another outside one has pores of various angles, are combined. And a quasiparticle can be shot at an arbitrary angle by rotating the outside. Inside the cell, we insert Quartz Tuning Fork (QTF) for observing momentum flux variation due to Andreev reflection.

We conducted an operation test of the stepping motor used to rotate the above measuring cell in the low temperature region and an experiment of the QTF necessary for the measurement.

- [1] T. Okuda, *et al.*, Phys. Rev. Lett. **80**, 2857(1998). [2] Y. Nagato, *et al.*, J. Low Temp. Phys. **110**, 1135(1998). [3] S. N. Fisher, *et al.*, Phys. Rev. Lett. **69**, 1073 (1992).

## P26.21 Superconductivity in model cuprate as an $S = 1$ pseudomagnon condensation

E. V. Vasinovich, A. S. Moskvin, and Yu. D. Panov

Ural Federal University, Ekaterinburg, Russia

Interest to the  $S = 1$  spin models is associated with the description both of strongly anisotropic magnets based on  $Ni^{2+}$  (conventional spin  $S = 1$ ), in particular  $NiCl_2SC(NH_2)_2$ , and “semi-hard-core” bosons or mixed-valence systems such as the system of charge “triplets”  $Cu^{1+,2+,3+}$  in cuprates<sup>1</sup>. We make use of the  $S = 1$  pseudospin formalism to describe the charge degree of freedom in a model high- $T_c$  cuprate with the on-site Hilbert space reduced to the three effective valence centers, nominally  $Cu^{1+,2+,3+}$ . The effective pseudospin Hamiltonian can be written as a sum of potential and kinetic energies:

$$H_{pot} = \sum_i (\Delta S_{iz}^2 - \mu S_{iz}) + V \sum_{ij} S_{iz} S_{jz},$$

$$H_{kin} = \sum_{ij} [t^p P_{i+} P_{j-} + t^n N_{i+} N_{j-} + \frac{1}{2} t^{pn} (P_{i+} N_{j-} + N_{i+} P_{j-}) - t^b S_{i+}^2 S_{j-}^2 + h.c.],$$

where  $P_{\pm} = \frac{1}{2}(S_{\pm} + T_{\pm})$ ,  $N_{\pm} = \frac{1}{2}(S_{\pm} - T_{\pm})$  and  $T_{\pm} = \{S_z, S_{\pm}\}$ . Starting with a parent cuprate as an analogue of the quantum paramagnet ground state and using the Schwinger boson technique<sup>2</sup> we found the pseudospin spectrum and conditions for the pseudomagnon condensation with phase transition to a superconducting state.

The research was supported by the Government of the Russian Federation, Program 02.A03.21.0006, by the Ministry of Education and Science of the Russian Federation, Projects nos. 2277 and 5719, and by the Competitiveness Enhancement Program - CEP 3.1.1.2-18.

1. A.S. Moskvin // JETP, V. 148(3), 549 (2015).

2. Han-Ting Wang, Yupeng Wang // Physical Review B, V. 71, 104429 (2005).

## P26.22 Orbital angular momentum in chiral superfluids

Yasuhiro Tada

Institute for Solid State Physics, The University of Tokyo, Japan

In fermionic chiral superfluids, the spontaneous orbital angular momentum (OAM) is expected to arise due to broken time reversal symmetry. Although the study on the OAM in chiral superfluids has a long history, it has been a paradoxical problem and is not well understood still now. In fact, the recent mean field studies suggest that OAM in a chiral superfluid depends on boundary conditions and shapes of a system, which would be rather counter-intuitive. We propose a simple physical description on the sensitivity of OAM within a mean field approximation, and demonstrate that the mean field results are essentially correct by a density matrix renormalization group calculation. Furthermore, we point out that these results do not contradict the standard thermodynamics, because there is no intensive external field conjugate to OAM with which a uniform superfluid can be realized.

1. Tada, Y. arXiv:1805.11226.

## P26.23 Charging effects around single vortex in chiral p-wave superconductor

Y. Masaki<sup>a</sup> and Y. Kato<sup>b</sup>

<sup>a</sup>Research and Education Center for Natural Science, Keio University

<sup>b</sup>Department of Basic Science, The University of Tokyo

We study the charging effects around a single vortex of chiral p-wave superconductors using an augmented quasiclassical theory. Chiral p-wave superconductors have two non-equivalent vortices in terms of the relative directions between vorticity and chirality of the Cooper pair; One is charged and the other is uncharged. We found that charged vortex has relatively large charge density compared with s-wave superconducting vortex. This is because the presence of the induced component of the order parameter. The validity of our scheme is investigated through the comparison with BdG theory and force balance relation in the asymptotic region. We also show the local density of states with asymmetric spectrum.

## P26.24 Theory of thermal expansion of chiral p-wave superconductors

R. Konno<sup>a</sup>, U. Kohara<sup>a</sup>, M. Nakamori<sup>a</sup>, and N. Hatayama<sup>a</sup>

<sup>a</sup>Kindai University Technical College, Japan

<sup>b</sup>Department of Physics, Dhaka University, Dhaka, Bangladesh

We investigated thermal expansion of chiral p-wave superconductors<sup>1</sup> near the superconducting transition temperature  $T_{sc}$  by using Ginzburg and Landau expansion of the free energy. Takahashi's theory<sup>2</sup> was used in order to obtain thermal expansion. We find that thermo-dynamic Gruneisen's relation is satisfied theoretically near  $T_{sc}$ . It is found that the thermal expansion coefficient has  $T$ -linear dependence near  $T_{sc}$ . Although the s-electron conduction band had been used in high  $T_{sc}$  superconductors theoretically, the wave number dependence of the static spin susceptibility at  $T=0K$  was studied by using the  $d_{x^2-y^2}$  conduction band.

1. Sato, M and Fujimoto, S. J. Phys. Soc. Jpn. 85, 072001, (2016) and references therein.
2. Takahashi, Y. (2013). "Spin Fluctuation Theory of Itinerant Electron Magnetism", Springer, and references therein.

## P26.25 Influence of Magnetic Domain Structure on the Ferromagnetic Superconductivity of $\text{UGe}_2$

A. Yamaguchi<sup>a</sup>, H. Tanaka<sup>a</sup>, T. Kotani<sup>a</sup>, G. Motoyama<sup>b</sup>, I. Kawasaki<sup>c</sup>, A. Sumiyama<sup>a</sup>, and T. Yamamura<sup>d</sup>

<sup>a</sup>Graduate School of Material Sciences, University of Hyogo, Japan

<sup>b</sup>Interdisciplinary Faculty of Science and Engineering, Shimane University, Japan

<sup>c</sup>Japan Atomic Energy Association, Japan

<sup>d</sup>Institute for Integrated Radiation and Nuclear Science, Kyoto University, Japan

We have recently carried out ac magnetic susceptibility measurement for a ferromagnetic superconductor  $\text{UGe}_2$  in different magnetized states, in temperature below 1 K and at pressure of 1.15 GPa.<sup>1</sup> It was revealed that the superconducting ac response depends on the magnetized state in high ac amplitude region, indicating superconducting ac shield ability is affected by presence of magnetic domain walls. The shielding ability seems to be enhanced by the emergence of the domain walls, and the observation would contradict the theory that regards them as weak links. Possible explanation for the enhancement will be presented.

1. H. Tanaka, A. Yamaguchi, I. Kawasaki, A. Sumiyama, G. Motoyama, and T. Yamamura, Phys. Rev. B 97, 020509(R) (2018).

## P26.26 Multiband superconductivity in $\text{PrPt}_4\text{Ge}_{12}$ probed by thermal transport

A. M. Strydom and D. Britz

Highly Correlated Matter Research Group, Physics Department, University of Johannesburg, PO Box 524, Auckland Park 2006, South Africa

Thermal conductivity  $\kappa(T)$  has been used as a direct probe into the superconducting gap morphology in conventional, correlated and multiband superconducting compounds [1]. The defining feature of nodal superconductors is their finite density of electronic states at  $T = 0$  within the superconducting state, caused by the superconducting gap vanishing at points on the Fermi surface. We present thermal conductivity data as function of temperature and applied magnetic field on the two cubic skutterudite compounds  $\text{PrPr}_4\text{Ge}_{12}$  ( $T_c = 7.9$  K) and  $\text{LaPt}_4\text{Ge}_{12}$  ( $T_c = 8$  K). We show that  $\text{PrPt}_4\text{Ge}_{12}$  is a nodal superconductor by comparison to  $\text{LaPt}_4\text{Ge}_{12}$  which is a conventional isotropically gapped superconductor [2]. The highly debated multiband nature of the superconducting state in  $\text{PrPt}_4\text{Ge}_{12}$  [3] we investigate by zero-field and low-field thermal conductivity measurements. Different characteristic regions in the thermal conductivity data below  $T_c$  provide compelling evidence for the existence of multiple superconducting states, similar to the thermal conductivity data reported in the well-known multiband superconductor  $\text{PrOs}_4\text{Sb}_{12}$  [4].

1. Shakeripour H., Petrovic C, and Taillefer L. (2009) New J. Phys **11** 055065.
2. Gumenuik R. *et al.* (2008) Phys. Rev. Lett. **100** 017002.
3. Zhang J.L. *et al.* (2013) Phys. Rev. B **87** 064502.
4. Seyfarth G. *et al.* (2006) Phys. Rev. Lett. **97** 236403.

## P26.27 Doping dependence of the local electronic structures around a nonmagnetic impurity in BiS<sub>2</sub>-based superconductors

Yun Liu and Bin Liu

Department of Physics, Beijing Jiaotong University, Beijing, China

In a superconductor, the crucial requirement is to confirm the symmetry of the superconducting (SC) state, since the understanding of the pairing symmetry will help to reveal the underlying SC mechanism. In this paper, we use local electronic structure around a single nonmagnetic impurity to probe the pairing symmetry in recently discovered BiS<sub>2</sub>-based superconductors, where no general consensus on the pairing symmetry has been reached so far. We find that the effect from a single nonmagnetic impurity scattering on the SC state with the conventional *s*-wave, the extended *s*-wave, the  $\pm s$ -wave, and the  $d_{x^2-y^2}$ -wave symmetries may induce qualitatively different resonance states as a result of unique nodal structures on the different FS topology with doping. Since these impurity induced resonance states can be verified directly by the scanning tunneling microscopy (STM) experiments, they are proposed as a test of the SC pairing symmetry in BiS<sub>2</sub>-based superconductors.

## P26.28 Even- and Odd-Frequency Superconductivity in Q1D Organic Superconductors under Magnetic Field

K. Fukui<sup>a</sup> and Y. Kato<sup>b</sup>

<sup>a</sup>Department of Physics, The University of Tokyo, Japan

<sup>b</sup>Department of Basic Science, The University of Tokyo, Japan

One of the organic superconductors (TMTSF)<sub>2</sub>X, called Bechgaard salts, have attracted a lot of interest since its discovery in 1980.<sup>1</sup> These compounds have high critical magnetic field  $H_{c2}$  in the direction parallel to the layers and their pairing symmetry seems to be different between low-field phase and high-field phase. In addition, recently, possibility of the realization of odd-frequency superconductivity was pointed out<sup>2,3</sup>. Therefore, we study pairing symmetry of Bechgaard salts under magnetic field with frequency-dependent pairing interaction due to spin and charge fluctuation. The model is given by the extended Hubbard model on a quasi-one-dimensional square lattice and the spin susceptibility and charge susceptibility for the effective pairing interactions are derived by random phase approximation under magnetic field. The theoretical scheme we use was introduced in our previous paper.<sup>4</sup>

1. K. Bechgaard *et al.*, Solid State Commun. **33**, 1119 (1980).
2. F. L. Pratt *et al.*, Phys. Rev. Lett. **110**, 107005 (2013).
3. K. Shigeta, S. Onari, and Y. Tanaka, J. Phys. Soc. Jpn. **82**, 104702 (2013).
4. K. Fukui and Y. Kato, J. Phys. Soc. Jpn. **87**, 014706 (2018).



## P26.29 Phase transition from Weyl to node-line superfluid: Antispacetime and novel effective electrodynamics

J. Nissinen<sup>a</sup> and G. E. Volovik<sup>a,b</sup>

<sup>a</sup>Low Temperature Laboratory, Aalto University, Finland

<sup>b</sup>Landau Institute for Theoretical Physics, Chernogolovka, Russia

In the topological classification of matter, symmetry protected node lines in the fermionic spectrum form a new phase of matter: A gapless 3d Fermi system with a stable line of zeroes. New physics arises from the massless nodal-line quasiparticle excitations: In the vicinity of a node-line or node, the low-energy fermions are quasirelativistic and couple to effective electromagnetic (EM) gauge fields and gravitational tetrads, giving rise to dimensional crossover phenomena in the effective EM and geometric response.

Thanks to the recent discovery of new phases of superfluid <sup>3</sup>He in nanoconfinement, it is experimentally feasible to make a continuous transition from a Weyl superfluid with point nodes (A-phase) to a node-line superfluid (polar phase) and back. We consider the fate of the low-energy fermions in this transition and predict that upon approaching the polar phase, the original Weyl superfluid experiences a crossover to a non-analytic effective EM response due to the node line<sup>1</sup>. The transition is accompanied by relativistic quantum field theory anomalies related to the discrete symmetries of parity and time-reversal for the effective electrodynamics and gravitational tetrads (a.k.a. “antispacetime”).

We propose that these effects could be experimentally accessible by manipulating the order parameter textures in polar distorted phases of superfluid <sup>3</sup>He.

1. Nissinen, J. and G.E. Volovik (2018). “Dimensional crossover of effective orbital dynamics in polar distorted <sup>3</sup>He-A: Transitions to antispacetime”. *Phys. Rev. D* **97**, 025018.

## P26.30 Disorder-dressed evolution in edge-mode transport and beyond

C. Gneiting<sup>a</sup> and F. Nori<sup>b</sup>

<sup>a</sup>RIKEN, Wako-shi, Saitama, Japan

<sup>b</sup>RIKEN, Wako-shi, Saitama, Japan and University of Michigan, Ann Arbor, Michigan, USA

The possibility of backscattering-free transport in topological insulators renders them promising candidates for applications in quantum information processing, where reliable transmittance of quantum states is a prerequisite for successful implementations. However, while edge states are robust against backscattering, they are not immune to disorder effects such as dephasing, posing potential obstacles to their successful deployment as carriers of quantum information. We analyze disorder-induced dephasing and related effects in backscattering-free quantum transport. To this end, we present a method to formulate disorder-dressed evolution equations, which allows us to interpret disorder in analogy to a quantum environment. As we argue, this method can also be applied to describe—and understand—the impact of disorder on, e.g., the stability of flat bands or spin-dependent edge propagation.

1. C. Gneiting, F. Nori. “Quantum evolution in disordered transport”. *PRA* 96, 022135 (2017).
2. C. Gneiting, F. Nori. “Disorder-induced dephasing in backscattering-free quantum transport”. *PRL* 119, 176802 (2017).
3. C. Gneiting, Z. Li, F. Nori. “Lifetime of flatband states”. arXiv:1803.00813.

## P26.31 Decoherence-free interaction between giant atoms in waveguide QED

A. F. Kockum<sup>a</sup>, G. Johansson<sup>b</sup>, and F. Nori<sup>a</sup>

<sup>a</sup>Theoretical Quantum Physics Laboratory, RIKEN, Saitama 351-0198, Japan

<sup>b</sup>MC2, Chalmers University of Technology, SE-412 96 Gothenburg, Sweden

In quantum-optics experiments with both natural and artificial atoms, the atoms can usually be approximated as point-like compared to the wavelength of the electromagnetic radiation they interact with. However, superconducting qubits coupled to a meandering transmission line, or to surface acoustic waves<sup>1,2</sup>, can realize “giant artificial atoms” that couple to a bosonic field at several points which are wavelengths apart<sup>3,4</sup>. Here, we study setups with multiple giant atoms coupled at multiple points to a one-dimensional (1D) waveguide<sup>5</sup>. We show that the giant atoms can be protected from decohering through the waveguide, but still have exchange interactions mediated by the waveguide. Unlike in decoherence-free subspaces, here the entire multi-atom Hilbert space is protected from decoherence. This is not possible with “small” atoms. We further show how this decoherence-free interaction can be designed in setups with multiple atoms to implement, e.g., a 1D chain of atoms with nearest-neighbor couplings or a collection of atoms with all-to-all connectivity. This may have important applications in quantum simulation and quantum computing.

1. M. V. Gustafsson *et al.*, *Science* **346**, 207 (2014).
2. R. Manenti *et al.*, *Nat. Commun.* **8**, 975 (2017).
3. A. F. Kockum *et al.*, *Phys. Rev A* **90**, 013837 (2014).
4. L. Guo *et al.*, *Phys. Rev. A* **95**, 053821 (2017).
5. A. F. Kockum *et al.*, *Phys. Rev. Lett.* **120**, 140404 (2018).

## P26.32 <sup>3</sup>He Purification System with an Acoustic Cavity for Purity Monitoring

Y. Lee, W. G. Jiang, C. B. Perez, C. S. Barquist, and B. Popovic

Department of Physics, University of Florida, Gainesville, USA

A system for helium extraction and purification (SHeEP) is constructed to remove <sup>4</sup>He contamination from <sup>3</sup>He gas, utilizing a chromatographic cylinder filled with activated charcoal.<sup>1</sup> For the purpose of monitoring the progress of purification, an acoustic cavity is designed that determines the average atomic mass of the mixture by measuring the speed of sound.<sup>2,3</sup> It is estimated to have a sensitivity of  $\approx 0.04\%$ , and provides a cheap and simple alternative to a mass spectrometer. We will discuss detailed design and the performance of the purification system and the acoustic cavity.

This work is supported by the National Science Foundation through DMR-1708818.

1. Dmitriev, V. V. (2004). “Purification of <sup>3</sup>He from a <sup>4</sup>He impurity using adsorption”. *Instrum. Exp. Tech. (USSR)* **47**, 567-569.
2. Kagiwada, R. S., and Rudnick, I. (1970). “Note on a simple method for determining the isotopic concentration of a <sup>3</sup>He-<sup>4</sup>He gas”. *J. Low Temp. Phys.* **3**, 113.
3. Lin, H., *et al.* (2013). “Improved determination of the Boltzmann constant using a single fixed-length cylindrical cavity”. *Metrologia* **50**, 417-432.

## P26.33 Chasing microkelvin electron temperatures in nanoelectronics

S. Autti<sup>a</sup>, D. I. Bradley<sup>a</sup>, A. M. Guénault<sup>a</sup>, D. Gunnarsson<sup>b</sup>, R. Haley<sup>a</sup>, H. Heikkinen<sup>b</sup>, S. Holt<sup>a</sup>, A. Jones<sup>a</sup>, S. Kafanov<sup>a</sup>, Y. Kalyoncu<sup>c</sup>, D. Maradan<sup>c</sup>, M. Palma<sup>c</sup>, Y. Pashkin<sup>a</sup>, J. Penttilä<sup>d</sup>, J. Prance<sup>a</sup>, M. Prunnila<sup>b</sup>, L. Roschier<sup>d</sup>, M. Sarsby<sup>a</sup>, C. Scheller<sup>c</sup>, D. Zmееv<sup>a</sup>, and D. Zumbühl<sup>c</sup>

<sup>a</sup>Lancaster University, Department of Physics, Lancaster University, Lancaster, LA1 4YB, UK

<sup>b</sup>VTT Technical Research Centre of Finland Ltd, P.O. Box 1000, 02044, VTT, Espoo, Finland

<sup>c</sup>Department of Physics, University of Basel, Klingelbergstrasse 82, CH-4056 Basel, Switzerland

<sup>d</sup>Aivon Oy, Valimotie 13A, 00380 Helsinki, Finland

It has been a longstanding challenge to cool electrons in nanoelectronic devices to a few millikelvin and then further into the elusive microkelvin regime. Those trying to build quantum computers, for instance, are likely to embrace any accessible cooling method capable of providing such temperatures. In this presentation we briefly review some of the best schemes implemented so far, and discuss ways to integrate them. We demonstrate our approach by cooling a Coulomb blockade thermometer, which allows measuring the electron temperature directly and unambiguously. We used a custom Lancaster fridge which achieves a base-temperature of 2.5 mK, and by immersing the device in the helium mixture we improve the thermal contact sufficiently to achieve a base electron temperature of 3.7 mK. To cool the electrons further below the host lattice temperature, one can use an on-chip demagnetisation stage which consists of microscopic copper islands [1,2] on a non-immersed device. Our implementation of this design requires minimal changes to any standard dilution refrigerator. It remains a task for the future to show that such cooling results in quantum devices that function better, or even entirely new physics.

[1] Sci. Rep. 7, 45566 (2017)

[2] Appl. Phys. Lett. 111, 253105 (2017)

## P26.34 Direct Measurement of Effectiveness of Silver Sinter with Different Boundary Conditions

S. Autti<sup>a</sup>, A.M. Guénault<sup>a</sup>, R.P. Haley<sup>a</sup>, A. Jennings<sup>a</sup>, S. Kafanov<sup>a</sup>, G.R Pickett<sup>a</sup>, R. Schanen<sup>a</sup>, A.A. Soldatov<sup>b</sup>, V. Tsepelin<sup>a</sup>, and D.E. Zmееv<sup>a</sup>

<sup>a</sup>Department of Physics, Lancaster University, UK

<sup>b</sup>P.L. Kapitza Institute for Physical Problems of Russian Academy of Sciences, Moscow, Russia

The mechanism of heat transfer between superfluid <sup>3</sup>He-B and sintered metal is still an open problem in low temperature physics. We present direct measurement of the effectiveness of sintered silver in cooling <sup>3</sup>He with two different boundary conditions: in pure <sup>3</sup>He versus the sinter covered by approximately two layers of solid <sup>4</sup>He. We created a heat pulse by movement of a large wire and we then measured the thermal response of nearby vibrating wire and tuning fork thermometers. Measurements took place in the ballistic regime of <sup>3</sup>He-B below 0.25T<sub>c</sub>. Comparing the different boundaries shows that the presence of solid <sup>4</sup>He on the surface leads to a doubling of the boundary resistance. This is consistent with the idea that magnetic channel of energy transfer formed when solid <sup>3</sup>He is adsorbed on the surface of the sinter plays an important role.<sup>1</sup> No temperature dependence of the effectiveness was seen with either of the boundary conditions, indicating the Kapitza resistance in the ballistic regime is proportional to the quasi-particle density.<sup>2</sup>

1. R. Konig *et al.*, J. of Low Temp. Phys. **113**, 969 (1998).

2. C.A. Castelijns *et al.*, Phys. Rev. Lett. **55**, 2021 (1985).

## P26.35 **Developing high sensitive gyroscope to detect angular momentum of $^3\text{He-A}$ in slab geometry**

J. Jeong<sup>a</sup>, H. Byun<sup>a</sup>, S. Kim<sup>c</sup>, S. Sim<sup>b</sup>, J. Suh<sup>b</sup>, and H. Choi<sup>a</sup>

<sup>a</sup>Department of Physics, KAIST, Daejeon, Korea

<sup>b</sup>Korea Research Instituted for Standard and Science, Daejeon, Korea

<sup>c</sup>IBS, Daejeon, Korea

As a prototypical Weyl superconductor,  $^3\text{He-A}$  is expected to carry a chiral edge current of Majorana fermions when confined in a (quasi) two dimensional slab geometry. This chiral current contributes to a ground state intrinsic angular momentum exact value of which has been controversial for more than 40 years. Recent theoretical estimates seem to be resolving the angular momentum paradox as the estimates converge to  $N\hbar/2$  consistently. The experimental measurement of this value is still of great challenge and we are developing micro-machined planar gyroscopes which have angular momentum sensitivity about  $10^{14}\hbar$ . We present the design and performance of our gyroscope and discuss the outlook of the device development in the future.

## P26.36 **Research Activity for New Types of Superfluidity by a NPO**

M. KUBOTA, T. AOKI, Y. CHIZAKI, S. GOTOH, S. HARADA, Y. HIRESAKI, M. IKEUCHI, Y. KATO, T. SHIGEMATSU, H. SUZUSHIKA, K. TOZAKI, and H. UEDA

NPO(Non Profit Organization) Institute for New Types of Superfluidity, Hachioji, Tokyo, Japan

We present the aim and the research activities of a NPO, Institute for New Types of Superfluidity. This movement was originally started from an internal group activity encouraged by Cryogenics and Superconductivity Society of Japan as a "Chosa KenkyuKai (Study Group)" in March 2013. After 3 years of preparation with such a support, we established a Non Profit Organization "Institute for New Types of Superfluidity" in 2015. The members are from researchers in universities or companies where some low temperature activities as well as school teachers and management or other duties in private companies, who are eager to pursuit activities of the NPO Institute for New Types of Superfluidity. Research activity is one of the four activity fields of the present NPO and the financial resources are limited to membership fees and donations by law. We are starting up a laboratory, basically, using closed cycle He refrigerator to produce low temperatures. Essential tools to study superfluidity are various kinds of oscillators. And we have been studying the influence of the vibrations from the pulsed tube refrigerator and other vibration sources<sup>1</sup>. We discuss as to what could be studied for the vortex physics in hcp  $^4\text{He}$ ,<sup>2</sup> as well as H(D) in PdH(D)<sub>x</sub> systems<sup>3</sup>.

1. Harada S., Aoki T., Ikeuchi M., Ueda H., Kato Y., Kubota M., Sigematsu T., Suzushika H., Chizaki Y., Tozaki K., Hiresaki Y., Proc. Cryogenics & Superconductivity Society Japan Spring Meeting 2017. p.48, "Various mechanical Oscillator techniques for new types of superfluidity study and pulse tube refrigerator I". 2. Kubota M. J. Low Temp Phys., vol.169 (2012) 228. 3. Harada S., et al. ibid, 162 (2011) 724.

**July 27 (Friday)**



# July 27 (Friday) Oral Presentations

## O27.1 Topological Defects and Phase Transitions

J. Michael Kosterlitz

Department of Physics, Brown University, Providence, RI 02912

This talk reviews some of the applications of topology and topological defects in phase transitions in two-dimensional systems for which Kosterlitz and Thouless split half the 2016 Physics Nobel Prize. The theoretical predictions and experimental verification in two dimensional superfluids, superconductors and crystals will be reviewed because they provide very convincing quantitative agreement with topological defect theories.

PLENARY TALK

## O27.2 The Road to the KT Transition; Experiments with Thin $^4\text{He}$ Films

John D. Reppy

Laboratory of Atomic and Solid State Physics, Cornell University, Ithaca NY 14851, USA.

The study of the properties of  $^4\text{He}$  films adsorbed on a variety of substrates allows an insight into the influence of topology on the nature of superfluidity in two and three-dimensional systems. A variety of experimental techniques have been applied in these studies, including persistent current, 3rd sound, vibrating microbalance, heat capacity, and torsional oscillator measurements. Of particular interest here will be the physical realization of the Berzinskii-Kosterlitz-Thouless transition for  $^4\text{He}$  films adsorbed on 2-D substrates as demonstrated in microbalance, 3rd sound and torsional oscillator measurements. Although the original description of the superfluid transition for thin  $^4\text{He}$  films, as given by Kosterlitz and Thouless, applies to the static case, their approach can be extended to the dynamic situation appropriate for the actual experimental measurements. The temperature dependence of the dissipation and superfluid mass of the 2-D  $^4\text{He}$  film, such as observed in torsional oscillator measurements, provides excellent agreement with the predictions of the dynamic KT theory.

PLENARY TALK

### O27.3 Spin liquid, Mott transition and BEC-BCS crossover exhibited by interacting electrons on triangular lattices

K. Kanoda

Department of Applied Physics, University of Tokyo, Japan

The interacting spins on geometrically frustrated lattices may exhibit non-trivial magnetic states called spin liquids. The triangular lattice is the representative of such stages.<sup>1</sup> In this symposium, after briefly reviewing the experimental status of the spin-liquid research, I focus on interacting electrons in organic materials with triangular lattices, which provided the first example of electronic spin liquid. I discuss anomalous spin excitations observed in a spin liquid<sup>1</sup> and their possible relevance to the peculiar Mott transition of the spin liquid.<sup>2</sup> Remarkably, an antiferromagnetic order in a less frustrated material, when X-ray irradiated, disappears and gapless spin excitations emerge.<sup>3</sup> Randomness appears to act for rather than against the emergence of the spin liquid. This issue will be theoretically discussed by Kawamura in this symposium. I also talk about a triangular-lattice material, in which a half-filled band is 11% hole doped. Spin susceptibility is nearly perfectly scaled to that of a non-doped spin liquid insulator in spite of a metallic state, indicating the realization of a doped spin liquid.<sup>4</sup> This material undergoes superconductivity, which shows a pressure-induced BEC-BCS crossover. The work presented here was performed in collaboration with T. Furukawa, H. Oike, J. Ibuka, M. Urai, Y. Suzuki, Y. Seki, K. Miyagawa, Y. Shimizu, M. Ito, H. Taniguchi and R. Kato, M. Saito, S. Iguchi and T. Sasaki.

1. Y. Zhou, K. Kanoda, and T.-K. Ng: *Rev. Mod. Phys.* **89**, 025003 (2017). 2. T. Furukawa *et al.*: *Nature Commun.* **9**, 307 (2018). 3. T. Furukawa *et al.*: *Phys. Rev. Lett.* **115**, 077001 (2015). 4. H. Oike *et al.*: *Nature Commun.* **8**, 756 (2017); *Phys. Rev. Lett.* **114**, 067002 (2015).

PLENARY TALK

### O27.4 Randomness-Induced Quantum Spin Liquids in Frustrated Magnets: Application to 2D <sup>3</sup>He and Organic Salts

H. Kawamura

Graduate School of Science, Osaka University, Japan

Experimental quest for the hypothetical “quantum spin liquid (QSL)” state recently met several promising candidate materials on geometrically frustrated lattices such as triangular and kagome lattices. Its first realization might be the nuclear spins in the second-layer solid <sup>3</sup>He adsorbed on graphite, which can be viewed as the  $s = 1/2$  Heisenberg triangular-lattice system possessing a considerable amount of multiple spin exchange. A gapless QSL behavior accompanied by the temperature ( $T$ )-linear specific heat was observed there. More recently, similar gapless QSL behaviors are observed in several frustrated antiferromagnets including the triangular organic salts  $\kappa$ -(ET)<sub>2</sub>Cu<sub>2</sub>(CN)<sub>3</sub> and EtMe<sub>3</sub>Sb[Pd(dmit)<sub>2</sub>]<sub>2</sub>, and the kagome herbertsmithite CuZn<sub>3</sub>(OH)<sub>6</sub>Cl<sub>2</sub>. We have argued that these compounds might contain significant amount of (effective) randomness or inhomogeneity, and this randomness or inhomogeneity might be essential in realizing the experimentally observed QSL behaviors. The origin of the effective randomness or inhomogeneity could be of variety: the disordered arrangement of <sup>3</sup>He atoms in 2D <sup>3</sup>He, the freezing of the charge (dielectric) degrees of freedom in triangular organic salts, and the Zn<sup>2+</sup>/Cu<sup>2+</sup> intersite disorder in herbertsmithite. We model these magnets by the random-bond  $s=1/2$  Heisenberg model on geometrically frustrated 2D lattices, *e.g.*, the triangular lattice, numerically compute various physical quantities by the exact-diagonalization method, and demonstrate that, when the randomness exceeds a critical value, the model generically exhibits a randomness-induced gapless QSL-like state, a “random-singlet state”. The results seem to provide a consistent explanation of the recent experimental observations on 2D <sup>3</sup>He and organic salts.

INVITED TALK

## O27.5 New Quantum Spin Liquids in $^3\text{He}$ Monolayer on Hydrogen Plated Graphite

M. Kamada<sup>a</sup>, R. Nakamura<sup>a</sup>, K. Ogawa<sup>a</sup>, T. Matsui<sup>a</sup>, and Hiroshi Fukuyama<sup>a,b</sup>

<sup>a</sup>Department of Physics, The University of Tokyo, Japan

<sup>b</sup>Cryogenic Research Center, The University of Tokyo, Japan

We have found two different types of new quantum spin liquids (QSLs) in  $^3\text{He}$  monolayer adsorbed on graphite preplated with a bilayer of HD from specific heat ( $C$ ) measurements down to 0.3 mK. One of them was observed in a newly found commensurate (C3) phase which exists within a narrow density span (1%) centered  $4.74 \text{ nm}^{-2}$ . This phase must be stabilized by a large corrugation amplitude with a long periodicity of the adsorption potential due to the HD underlayer ( $9.1 \text{ nm}^{-2}$ ). It shows a curious  $T$ -dependence of  $C$  with a fractional power like  $C \propto T^{2/3}$  in the low- $T$  limit ( $T \leq 7 \text{ mK}$ ) below a broad peak around 20 mK. We notice that the magnetic susceptibility ( $\chi$ ) measured previously by other workers<sup>1</sup> also shows a curious  $T$ -dependence like  $\chi \propto T^{-1/3}$  down to 0.01 mK near the C3 phase. Therefore, even the Wilson ratio can be defined as  $R_W \approx 8$ . Unknown magnetic excitations in this QSL, if they exist, seem to obey an unusual dispersion of  $\epsilon \propto k^3$ . As the  $^3\text{He}$  density increases further, the other type of QSL (C2-like phase) emerges from the C3 phase through a first order transition. The C2-like phase is a highly compressible single phase where, upon a compression by 20%,  $C(T/J)$  falls on a universal curve with an even broader peak near  $T/J = 0.4$  and the characteristic exchange interaction ( $J$ ) reduces by a factor of 10. At the lowest  $T$ ,  $C$  varies as  $C \propto T$  here. These features resemble those of the C2 phase, a quantum liquid crystal phase proposed for the second layer of  $^3\text{He}$  on graphite.<sup>2</sup> The random distribution of  $J$  expected in quantum liquid crystal may play an essential role in the C2 and C2-like phases.

1. Masutomi *et al.*, PRL **92**, 025301 (2004).    2. S. Nakamura *et al.*, PRB **91**, 180501(R) (2016).

INVITED TALK

## O27.6 Helium in two dimensions and under nano-scale confinement: realizing quantum materials and topological mesoscopic superfluidity

F. Arnold<sup>a</sup>, A. Casey<sup>a</sup>, B. Cowan<sup>a</sup>, P. Heikkinen<sup>a</sup>, L. Levitin<sup>a</sup>, J. Nyeki<sup>a</sup>, J. Parpia<sup>b</sup>, X. Rojas<sup>a</sup>, A. Waterworth<sup>a</sup>, N. Zhelev<sup>a</sup>, and J. Saunders<sup>a</sup>

<sup>a</sup>Department of Physics, Royal Holloway University of London, U.K

<sup>b</sup>LASSP, Cornell University, U.S.A.

The study of helium allows us to address central questions in the field of strongly correlated quantum systems. Atomically layered helium films and helium confined in precisely engineered nanostructures are two complementary approaches. Helium films on graphite demonstrate: a Wigner-Mott-Hubbard transition into a putative quantum spin liquid; a heavy fermion state with quantum criticality; intertwined superfluid and density wave order; ideal 2D frustrated ferromagnetism. Does the Landau Fermi liquid survive in 2D? To address this question we can study  $^3\text{He}$  in surface states atop a superfluid  $^4\text{He}$  film. This provides a model coupled fermion-boson system, which we have probed by SQUID NMR to well below 1 mK. In the second approach we have made NMR studies of superfluid  $^3\text{He}$  confined in thin cavities of height ranging from one micron down to 100 nm. This work has demonstrated the profound influence of confinement on the phase diagram, and the ability to tune the surface scattering. We also find evidence for the stabilization of a spatially modulated superfluid phase, an FFLO-like state, but with two-dimensionally modulated superfluid order. Such precisely engineered nanoscale confinement opens up the field of topological mesoscopic superfluidity. Structures, with confinement as the control parameter, can be used to create new “materials” and high quality interfaces between them, for the study of emergent surface excitations.

PLENARY TALK



## O27.7 The solid-to-hexatic quantum melting phase transition

A.J. Beekman

Department of Physics, Keio University, Hiyoshi, Yokohama, Japan

In the 1970s Nelson, Halperin and Young wrote down the theory of melting of two-dimensional solids as an unbinding of dislocation topological defects, following the vortex-unbinding transition by Kosterlitz and Thouless. This led to the prediction of a phase with translational symmetry but rotational rigidity which they called the *hexatic*.

Here we consider the two-dimensional solid-to-hexatic zero-temperature *quantum* phase transition as a Bose–Einstein condensation of dislocations.<sup>1</sup> We employ a duality transformation where the phonons of the solid phase are represented by gauge fields, which mediate the interactions between dislocations. When dislocations condense, the gauge field related to shear becomes gapped, indicating the loss of shear rigidity in the hexatic. At the same time, a Nambu–Goldstone mode related to rotational symmetry breaking emerges once translational symmetry is restored.

I will also present some preliminary results on the critical properties of this quantum phase transition. This ties in to recent specific heat measurements showing evidence for the quantum hexatic phase in helium monolayers on a graphite substrate.<sup>2</sup>

1. A.J. Beekman, J. Nissinen, K. Wu, K. Liu, R.-J. Slager, Z. Nussinov, V. Cvetkovic. J. Zaanen. Phys. Rep. 683, 1 (2017).

2. S. Nakamura, K. Matsui, T. Matsui, H. Fukuyama. Phys. Rev. B 94, 180501 (2016).

INVITED TALK

## O27.8 Anomalous superfluid response in the second layer <sup>4</sup>He films adsorbed on graphite

Jaewon Choi<sup>†</sup>, Oleksiy Zadorozhko<sup>‡</sup>, Jeakyung Choi, and Eunseong Kim

Department of Physics, KAIST, Daejeon 34141, Republic of Korea

We investigated the superfluid response of the second layer of <sup>4</sup>He adsorbed on the atomically flat surface of graphite by using a double resonance torsional oscillator (TO). Crowell and Reppy [1] reported first reentrant superfluidity in the second layer of <sup>4</sup>He films adsorbed on Grafoam, which was reproduced recently [2, 3]. Both experiments suggest the existence of a possible 2D supersolid phase, although an ab initio Monte Carlo simulation disagrees with the interpretation [4]. Because a single resonance TO cannot distinguish the genuine superfluidity from the elasticity dependent response, we investigated <sup>4</sup>He on graphite by utilizing a TO with two different resonant frequencies. We found no frequency dependent TO response that can be attributed to the rigidity change in the 2<sup>nd</sup> layer helium films on graphite. Instead, frequency independent response, the evidence of superfluidity, appeared with a dissipation peak.

<sup>†</sup> present address: Physik Institut, University of Zurich, Switzerland

<sup>‡</sup> present address: Quantum Dynamics Unit, OIST, Okinawa, Japan

[1] P. A. Crowell and J. D. Reppy, Phys. Rev. B 53, 2701 (1996).

[2] Y. Shibayama, et al., J. Phys. Conf. Ser. 150, 032096 (2009).

[3] J. Nyeki et al., Nature Physics 35, 40 (2017).

[4] P. Corboz et al., Phys. Rev. B 78, 245414 (2008).

INVITED TALK

## O27.9 Multimode–excitations in liquid $^4\text{He}$ above the phonon–roton spectrum: Experiments and Theory

K. Beauvois<sup>ab</sup>, B. Fåk<sup>a</sup>, H. Godfrin<sup>b</sup>, [E Krotscheck](#)<sup>c</sup>, and J. Ollivier<sup>a</sup>

<sup>a</sup>Institut Laue-Langevin, CS 20156, 38042 Grenoble Cedex 9, France<sup>b</sup>Univ. Grenoble Alpes, CNRS, Grenoble INP, Institut Néel, 38000 Grenoble, France

<sup>c</sup>Department of Physics, University at Buffalo, SUNY Buffalo NY 14260

The dynamic structure factor of liquid  $^4\text{He}$  shows above the familiar phonon–roton spectrum a weak, but rich structure which can be attributed to the decay of induced density fluctuations into elementary excitations. Recent high–precision neutron scattering experiments at very low temperatures<sup>1</sup> and parallel theoretical calculations<sup>2</sup> show clear features such as (a) an extension of the phonon branch into the continuum, (b) the extension of the Pitaevskii–plateau to long wave lengths, and, for the first time, (c) the “Cherenkov” decay of a  $R_+$ -roton into a long–wavelength phonon and a lower–energy  $R_+$  roton<sup>3</sup> around saturation density.

1. K. Beauvois *et al.*: arXiv:1802.08120

2. C. E. Campbell, E. Krotscheck, and T. Lichtenegger: Phys. Rev. **B 91**, 184510 (2015).

3. A. B. Burkova, Sov. Phys. - JETP **54:2**, 320 (1981)

INVITED TALK

## O27.10 Quantum turbulence in $^4\text{He}$ as a source of non–thermal rotons and of quantum evaporation

[L. Reatto](#)<sup>a</sup>, I. Amelio<sup>b</sup>, and D. E. Galli<sup>a</sup>

<sup>a</sup>Dipartimento di Fisica “Aldo Pontremoli”, Università degli Studi di Milano, via Celoria 16, I-20133 Milano, Italy

<sup>b</sup>Dipartimento di Fisica, Università di Trento, via Sommarive 14, I-38050 Povo, Italy

We propose a new way to study a quantum vortex tangle in superfluid  $^4\text{He}$  by measurement of quantum evaporation processes from the free surface of the superfluid. State of the art quantum simulation of  $^4\text{He}$  shows that the vortex core in this superfluid has the character of a density modulation and is not a simple rarefaction region as found in clouds of cold bosonic atoms. We find that the vortex density profile can be well represented as a wave packet of bulk excited states in which rotons are the major component: The vortex density modulation can be viewed as a cloud of virtual excitations, mainly rotons, sustained by the phase of the vortex wave function. This suggests that in a vortex reconnection some of these rotons become real so that a vortex tangle is predicted to be a source of non–thermal rotons. The presence of such vorticity–induced rotons can be verified by measurements at low temperature of quantum evaporation of  $^4\text{He}$  atoms. We estimate the rate of evaporation and this turns out to be detectable by current instrumentation. Additional information on the microscopic processes in the decay of quantum turbulence will be obtained if quantum evaporation also by high-energy phonons would be detected.

INVITED TALK

## O27.11 Inchworm Driving of $^4\text{He}$ Crystals in Superfluid

R. Nomura, T. Yoshida, A. Tachiki, and Y. Okuda

Tokyo Institute of Technology, Japan

It is a difficult task to remotely move a solid object through a superfluid over a long distance. Moving a  $^4\text{He}$  quantum crystal in a superfluid is even more difficult, and at present there is no known means of accomplishing this in a well-controlled manner. In the present work, we demonstrated that a  $^4\text{He}$  crystal can in fact undergo motion on a oscillating plate as the result of employing an inchworm driving<sup>1,2</sup>, a technique that is employed to impart motion to classical solid objects based on the difference between static and dynamic friction forces. However, the observed motion was quite different from the ordinary behavior of classical objects. The crystal was only deformed initially by the oscillations and eventually moved after this deformation. Furthermore, the distance traversed was one order of magnitude larger than expected from the oscillation amplitude. Since the initial deformation appears to be consistent with contact line depinning, the subsequent motion was also likely induced by depinning, rather than by crystal slip on the plate. The extended movement of these crystals can be attributed to the crystal-superfluid transition, namely crystallization on one side and melting on the other, assisted by superflow induced during the oscillation process.

1. T. Yoshida, A. Tachiki, R. Nomura, and Y. Okuda (2017). “Inchworm Driving of  $^4\text{He}$  Crystals in Superfluid”. *J. Phys. Soc. Jpn.* **86**, 074603.

2. K. Kono (2017). “Quantum Conveyance of Helium Crystals”. *JPSJ News Comments* **14**, 07.

INVITED TALK

## July 27 (Friday) Poster Presentations

### P27.1 Differential conductance anomalies in superconducting nanoconstrictions by hydrogen adsorption

K. Miyakawa<sup>a</sup>, H. Takata<sup>a</sup>, Y. Kajiwara<sup>a</sup>, Y. Inagaki<sup>a</sup>, K. Hashizume<sup>b</sup>, and T. Kawae<sup>a</sup>

<sup>a</sup>Department of Applied Quantum Physics, Kyushu University

<sup>b</sup>Department of Engineering Science, Kyushu University

We study the effect of hydrogen (H) adsorption on metallic surface by measuring the differential conductance  $dI/dV$  spectra for Josephson contacts made by lead (Pb) and niobium (Nb) nanoconstrictions, which are prepared by a mechanically controllable break junction technique. In pure nanoconstrictions,  $dI/dV$  spectra show several anomalies due to the Andreev reflection inside the superconducting gap, when the temperature is lowered below the superconducting transition temperature  $T_c$ .

The spectra change drastically by covering the surface with H, which is done by the following procedure. After exposing nanoconstrictions in gas  $H_2$ ,  $H_2$  is evacuated from the experimental cell at  $T \sim 20$  K, ensuring that a few layers of  $H_2$  films are adsorbed on the nanoconstrictions. In the both nanoconstrictions of Pb and Nb, a number of anomalies appear in  $dI/dV$  spectra, where the gap between the anomalies is almost the same value of  $\sim 0.1$  mV. Moreover, the position at the anomalies is temperature independent. The result suggest that the H adsorption leads to a drastic change of the electronic structure for the base metal.

### P27.2 Low-temperature hydrogen absorption in vanadium nano-contacts

H. Takata<sup>a</sup>, K. Ienaga<sup>b</sup>, Y. Inagaki<sup>a</sup>, K. Hashizume<sup>c</sup>, H. Tsujii<sup>d</sup>, and T. Kawae<sup>a</sup>

<sup>a</sup>Department of Applied Quantum Physics, Kyushu University, Japan

<sup>b</sup>Department of Science, Tokyo Institute of Technology, Japan

<sup>c</sup>Department of Advanced Energy Engineering Science, Kyushu University, Japan

<sup>d</sup>Department of Education, Kanazawa University, Japan

We study hydrogen (H) absorption in vanadium (V) nano-contacts at low temperature using the Point-contact spectroscopy (PCS) technique. In palladium (Pd) nano-contacts, we report that H absorption is induced even at  $T \leq 20$  K, where H diffusion hardly progress, by phonon vibrations excited through PCS measurements.<sup>1</sup>

As in the case of Pd nano-contacts, hydride is synthesized at  $T \leq 20$  K in V nano-contacts. Moreover, the differential conductance ( $dI/dV$ ) spectrum changes drastically from peak- to dip-shape with increasing H concentration, while the dip-shape anomaly disappears after H desorption from the nano-contacts. These indicate that the change does not originate from defects or lattice distortions in the nano-contacts, but from the variation of electrical property. According to the theoretical calculation<sup>2</sup>, the electronic density of states for V with high H concentration exhibits the chromium (Cr)-like structure. Actually, the dip-shape spectrum is observed in Cr nano-contacts for PCS measurements, suggesting that the magnetic moment might appear in V by H absorption.

1. Ienaga, K. *et al.* (2015). "Spectroscopic study of low-temperature hydrogen absorption in palladium". *Appl. Phys. Lett.* 2. Andersson, P. H. *et al.* (1998). "Theoretical study of structural and electronic properties of  $VH_x$ ". *Phys. Rev. B*

### P27.3 Collective Motion of Hydrogen Atoms via Quantum Tunneling in Niobium Nanocontacts

H. Takata<sup>a</sup>, K. Ienaga<sup>b</sup>, S. Islam<sup>a</sup>, K. Hashizume<sup>c</sup>, and T. Kawae<sup>a</sup>

<sup>a</sup>Department of Applied Quantum Physics, Faculty of Engineering, Kyushu University, Japan

<sup>b</sup>Department of Physics, Tokyo Institute of Technology, Japan

<sup>c</sup>Department of Advanced Energy Engineering Science, Kyushu University, Japan

We study the kinetics of hydrogen (H) atoms in niobium (Nb) nanocontacts using point-contact spectroscopy measurement, which is a sensitive tool for investigating phonon excitations. In the present research, the hydride sample is prepared by low-temperature H absorption (LTHA), where H atoms are loaded from liquid H<sub>2</sub> by applying a bias voltage between the nanocontacts<sup>1,2</sup>. The kinetic behavior is tracked by the  $dI/dV$  spectra and the derivative  $d^2I/dV^2$  spectra simultaneously through the differential conductance measurements with a lock-in technique. The differential conductance in hydrogenated Nb nanocontacts prepared by LTHA show several spikes in the  $d^2I/dV^2$  spectra without polarity and hysteresis in the bias sweep, which reflects H transfer arising from quantum tunneling between the occupied and vacant sites assisted by electron-excited phonon vibrations. When the spectra are plotted as a function of the product of current and voltage,  $I \times V$ , the spike positions show good agreement between different sized contacts. These suggest that a number of H atoms in the contact move collectively via quantum tunneling.

[1]. Ienaga, K. Yokota, T. Nakashima, N. Inagaki, Y. Tsujii, H. and Kawae, T. (2012). *J. Phys. : Conf. Ser.* **400**, 042019. [2]. Ienaga, K. Takata, H. Onishi, Y. Inagaki, Y. Tsujii, H. Kimura, T. and Kawae, T. (2015) *Appl. Phys. Lett.* **106**, 021605.

### P27.4 Non-ohmic currents of Wigner solid on helium in 3-terminal microchannel structure.

A. O. Badrutdinov<sup>a</sup>, D. Rees<sup>b</sup>, A. V. Smorodin<sup>a</sup>, J. Y. Lin<sup>a</sup>, and D. Konstantinov<sup>a</sup>

<sup>a</sup>Okinawa Institute of Science and Technology (OIST) Graduate University, Japan

<sup>b</sup>National Chiao Tung University, Taiwan

We report time-resolved transport measurements of surface electrons on liquid helium confined in a three-terminal microchannel device, which consists of three reservoirs connected by a T-shaped channel structure. When electrons flow from a source reservoir into two drain reservoirs, the electron current must split at the junction of the T-channel. For Ohmic electron transport, the current should split equally. However, this is not always observed; the current splitting becomes completely asymmetric when electrons are in the Wigner solid state and under certain conditions of temperature and electron density. In this asymmetric case, all the current flows into one drain reservoir, while no current flows into another. We interpret this as a manifestation of the strong coupling between the Wigner solid and helium surface waves that are generated by the electron motion<sup>1</sup>.

1. Dykman, M. and Rubo, Y. (1997). "Bragg-Cherenkov Scattering and Nonlinear Conductivity of a Two-Dimensional Wigner Crystal". *Phys. Rev. Lett.* **78**, 4813.

## P27.5 Experiments on ac Driven Wigner Solid on Liquid Helium Confined in a Microchannel and Subjected to an External Periodic Potential

J.-Y. Lin, A. V. Smorodin, A. O. Badrutdinov, and D. Konstantinov

Quantum Dynamics Unit, Okinawa Institute of Science and Technology (OIST) Graduate University, Japan

Wigner solids (WS) on the surface of liquid helium<sup>1</sup> is one of the ideal 2D systems for studying many-body physics. Motivated by the Frenkel-Kontorova model<sup>2</sup>, we employed the WS of surface-state electrons on liquid helium as the chain of particles, and introduce an external periodic electrostatic potential as a substrate potential in order to study their driven dynamic interactions. Here we show one of the interesting experimental findings that the Bragg-Cherenkov scattering<sup>3</sup> effect is gradually suppressed by the increase of external periodic potential amplitude under the condition of coverage parameter  $\theta = 4$ , i.e. 4 particles per substrate period.

1. Grimes, C. C. and Adams, G. (1979). “Evidence for a Liquid-to-Crystal Phase Transition in a Classical, Two-Dimensional Sheet of Electrons”. *Physical Review Letters*, 42, 795.
2. Braun, O. M. and Kivshar, Y. S. (2004). “The Frenkel-Kontorova Model: Concepts, Methods, and Applications”. Springer-Verlag Berlin Heidelberg.
3. Dykman, M. I. and Rubo, Y. G. (1997). “Bragg-Cherenkov Scattering and Nonlinear Conductivity of a Two-Dimensional Wigner Crystal”. *Physical Review Letters*, 78, 4813.

## P27.6 Critically charged superfluid <sup>4</sup>He surfaces in inhomogeneous electric fields

P. Leiderer<sup>a</sup>, Th. B. Möller<sup>a</sup>, P. Moroshkin<sup>b</sup>, E. Scheer<sup>a</sup>, and K. Kono<sup>c</sup>

<sup>a</sup>University of Konstanz, Konstanz, Germany

<sup>b</sup>Okinawa Institute of Science and Technology, Okinawa, Japan

<sup>c</sup>National Chiao Tung University, Hsinchu, Taiwan

We have studied the spatial distribution of charges trapped at the surface of superfluid helium in the inhomogeneous field of a metallic tip close to the surface. The electrostatic pressure generates a deformation of the liquid surface, leading to a “hillock” or “dimple”, depending on whether the tip is placed above or below the surface. These experiments are complemented by finite-elements simulations for the surface profile and the corresponding charge densities in vicinity of the tip. Typical applied electric fields  $E$  are in the range of a few kV/cm, the maximum equilibrium surface deformations are below 0.5 mm, related to the capillary length of liquid <sup>4</sup>He. As the elongation of the surface is increased by raising  $E$  beyond a critical value (depending on the available amount of charges at the surface), an electrohydrodynamic instability develops, which in the case of hillocks is known from classical liquids as Taylor cone breakdown. Our results provide direct access to determining the total number and the local density of electrons or ions from an observation of the liquid profile. They also show that in equilibrium the maximum density of surface state electrons in a dimple is limited to  $n < 10^{10} \text{ cm}^{-2}$ , where the electrons behave like a classical-particle system. However, distinctly higher densities should be achievable for short times ( $\ll \text{ms}$ ) using pulsed electric fields, which opens a route towards the degenerate regime of surface state electrons.

## P27.7 Elasticity Measurements of Neon Films on a Porous Glass Substrate

T. Makiuchi, K. Yamashita, M. Tagai, Y. Nago, and K. Shirahama

Department of Physics, Keio University, Japan

Elastic constants of bosonic  $^4\text{He}$  and fermionic  $^3\text{He}$  films on a porous glass substrate anomalously increase at low temperatures for small coverages.<sup>1</sup> This stiffening is explained by localization and thermal activation of adsorbed He atoms, which were first proposed in a heat capacity study of  $^4\text{He}$  films by Tait and Reppy<sup>2</sup>. The heat capacity exponentially drops at a characteristic temperature below which He atoms are localized. Similar heat capacity features were observed for  $\text{H}_2$  film on porous Vycor<sup>2</sup> and Ne film on graphite<sup>3</sup>. Therefore, the stiffening of adsorbed film at  $T \rightarrow 0$  is expected for any molecules physisorbed on any substrates. We have executed elasticity measurements for Ne films with the same torsional oscillator as the He-film study<sup>1</sup> in the temperature range 1–22 K. We have found that Ne films show similar stiffening to that of He films, which is seen as an increase of elasticity accompanied by a dissipation peak. However, the coverage dependence of the onset of stiffening differs significantly from that of He films. The onset temperatures remain constant at coverages  $10 < n < 35 \mu\text{mol}/\text{m}^2$ , while the onset in  $^4\text{He}$  and  $^3\text{He}$  vanishes at a critical coverage  $n_c \approx 20 \mu\text{mol}/\text{m}^2$ , indicating a quantum phase transition. This difference suggests that Ne films form 2D solid puddles and the softening at high  $T$  occurs by sublimation of Ne atoms to a 2D gas phase.

1. T. Makiuchi, *et al.*, another poster; T. Makiuchi, M. Tagai, Y. Nago, D. Takahashi and K. Shirahama, in preparation. 2. R. H. Tait and J. D. Reppy, *PRB* **20**, 997 (1979). 3. R. H. Torii, H. J. Maris and G. M. Seidel, *PRB* **41**, 7167 (1990). 4. G. B. Huff and J. G. Dash, *J. Low Temp. Phys.* **24**, 155 (1976).

## P27.8 Kosterlitz-Thouless Superfluid Transition of $^4\text{He}$ Films on Planar Gold

M. Hieda<sup>a</sup>, H. Yamaguchi<sup>b</sup>, T. Matsushita<sup>b</sup>, and N. Wada<sup>b</sup>

<sup>a</sup>College of Liberal Arts and Sciences, Tokyo Medical and Dental University, Chiba, Japan

<sup>b</sup>Department of Physics, Nagoya University, Nagoya, Japan

The Kosterlitz-Thouless (KT) superfluid transition<sup>1</sup> of  $^4\text{He}$  films has been studied extensively for about last half century. The dynamic extension<sup>2</sup> of the static theory is needed to understand experiments with a finite frequency. This dynamic theory was strictly tested in the experiments of 2D  $^4\text{He}$  on Mylar by torsional oscillators.<sup>3,4</sup> In the monolayer region, the fits to temperature dependence of the superfluid response were greatly successful. However, in the submonolayer region, those were considerably failure. To solve this mystery, further studies on pure 2D  $^4\text{He}$  are still required. In this presentation, we report data of submonolayer superfluidity of  $^4\text{He}$  films on planar gold substrate at various submonolayer coverages ( $0.1 < T_{\text{KT}} < 0.8$  K) using a quartz crystal microbalance (QCM) at 60 MHz. We succeeded in describing the entire region of temperature dependence of  $\rho_s$  and  $\Delta Q^{-1}$  at all measured coverages by the dynamic KT theory.

1. J. M. Kosterlitz and D. J. Thouless, *J. Phys. C* **6**(8), 1181 (1973).
2. V. Ambegaokar, B. I. Halperin, D. R. Nelson, and E. D. Siggia, *Phys. Rev. B* **21**, 1806 (1980).
3. G. Agnolet, D. F. McQueeney, and J. D. Reppy, *Phys. Rev. B* **39**, 8934 (1989).
4. H. Yano, T. Joha, and N. Wada, *Phys. Rev. B* **60**, 543 (1999).

## P27.9 Prediction for two spatially modulated superfluids: $^4\text{He}$ on fluorographene and on hexagonal BN

M. Nava<sup>a</sup>, P.L. Silvestrelli<sup>b</sup>, F. Ancilotto<sup>b</sup>, and L. Reatto<sup>c</sup>

<sup>a</sup>Department of Chemistry, University of Illinois, Urbana, Illinois 61801, United States

<sup>b</sup>Dipartimento di Fisica e Astronomia “Galileo Galilei” and CNISM, Università’ di Padova, via Marzolo 8, 35122 Padova, Italy; CNR-IOM Democritos, via Bonomea, 265 - 34136 Trieste, Italy

<sup>c</sup>Dipartimento di Fisica, Università’ degli Studi di Milano, via Celoria 16, 20133 Milano, Italy

We have derived the adsorption potential of  $^4\text{He}$  atoms on fluorographene (GF) and on hexagonal boron nitride (hBN) by a recently developed *ab initio* method which incorporates the van der Waals interaction. The  $^4\text{He}$  monolayer is studied by state-of-the-art quantum simulations at  $T=0$  K. With our adsorption potentials we find that in both cases the ground state of  $^4\text{He}$  monolayer is a superfluid and not an ordered state with localized atoms as on graphite and on graphene. In the case of GF the present result is in qualitative agreement with a previous result<sup>1</sup> that was obtained using an empirical adsorption potential. Superfluidity on GF and on hBN is characterized by a very large density modulation and at the equilibrium density the ratio  $\Gamma$  between the largest and the smallest local density along the direction of two neighboring adsorption sites and averaged over the perpendicular direction is  $\Gamma \sim 1.9$  for GF and  $\Gamma \sim 1.7$  for hBN. Recent experiments<sup>2</sup> have discovered that the superfluid phase of the second layer  $^4\text{He}$  has anomalous thermal properties. This gives a strong motivation for an experimental study of monolayer  $^4\text{He}$  on GF and on hBN that we predict to be a spatially anisotropic superfluid.

1. M. Nava et al., Phys. Rev. B **86**, 174509 (2012).

2. J. Nyeki et al., Nature Physics **13**, 455 (2017).

## P27.10 Quantum Phase Diagram of $^3\text{He}$ Monolayer on Hydrogen Plated Graphite

M. Kamada<sup>a</sup>, R. Nakamura<sup>a</sup>, K. Ogawa<sup>a</sup>, T. Matsui<sup>a</sup>, and Hiroshi Fukuyama<sup>a,b</sup>

<sup>a</sup>Department of Physics, The University of Tokyo, Japan

<sup>b</sup>Cryogenic Research Center, The University of Tokyo, Japan

In the second layer of  $^3\text{He}$  on graphite (bilayer system), various quantum phases are known to emerge with increasing density ( $\rho$ ) such as the gas-liquid coexistence (G-L), Fermi liquid (FL), possible quantum liquid crystal (C2), and incommensurate (IC) solid. Recently, we have determined a whole phase diagram of  $^3\text{He}$  monolayer on graphite preplated with a bilayer of HD ( $^3\text{He}/\text{HD}/\text{HD}/\text{gr}$ ) from specific heat measurements over wide temperature (0.3–90 mK) and density (0–13  $\text{nm}^{-2}$ ) ranges. The purpose of this study is to elucidate a role of the potential corrugation produced by the underlayer. In  $^3\text{He}/\text{HD}/\text{HD}/\text{gr}$ , the corrugation periodicity is much longer and the corrugation amplitude is much larger than in the bilayer system. We found a new phase stabilized within a narrow density range ( $< 1\%$ ) at  $4.74 \text{ nm}^{-2}$  between the FL and C2-like phases. This is most likely a new commensurate (C3) phase registered to the potential corrugation. It was also found that the C2-like phase, a previously known possibly localized phase, has a remarkably similar nuclear magnetic specific heat to that of the C2 phase. Moreover, the C2-like phase can be compressed over a much wider density range ( $\approx 20\%$ ) than the C2 phase. From these facts, the C2 and C2-like phases are essentially the same phase and would not be a simple commensurate phase like the  $4/7$  phase or else. Other regions of the phase diagram of  $^3\text{He}/\text{HD}/\text{HD}/\text{gr}$ , i.e., the G-L and IC phases, are similar to the bilayer system. By analyzing the substrate heterogeneity effects very carefully, we reexamined critical behaviors of the  $^3\text{He}$  effective mass and spin fluctuations in the FL phase as  $\rho$  increases toward the C3 phase finding quantitatively different results from the previous work.



## P27.11 Randomness-induced quantum spin liquid behavior in the two-dimensional $^3\text{He}$

K. Uematsu and H. Kawamura

Graduated School of Science, Osaka University, Japan

Two-dimensional  $^3\text{He}$  adsorbed on graphite shows gapless quantum spin liquid (QSL)-like behaviors down to low temperatures. Theory suggests that the  $s = 1/2$  Heisenberg model on the triangular lattice with the ferromagnetic two-body exchange interaction together with the four-body exchange interaction, which is expected to describe the nuclear magnetism of 2D  $^3\text{He}$ , exhibits a gapped QSL phase. Recently, it was reported that the inhomogeneity or randomness associated with spatial arrangement of 2D  $^3\text{He}$  atom could be crucial in the nuclear magnetism of the 2D  $^3\text{He}$  system. We study the  $s = 1/2$  random Heisenberg model on the triangular lattice with the multiple-spin exchange interaction by using the exact diagonalization method. We then find the randomness-induced gapless nonmagnetic phase (the random singlet phase) for stronger randomness, which is quite consistent with the experimentally observed C2-like phase. The computed thermodynamic properties including the specific heat, the susceptibility, and the magnetization curve are presented, and the properties of the randomness-induced phase are discussed.

## P27.12 The Frank-Read mechanism in the crystalline bilayer of He-4

T. Minoguchi

Institute of physics, The University of Tokyo, Komaba, Japan

The dynamical instability of the bilayer of crystalline He-4 typically formed on graphite is explained with emphasis on the role of the Frank-Read source, a piece of line dislocation with pinned endpoints. With a sufficiently large shear stress between the bilayer, the Frank-Read source generates multiple dislocations resulting in the density imbalance between layers. Such an imbalance causes a 'mass pumping' from the first layer (the nearest solid layer to the substrate) to the second solid layer, and from the second solid layer to the upper liquid overlayers. As a result, the first layer can include appreciable random vacancies and demonstrates a long-lived mass decoupling response as speculated.<sup>1</sup>

In the presence of a superfluid (SF) overlayer, on the other hand, the deformation of the line dislocation is annihilated and reforms a straight line shape through the mass flow in SF: That is, the Frank-Read mechanism does not work and the first layer is protected from the structural damage. It is consistent with our 'dynamical sticking' mechanism of solid layer previously proposed.<sup>2</sup>

1. Minoguchi, T. (2017). "Highly mobile metastable state of He-4 thin films: A glass transition by mechanical perturbation?". *J. Low Temp. Phys.* 187, 354-360.

2. Hosomi, N., Taniguchi, J., Suzuki, M. and Minoguchi, T. (2009). "Dynamical sticking of a solid He-4 film with superfluid overlayer". *Phys. Rev.* B79, 172503.

## P27.13 Mass Decoupling of $^3\text{He}$ - $^4\text{He}$ Mixture Films and Its Relaxation

K. Ishibashi, J. Taniguchi, and M. Suzuki

Department of Engineering Science, University of Electro-Communications,  
1-5-1 Chofugaoka, Chofu, Tokyo 182-8585, Japan

We measured the mass decoupling for  $^3\text{He}$ - $^4\text{He}$  mixture films adsorbed on Grafoil using a 5 MHz quartz-crystal microbalance. For a mixture film composed of  $^4\text{He}$  with 31.6 atoms/nm<sup>2</sup> and  $^3\text{He}$  with 0.2 atoms/nm<sup>2</sup>, solid  $^4\text{He}$  layers undergo decoupling from a largely oscillating substrate below a certain temperature, and this decoupling remains metastable after switching from a large to a small oscillation amplitude before relaxing to the sticking state. The observed relaxation is significantly different from that of pure  $^4\text{He}$  films. In the case of pure  $^4\text{He}$  films, the mass decoupling decreases exponentially with respect to waiting time<sup>1</sup>, while it decreases abruptly at a certain waiting time  $t_a$ . In addition,  $t_a$  depends strongly on temperature and obeys to the Arrhenius law as  $t_a = t_{a0} \exp(E/k_B T)$ , where  $t_{a0} \sim 10^3$  s and  $E \sim 8$  K. The observed relaxation can be explained as follows: the sticking area is nucleated in the highly mobile state by overcoming a potential barrier, and it expands rapidly.

1. N Hosomi, A. Tanabe, M Suzuki, and M. Hieda, Phys. Rev. B **75**, 064513 (2007).

## P27.14 Wetting Property of $^4\text{He}$ Crystals on a Rough Wall

R. Nomura<sup>a</sup>, T. Takahashi<sup>a</sup>, H. Minezaki<sup>a</sup>, A. Suzuki<sup>a</sup>, K. Obara<sup>b</sup>, K. Itaka<sup>c</sup>, and Y. Okuda<sup>a</sup>

<sup>a</sup>Tokyo Institute of Technology, Japan

<sup>b</sup>Osaka City University, Japan

<sup>c</sup>Hirosaki University, Japan

In the case of classical fluids, the roughness of a wall assists repulsion and alters the contact angle, which is referred to as the lotus effect. Such effect are predicted to occur also in nano-crystals which can transform the shape in a short period<sup>1</sup>, but never in bulk crystals. Bulk  $^4\text{He}$  crystals, however, are known to relax to the lowest energy shape quickly and thus should exhibit the lotus effect. To investigate whether controlling the contact angle of a  $^4\text{He}$  crystal in superfluid is possible or not, contact angles of  $^4\text{He}$  crystals were measured on rough and smooth walls<sup>2</sup>. A rough surface was made by coating a surface of a glass plate with a commercially available coating agent. Contact angles of  $^4\text{He}$  crystals were found to increase by about 10 degrees on the rough wall coated with the agent. Therefore, the increase of repellency of  $^4\text{He}$  crystals in superfluid was demonstrated to be possible on the very rough surface. From the comparison of the contact angles and SEM image of the rough surface, the Cassie-Baxter state was likely to be realized on the rough surface; the  $^4\text{He}$  crystal had a contact with the protruding parts of the rough surface but superfluid was entrapped between the crystal and the hollow parts of the wall.

1. M. Ignacio, Y. Saito, P. Smereka, and O. Pierre-Louis (2014). “Wetting of Elastic Solids on Nanopillars”. Phys. Rev. Lett. **112**, 146102.
2. T. Takahashi, H. Minezaki, A. Suzuki, K. Obara, K. Itaka, R. Nomura, and Y. Okuda (2016). “Control of the Wetting Properties of  $^4\text{He}$  Crystals in Superfluid”. Phys. Rev. E **93**, 052806.

## P27.15 Conventional magnon BEC in antiferromagnets

Yu. M. Bunkov<sup>a</sup>, A. V. Klochkov<sup>a</sup>, T. R. Safin<sup>a</sup>, K. R. Safiullin<sup>a</sup>, and M. S. Tagirov<sup>b</sup>

<sup>a</sup>Kazan Federal University, Kazan, Russia

<sup>b</sup>Institute of Applied Research, Tatarstan Academy of Sciences, Kazan, Russia

The NMR in antiferromagnets with Suhl-Nakamura interaction described by the Landau-Lifshitz-Gilbert equations.<sup>1</sup> The Bose-Einstein condensation (BEC) of magnons is possible for the case, when density of magnons is larger than the critical density. According<sup>2</sup> the critical density of magnons in considered systems at temperature about 1.5 K correspond to a nuclear magnetization deflection on the angle of about  $3^\circ - 5^\circ$ . The magnon BEC forms at a minimum of energy at  $k=0$ . The frequency of magnon BEC precession is shifted up from Larmor frequency due to magnon-magnon repulsive interaction. At the conditions of pulsed NMR the chemical potential and frequency shift are determined by the number of excited magnons. In the case of small continuous wave (CW) pumping, the magnon BEC state forms with the frequency of RF pumping.<sup>3</sup> This state has elasticity. The Goldstone mode of magnon BEC was observed in.<sup>4</sup> In conclusion, the magnon BEC in antiferromagnets demonstrates a number of effects, similar to magnon BEC in antiferromagnetic superfluid states of  $^3\text{He}$ .

This work was supported by the Russian Science Foundation, project no. 16-12-10359.

1. Abdurakhimov L. V., et al.,(2018) Phys. Rev. B 97, 024425.
2. Gazizulin R. R., et al.(2015), JETP Lett. 102, 876.
3. Tagirov, M. S., et al.(2014), J. Low Temp. Phys. 175, 167.
4. Bunkov Yu. M., et al.,(2017), JETP Lett. 106, 677.

## P27.16 Propagation of heat pulse through superfluid $^4\text{He}$ in 90% open aerogel

K. Matsumoto, R. Okamoto, S. Shibuya, A. Nakajima, and S. Abe

Department of Physics, Kanazawa University, Japan

Propagation of heat pulse through superfluid  $^4\text{He}$  in 90% open aerogel was studied below superfluid transition temperature. Commercially available Cernox sensor (Lake Shore) was used as detector. Signals corresponding to slow mode and bulk second sound were observed between 1 K and superfluid transition temperature. However, slow mode signal was difficult to detect below 1 K. Sound velocity was obtained from time of flight. The velocity of slow mode stayed those of second and forth sound. The pulse corresponding to second sound in aerogel became broadened and had almost the same velocity of second sound without gel. Velocity of slow mode and second sound had no significant pressure dependence.

## P27.17 Decoding quantum criticalities from the matrix product wave functions of one-dimensional topological states

G. M. Zhang

Department of Physics, Tsinghua University, Beijing, 100084, China

Under an appropriate symmetric bulk bipartition in a one-dimensional symmetry protected topological (SPT) phase with the Affleck-Kennedy-Lieb-Tasaki matrix product state wave function for the odd integer spin chains, a bulk critical entanglement spectrum can be obtained, describing the excitation spectrum of the critical point separating the SPT phase from the trivial (vacuum) state<sup>1</sup>. Such a critical point is beyond the standard Landau-Ginzburg-Wilson paradigm for symmetry breaking phase transitions. Recently, the framework of matrix product states for topological phases with Majorana fermions/parafermions have been established using the Fock representation. The defining feature of these topological phases is the presence of Majorana/parafermion zero modes localized at the edges. It is shown that the single-block bipartite entanglement spectrum and its entanglement Hamiltonian are described by the effective coupling between two edge quasiparticles. Furthermore, we demonstrate that sublattice bulk bipartition can create an extensive number of edge quasiparticles in the reduced subsystem, and the symmetric couplings between the nearest neighbor edge quasiparticles lead to the critical entanglement spectra, characterizing the topological phase transitions from the fermionic/parafermionic topological phases to its adjacent trivial phase<sup>2</sup>. The corresponding entanglement Hamiltonians for the critical entanglement spectra can also be derived.

1. W. J. Rao, X. Wan, G. M. Zhang, Phys. Rev. B 90, 075151 (2014); 93, 115125 (2016).
2. Z. Q. Wang, G. Y. Zhu and G. M. Zhang, arXiv:1802.04542.

## P27.18 Localization of Chiral-like Spin Solitons with Carriers in the Layered organic $k\text{-(ET)}_2\text{Cu}_2(\text{CN})_3$

I. Kanazawa, M. Nakajima, R. Maeda, and Shun Nakajima

Department of Physics, Tokyo Gakugei University

Shimizu et al.[1] found no indication of long-range magnetic ordering down to 32 mK, and have suggested that a quantum spin liquid is realized in the close proximity of the superconducting state appearing under pressure in the layered organic conductor  $k\text{-(ET)}_2\text{Cu}_2(\text{CN})_3$ . On the other hand, Kawamoto et al.[2] have proposed that the origin of this insulator phase does not correspond to a spin liquid state but to localization of carriers. In addition, a number of important questions have been raised such as the nature of the low-energy. The present author[3] has explained theoretically the important relationship between the superconducting critical temperature  $T_c$  and the effective mass of holes, which was observed by Caulfield et al.[4] in the layered organic superconductors. The present author [5] has proposed freezing mechanism of chiral-like spin solitons in the spin glass phase. In this study, we will present the localization mechanism of hole-induced chiral-like spin solitons in the layered organic conductor with triangular lattice, using the previous theory [6]. For the first time, we have proposed that the layered organic  $k\text{-(ET)}_2\text{Cu}_2(\text{CN})_3$  might have the glass phase of chiral-like spin solitons.

- [1] Y. Shimizu et al. Phys. Rev. Lett. 91, 107001 (2003) [2] A. Kawamoto et al., Phys. Rev. B 74, 212508 (2006)  
[3] I. Kanazawa, Physica C 282-287, 1891 (1997) [4] J. Caulfield et al., J. Phys. C 6, 2911 (1994) [5] I. Kanazawa, Physica B 328, 1051 (2003) [6] I. Kanazawa, R. Maeda, J. Supercond Nov Magn 30, 49 (2017)

P27.19 **The optical conductivity for a spin-Peierls ground state of  $(\text{TMTTF})_2\text{PF}_6$  with tetramer formation**

T. Yamaguchi and K. Iwano

Institute of Materials Structure Science, High Energy Accelerator Research Organization (KEK), Tsukuba, Japan

We consider a  $1/4$ -filled one-dimensional extended Hubbard model with tetrameric molecules of TMTTF and investigate the optical conductivity of  $(\text{TMTTF})_2\text{PF}_6$  within the framework of the exact diagonalization method at  $T = 0$  by using appropriate parameters which have already been reported.<sup>1,2,3</sup> Since some experiments indicate the formation of a tetramer in the spin-Peierls ground state of  $(\text{TMTTF})_2\text{PF}_6$  from observed molecular displacements<sup>3</sup> and charge configurations of molecules,<sup>4</sup> our results are useful to understand the effects of tetramarization on the optical properties of  $(\text{TMTTF})_2\text{PF}_6$ .

1. H. Seo, *et. al.*, J. Phys. Soc. Jpn. **75**, 051009 (2006).
2. A. C. Jacko, *et. al.*, Phys. Rev. B **87**, 155139 (2013).
3. S. Kitou, *et. al.*, Phys. Rev. Lett. **119**, 065701 (2017).
4. A. Pustogow, *et. al.*, Phys. Rev. B **94**, 195125 (2016).

P27.20 **Quasiperiodicity and valence fluctuation in the spin-1/2 Falicov-Kimball model**

J. Nasu, R. Shinzaki, and A. Koga

Department of Physics, Tokyo Institute of Technology, Meguro, Tokyo 152-8551, Japan

Strongly correlated electron systems with quasiperiodicity have attracted much attention since the discovery of quantum criticality in the compound  $\text{Au}_{51}\text{Al}_{34}\text{Yb}_{15}$  with quasiperiodic structure. In this material,  $f$  electrons of Yb ions are considered to be in intermediate valence regime, and hence valence fluctuations should play an essential role for this exotic phenomenon in addition to the quasiperiodicity.

In this study, to clarify the many-body effect and valence fluctuation in quasiperiodic systems, we introduce, as a simplest model, a spin-1/2 Falicov-Kimball model on a two dimensional Penrose lattice. We analyze the finite temperature properties of this model using real-space dynamical mean-field theory (RDMFT). In the Falicov-Kimball model, we can exactly evaluate an effective impurity problem in RDMFT. This enables us to perform calculations at very low temperatures.

At high temperatures, the  $f$  electron occupancy does not depend on sites of the Penrose lattice due to thermal fluctuations. In the intermediate temperature range, the site dependence appears, which is classified by its coordination number. Further decrease of temperature leads to the  $f$  electron distribution reflecting wider surrounding structure. However, at the lowest temperature, we find that this structure disappears associated with nonmonotonic temperature dependence.

## P27.21 Magnetic properties in the metallic magnets with large anisotropy

Y. Taguchi<sup>a</sup>, J. Nasu<sup>a</sup>, A. Koga<sup>a</sup>, T. Yoshioka<sup>b,c,d</sup>, and H. Tsuchiura<sup>b,c,d</sup>

<sup>a</sup>Department of Physics, Tokyo Institute of Technology, Meguro, Tokyo 152-8551, Japan

<sup>b</sup>Department of Applied Physics, Tohoku University, Aoba, Sendai 980-8579, Japan

<sup>c</sup>ESICMM, National Institute for Materials Science, Tsukuba 305-0047, Japan

<sup>d</sup>Center for Spintronics Research Network, Tohoku University, Sendai 980-8577, Japan

Rare-earth based permanent magnets such as Nd-Fe-B are not only of practical interest in technology but also provide challenging theoretical problems in fundamental physics. Their magnetic properties have been extensively examined experimentally. Theoretical descriptions, however, have not been provided in a consistent way. The static properties such as magnetocrystalline anisotropy can be described for  $T = 0$  by using first-principles calculations, and temperature dependences or several dynamical behavior of the systems are treated within rather phenomenological classical localized spin models despite that the systems are metallic. Here, it is highly desirable to give a consistent description of the dynamical properties based on a microscopic model consists of the localized orbitals for  $4f$  electrons interacting with itinerant  $3d$  electronic systems.

In the study, we consider the extended double exchange model as one of the simplest models for the permanent magnets Nd-Fe-B. Then, we take into account itinerant electrons, localized spins and realistic crystalline electric field. First, we determine the model parameters, which should describe the magnets qualitatively. Then, using the Monte Carlo simulations, we discuss the itinerant electron-mediated ferromagnetic transition and reorientation transition at low temperatures.

## P27.22 Thermodynamic Properties of 2D Spin-Pseudospin Model

V. V. Ulitko, Yu. D. Panov, K. S. Budrin, A. A. Chikov, and A. S. Moskvina

Ural Federal University, Ekaterinburg, 620002, Russia

One of the topical problems in the physics of high- $T_c$  cuprates is the coexistence and competition of spin, superconducting, and charge ordering. To consider the competition of spin and charge ordering in cuprates, a simplified static 2D spin-pseudospin model was proposed<sup>1-3</sup>, which takes into account both the conventional spin exchange interaction and the on-site and inter-site charge correlations. In the static limit, this model is equivalent to the 2D dilute antiferromagnetic Ising model with charged impurities. In the model, five different phases are realized in the ground state, depending on the concentration of charged impurities and the ratio between the exchange and the inter-site charge interaction constants and the on-site correlation parameter. It is shown that the cases of strong exchange and strong charge correlation differ qualitatively. For a strong exchange, the antiferromagnetic phase is unstable with respect to the phase separation into the charge (pseudospin) and spin subsystems, which behave like immiscible quantum liquids. An analytical expression is obtained for critical temperature of phase separation, and we found that it agrees well with the results of Monte Carlo simulation. The work supported by Act 211 Government of the Russian Federation, agreement No 02.A03.21.0006, by the Ministry of Education and Science of the Russian Federation, projects Nos. 2277 and 5719, and by RFBR project No 18-32-00837\18.

1. Yu.D. Panov, A.S. Moskvina, A.A. Chikov, I.L. Avvakumov, J. Supercond. Nov. Magn. 29, 1077 (2016)
2. Yu.D. Panov, A.S. Moskvina, A.A. Chikov, K.S. Budrin, J. Low Temp. Phys. 187, 646 (2017)
3. Yu.D. Panov, K.S. Budrin, A.A. Chikov, A.S. Moskvina, JETP Letters 106, 440 (2017)

## P27.23 Diagram approach to the problem of the normal phase properties of the spin polaron ensemble in cuprate superconductors

V. V. Val'kov<sup>a</sup>, V. A. Mitskan<sup>a</sup>, M. M. Korovushkin<sup>a</sup>, D. M. Dzebisashvili<sup>a</sup>, and A. F. Barabanov<sup>b</sup>

<sup>a</sup>Kirensky Institute of Physics, Federal Research Center KSC SB RAS, 660036 Krasnoyarsk, Russia

<sup>b</sup>Vereshchagin Institute for High Pressure Physics, 108840 Troitsk, Moscow, Russia

Taking into account the real crystalline structure of the CuO<sub>2</sub> plane within the spin-fermion model and using the Feynman diagram technique and the diagram technique for the spin operators, the spin polaron concept of the fermionic excitations in cuprates is implemented. The developed theory is based on the well-known statement on significant interplay between the spin and charge degrees of freedom of the localized and collective subsystems. It is shown that the self-energy part  $\Sigma(\vec{p}, i\omega_n)$ , which enters the Dyson equation for the one-electron Green function, can be represented in the form  $\Sigma(\vec{p}, i\omega_n) = \Sigma_{(1)}(\vec{p}, i\omega_n) + \Sigma_{(2)}(\vec{p}, i\omega_n) + \dots$ . Each term  $\Sigma_{(m)}(\vec{p}, i\omega_n)$  arises as a result of an account for the spin-fermion scattering processes in all the orders of the perturbation theory, which are connected to the  $m$ -site spin correlations. The exact recurrence relation between the one-site cumulants  $K_l = -K_{l-1}$ ,  $l = 3, 4, \dots$ ;  $K_2 = 3/4$  and the analytical expression for the  $\Sigma_{(1)}(\vec{p}, i\omega_n)$  are obtained. The spin-polaron excitations spectrum is found from the self-consistent integral equation  $\omega = \varepsilon_p + \Sigma_{(1)}(\vec{p}, \omega) + \Sigma_{(2)}(\vec{p}, \omega)$ . The lower energy band corresponds to the spin polaron quasiparticles of finite radius. The analytical expression for the effective spin-fermion interaction is obtained, and it allows one to calculate  $\Sigma_{(2)}(\vec{p}, i\omega_n)$  in a simple way. It is shown that the spin-polaron spectrum is in a good agreement with the experimental data on cuprates.

The work is supported by the RFBR (nos. 16-02-00304, 18-02-00837) and partly by the Government of Krasnoyarsk Region and the Krasnoyarsk Region Science and Technology Support Fund (nos. 18-42-243002, 18-42-243018), as well as the grant of the President of the Russian Federation (MK-1398.2017.2).

## P27.24 Low Temperature Study of Superconducting Graphite Intercalation Compound BaC<sub>6</sub>

A. Yamaguchi<sup>a</sup>, S. Heguri<sup>b</sup>, N. Kawade<sup>a</sup>, T. Fujisawa<sup>a</sup>, A. Sumiyama<sup>a</sup>, K. Tanigaki<sup>c</sup>, and M. Kobayashi<sup>a</sup>

<sup>a</sup>Graduate School of Material Sciences, University of Hyogo, Japan

<sup>b</sup>Faculty of Engineering, Osaka Institute of Technology, Japan

<sup>c</sup>WPI-AIMR, Tohoku University, Japan

We have recently reported superconductivity in the graphite intercalation compound BaC<sub>6</sub> below  $T_c = 65$  mK<sup>1</sup>. Here we present additional results on the superconducting property of BaC<sub>6</sub>, as well as the experimental details. Two batch of BaC<sub>6</sub> samples were investigated by ac and dc magnetization measurements down to 34 mK. Temperature dependence of ac susceptibility shows a clear drop below 65 mK with the batch dependent Meissner fractions. The zero-temperature upper critical field was estimated as 14 Oe using the WHH model. Dc magnetization measurements revealed the superconducting phase in BaC<sub>6</sub> shows type II behavior but magnetic flux pinning is relatively weak above 34 mK. We will discuss the results in relation to the superconducting CaC<sub>6</sub> with the high superconducting transition temperature of  $T_c = 11.5$  K.

1. S. Heguri, N. Kawade, T. Fujisawa, A. Yamaguchi, A. Sumiyama, K. Tanigaki, and M. Kobayashi, Phys. Rev. Lett. 114, 247201 (2015).

## P27.25 Specific heat and magnetic susceptibility of single-crystal Pd *A low-temperature study*

A. M. Strydom and S. Baidyanath

Highly Correlated Matter Research Group, Physics Department, University of Johannesburg, PO Box 524, Auckland Park 2006, South Africa

Palladium is one of the elements found in many binary and ternary compounds of the strongly correlated electron materials class. Especially in heavy-fermion systems harboring a quantum critical point it becomes essential to map the entropy landscape of quasi-particle excitations at very low temperatures. This requires the ability to isolate the free-electron as well as collective electronic phenomena from the influence of lattice vibrations on the total measurable specific heat. Moreover, when one or more of the elements in a compound possesses a nuclear moment, nuclear hyperfine interactions of magnetic origin may result. Interactions of electrostatic origin may arise on the other should a nucleus with a quadrupole moment be immersed in an electric field gradient.  $^{105}\text{Pd}$  is the only stable isotope of this element having a sizable natural abundance as well as nuclear magnetic and nuclear quadrupole moments. There are several reports on relevant thermal properties of Pd, -see for example Boerstoeel *et al.* and references within [1] for specific heat studies down to 0.4 K. In this study we contribute results of specific heat and *ac*-magnetic susceptibility, both down to 0.05 K, on a high-purity oriented single crystal of Pd and in various applied magnetic fields. The nuclear effects on the specific heat are demonstrated, which now enables these contributions to be isolated from future compound studies.

1. Boerstoeel, B.M., Zwart J.J., and Hansen J. (1971). "The specific heat of palladium, platinum, gold and copper below 30 K.". *Physica* **54** (1971) 442.

## P27.26 Spin-spin interaction as a nature of microwave absorption in superfluid helium

K.A. Chishko and A.S. Rybalko

B. Verkin Institute for Low Temperature Physics and Engineering, Kharkov, Ukraine

Experimentally observed with dielectric disc resonator (DDR) technique [1] microwave absorption-amplification in liquid He II below  $\lambda$ -point has been interpreted theoretically as a phenomenon in electrically active dielectric medium with low-energy excitations near the ground state of the two-electron helium shell due to spin-spin electronic interaction. The registered absorption line is  $f_0 = 180.3\text{GHz}$  at  $T = 1.4\text{K}$ , and  $f_0 = 151.3\text{GHz}$  at  $T = 2.1\text{K}$ . The phenomenon can be summarized as follows: i) the microwave adsorption can be detected definitely only within superfluid phase (above  $\lambda$ -point only weak response can be detected); ii) when the temperature decreases, the adsorption peak shifts to lower frequencies, broadens, decreases in magnitude, and vanishes as approaching  $T_\lambda$ ; iii) it means that we observe a macroscopically cooperative effect caused by interatomic interactions and destroyed by density fluctuations within condensed helium phase; iv) the observed low-temperature phenomenon can be interpreted only at presence of low-energy atomic excitations near the ground state of the helium atom.

To interpret the observed phenomenon we consider relativistic corrections of order  $1/c^2$  to the ground state of  $^4\text{He}$  atom and interatomic bond within  $^4\text{He}_2$  dimer [2]. After averaging over the ground state [2] we obtain two-level spin density matrix  $\hat{H}_{ss} = A_{ss} \hat{\sigma}_a \hat{\sigma}_b$  with  $A_{ss} = 2.015\text{K}$  and the gap between the two states is estimated as  $4A_{ss} = 8.06\text{K} = 167.9\text{GHz}$ . The gap depends on interatomic distances, and it is a basis for spin-phonon coupling which leads to 'roton minimum' on the helium phonon spectrum.

1. A. Rybalko, S. Rubets, E. Rudavskii, et.al., *Phys. Rev. B* **76**, 140503 (2007).
2. K.A.Chishko, *Low Temp. Phys.* **44**, No.10 (2018), online accessible.



## P27.27 Superfluid Brillouin laser

A. Sawadsky, C. Baker, X. He, Y. Sachkou, S. Forstner, Y. Sfindla, G. Harris, and W.P. Bowen

Centre for Engineered Quantum Systems, School of Mathematics and Physics, The University of Queensland, Australia

Enabled by superfluid helium's ultralow viscosity, we propose and experimentally demonstrate a superfluid Brillouin laser with ultra-high gain. Our experimental setup consists of an evanescently coupled silica microresonator covered by a nanometer-thick superfluid  $^4\text{He}$  film [1,2]. Regions of high light intensity inside the resonator pull in more superfluid due to the optical radiation pressure force (*i.e.* the optical gradient force), creating a spatially modulated refractive index grating, in turn scattering more light, leading to spontaneous Brillouin lasing with  $\mu\text{W}$  threshold. In contrast to the commonly studied Brillouin scattering in solids, whereby the light intensity strains the material through electrostrictive forces, this superfluid based approach provides orders of magnitude larger gain. This dramatic enhancement can be intuited by comparing the difficulty of straining a high Young's modulus material such as silica, compared to the ease with which light can continuously deform a (super)fluid interface. This work has applications in terms of ultra-narrow linewidth lasers and optical stirring of quantum fluids.

1. Harris, G. I. *et al.*. "Laser Cooling and Control of Excitations in Superfluid Helium." *Nature Physics* **12**, 8, 2016.
2. Baker, Christopher G. *et al.*. "Theoretical Framework for Thin Film Superfluid Optomechanics: Towards the Quantum Regime." *New Journal of Physics* **18**, 12, 2016.

## P27.28 Cooling of $^3\text{He}$ and $^3\text{He}$ - $^4\text{He}$ mixture beyond the Kapitza resistance bottleneck by adiabatic melting of solid $^4\text{He}$ in liquid $^3\text{He}$

T. S. Riekkii<sup>a</sup>, A. P. Sebedash<sup>b</sup>, and J. T. Tuoriniemi<sup>a</sup>

<sup>a</sup>Low Temperature Laboratory - Department of Applied Physics, Aalto University, Finland

<sup>b</sup>P. L. Kapitza Institute for Physical Problems RAS, Kosygina 2, 119334 Moscow, Russia

One grand open question of low temperature physics concerns the anticipated superfluidity of  $^3\text{He}$  diluted by  $^4\text{He}$ . In an effort to approach the temperature range of interest, we are utilizing a new cooling method which bypasses the huge barrier imposed by the steeply increasing thermal boundary resistance (Kapitza resistance) to any external cooling agent at ultra-low temperatures. In the adiabatic melting method, solid  $^4\text{He}$  is melted and mixed with liquid  $^3\text{He}$  producing cooling power due to the latent heat of mixing. Since the cooling occurs directly in the helium liquid, the thermal boundary resistance is no longer the main factor limiting the final temperature. We study the potential of our method to cool both the isotopic mixture and the pure  $^3\text{He}$  in an experimental cell to temperatures well below  $100\ \mu\text{K}$ . We analyze the significance of the starting conditions, the required efficiency of the melting/mixing process, and the optimal melting procedure in order to achieve the target range of temperatures. These are compared with the observations from a running experiment.

## P27.29 Effects of $^4\text{He}$ film on quartz tuning forks in $^3\text{He}$ at ultra-low temperatures

T. S. Riekkii<sup>a</sup>, J. Rysti<sup>a</sup>, A. P. Sebedash<sup>b</sup>, V. B. Eltsov<sup>a</sup>, and J. T. Tuoriniemi<sup>a</sup>

<sup>a</sup>Low Temperature Laboratory, Department of Applied Physics, Aalto University, Finland

<sup>b</sup>P. L. Kapitza Institute for Physical Problems RAS, Kosygina 2, 119334 Moscow, Russia

Quartz tuning fork oscillators have become widely adopted sensors in liquid helium, often used as thermometers. In liquid  $^3\text{He}$ – $^4\text{He}$  mixtures, the use of quartz tuning forks for thermometry becomes problematic due to the superfluid  $^4\text{He}$  film covering the oscillator surface and making the response non-trivial at dilution refrigerator temperatures [1].

With liquid  $^3\text{He}$ – $^4\text{He}$  mixture at low temperatures, all surfaces of the system are coated with  $^4\text{He}$ , including the surface of the oscillator residing in the pure  $^3\text{He}$  phase of the phase separated mixture. The thin layer of  $^4\text{He}$  becomes superfluid at temperatures below 100 mK [2].

In pure  $^3\text{He}$  at ultra-low temperatures, the tuning fork oscillator response is expected to saturate when the dissipation caused by the superfluid medium becomes substantially smaller than the internal dissipation of the oscillator. Even with small amounts of  $^4\text{He}$  present, however, we have observed saturation, with rather poor Q-values, already at significantly higher temperatures than anticipated, where we have other indicators to prove that the  $^3\text{He}$  liquid is still cooling. Furthermore, we have found that this anomalous behavior has a rather strong pressure dependence, and it practically disappears above the crystallization pressure of  $^4\text{He}$ . Long time-dependent anomalous fork response is also observed in a sample installed in a rotating cryostat after change of the angular velocity. We suggest that the anomalous behavior originates from the superfluid  $^4\text{He}$  film on the oscillator surface.

1. Boldarev *et al.*, *Instrum. Exp. Tech.* **54**, 740 (2011). 2. Agnolet *et al.*, *Phys. Rev. B* **39**, 8934 (1989).

## P27.30 Fabrication of Micro-slit Structures for Studies of Topological Properties of Quasi-two Dimensional Superfluid $^3\text{He}$

T. Tani<sup>a</sup>, S. Murakawa<sup>b</sup>, R. Wada<sup>a</sup>, K. Kaiya<sup>a</sup>, K. Yamada<sup>c</sup>, K. Itoh<sup>c</sup>, Y. Mita<sup>d</sup>, and K. Shirahama<sup>a</sup>

<sup>a</sup>Department of Physics, Keio University, Yokohama, Japan

<sup>b</sup>Cryogenic Research Center, University of Tokyo, Tokyo, Japan

<sup>c</sup>Department of Applied Physics and Physico-Informatics, Yokohama, Japan

<sup>d</sup>Department of Electrical Engineering and Information Systems, Tokyo, Japan

Topological properties of Superfluid  $^3\text{He}$  confined in microstructures have been attracting much interest. Some experiments have been performed using closed micro slab geometries. Nowadays, the development of semiconductor processing techniques enable us to fabricate deep micro slit structures with through-hole. Here we report fabrication of multiple deep micro slit structures where dimensions of each slit are  $1\mu\text{m}\times 100\mu\text{m}\times 50\mu\text{m}$ . Using such micro slit structures, we will perform a direct flow experiment to detect phase slippage by (half)quantum vortices<sup>1</sup>, and ultrasound studies of edge related surface collective (Higgs) modes<sup>2,3</sup>. We will discuss fabrication techniques including deep reactive ion etching (BOSCH process) and progress of preparation of superfluid experiments.

1. S. Backhaus, *et al.*, *Nature* **392**, 687 (1998)

2. Takeshi Mizushima and J. A. Sauls, arXiv preprint, arXiv:1801.02277 (2018)

3. Takeshi Mizushima, Masatoshi Sato, and Kazushige Machida, *Phys. Rev. Lett.* **109**, 165301 (2012)

## P27.31 Development of a sub-mK Continuous Nuclear Demagnetization Refrigerator

D. Schmoranzner, R. Gazizulin, S. Triqueneaux, E. Collin, and A. Fefferman

Institut Néel, CNRS and Université Grenoble Alpes

Demagnetization techniques are well-established methods of refrigeration capable of covering the entire temperature range from 300 K to ultra low temperatures, while avoiding the use of cryoliquids or moving parts. In particular, adiabatic nuclear demagnetization of Cu or van Vleck paramagnets has become an indispensable technique for reaching  $\mu\text{K}$  temperatures, despite the limited amount of experimental time available at very low T on standard demagnetization setups.

We present the development of a two-stage  $\text{PrNi}_5$  continuous demagnetization refrigerator in CNRS Grenoble and simulate its performance. The thermal model used in the simulations is presented in detail including the likely sources of heating. We demonstrate the effects of the heat conductivity of the  $\text{PrNi}_5$  and of the critical thermal links including superconducting heat switches. While the internal thermal resistance of the  $\text{PrNi}_5$  was not included in the simulation in [1], we account for the dependence of cooling power on the  $\text{PrNi}_5$  rod diameter. Entropy production due to external heat leaks, vibrational heating and eddy currents is compared on both  $\text{PrNi}_5$  demagnetization stages using estimates obtained in previous experiments. Our simulations show that if extreme care is taken to minimize the thermal resistance between the nuclear stages, a sample temperature of 1 mK can be maintained under a 20 nW heat load.

We acknowledge support from the ERC StG grant UNIGLASS No. 714692 and ERC CoG grant ULT-NEMS No. 647917.

[1] Ryo Toda et al 2018 *J. Phys.: Conf. Ser.* **969** 012093

## P27.32 Development of a Compact and Low Heat-dissipation Shielded Superconducting Magnet Usable at Sub-mK Temperature

S. Takimoto<sup>a,b</sup>, R. Toda<sup>b</sup>, S. Murakawa<sup>a,b</sup>, and Hiroshi Fukuyama<sup>a,b</sup>

<sup>a</sup>Department of Physics, The University of Tokyo, Japan

<sup>b</sup>Cryogenic Research Center, The University of Tokyo, Japan

The sub-mK environment is indispensable for studies of superfluid  $^3\text{He}$ . Recently, it became desirable in studies of  $^4\text{He}$  as well, for example, 1D superfluidity and quantum phase transitions in nanopores. To reduce barriers for sub-mK experiments, we are developing a compact and continuous NDR (CNDR) with two  $\text{PrNi}_5$  stages enclosed in small shielded superconducting (SC) magnets ( $B_{\text{max}} = 1.2$  T, *i.d.* = 22 mm, *o.d.* = 34 mm, 161 mm long) in vacuum.<sup>1</sup> The most standard magnetic shielding for such compact magnets is to combine a SC shield and an active shield, a counter-wound magnet.<sup>2</sup> Instead, based on numerical calculations of the field distribution under various high-permeability materials, we decided to use a FeCoV shield. The numerical calculation indicates that the magnetic field is 0.1 mT at a 56 mm radius from the center of the magnet. The SC wire generates heat because of the hysteresis of the magnetization curve of the wire. Therefore, we also simulated the  $T$  distribution inside the magnet and a copper bobbin based on the heat dissipation in the SC wire, and the result indicates that we can maintain the magnet temperature less than 0.86 K by thermally anchoring to the still (0.8 K) of a dilution refrigerator. We will report details of the design and measured performances of a magnet we recently assembled.

1. Toda, R. *et al.*, *J. Phys.: Conf. Ser.* **969** 012093 (2018).

2. Israelsson, U. E. and Gould, C. M., *Rev. Sci. Instrum.* **55**, 1143 (1984).

### P27.33 Melting curve thermometry in $^3\text{He}$ - $^4\text{He}$ mixtures at ultra-low temperatures.

A. Sebedash

Russian Academy of Sciences, P.L. Kapitza Institute for Physical Problems, Moscow, Russian Federation

Exploiting the properties of the melting curve of pure  $^3\text{He}$  for high precision thermometry at millikelvin temperatures can be applied also to isotopic mixtures of  $^3\text{He}$  in  $^4\text{He}$ . At sufficiently low temperatures equilibrium pressure in mixture at univariant curve depends solely on temperature. Melting curve thermometry have been demonstrated down to 0.5 mK.<sup>1</sup> Further applicability of the technique to lower temperatures becomes difficult because of decrease of sensitivity and severe problems with thermalization. We present new design of high sensitive pressure gauge, which potentially permit to reach 10 % sensitivity of temperature measurements at 0.1 mK. To increase sensitivity we developed differential pressure gauge with very thin membrane as flexible element. The membrane is supported from opposite side by unsaturated mixture at stabilized pressure. We discuss necessary conditions for appropriate behavior and present results of low temperature tests.

1.A. P. Sebedash, J. T. Tuoriniemi, S. T. Boldarev, E. M. Pentti, and A. J. Salmela, *AIP Conf. Proc.* **850**, 1591 (2006)

### P27.34 Development of cryogenic C-MOS and pHEMT amplifiers

H. Tanabe, K. Obara, H. Yano, and O. Ishikawa

Graduate School of Science, Osaka City University, Japan

In low temperature experiments, in general, sensors are located inside a cryostat and are connected to an amplifier which is located at the room temperature with long wires. When levels of current or voltage signals are small, the length of the wire may cause severe degradation of the signal; the most lucid reason is an incompleteness of a shielding, that is, the pickup noise. Second reason arises when one try to use a resonance technique that is sensitive to the resistance or the stray capacitance. These effects affect the signal-to-noise ratio of a read out of high impedance sensors such as a photo-diode and a quartz tuning-fork. In this sense, the length of the cable should be as short as possible to have better signal quality. The fundamental solution is to put the preamplifier into the cryostat. In addition, the Nyquist's thermal noise of the amplifier itself can be reduced by cooling the amplifier down. Hayashi *et al.* built up the trans-impedance amplifier using a commercially available C-MOS operational amplifier that could operate at 10 K [1]. On the other hand, cold amplifiers using HEMT devices have vigorously been developed in a high-frequency experiment, such as NMR and Microwave experiments. We have succeeded in developing the cryogenic amplifier using pHEMT devices[2]. In this presentation, we will show the details of a high-impedance C-MOS amplifier and a high-frequency pHEMT amplifier that can be used in either in the room temperature, liquid nitrogen and liquid helium.

[1] K. Hayashi, K. Saitoh, Y. Shibayama, K. Shirahama, *J. Phys. C: Conf. Ser.* **150**, 012016 (2009)

[2] T.Hirata, T.Okazaki, K.Obara, H.Yano, and O.Ishikawa, *J. of Low Temp. Phys.*, **187**, 596-601 (2017)

**July 28 (Saturday)**



# July 28 (Saturday) Oral Presentations

## O28.1 Topological matter:

### Weyl fermions, Higgs bosons, quantum gravity and room- $T$ superconductivity

G. E. Volovik

Low Temperature Laboratory, Aalto University, Finland  
Landau Institute for Theoretical Physics, Chernogolovka, Russia

A-phase and polar phase of superfluid  $^3\text{He}$  – gapless topological superfluids with Weyl fermions and Dirac nodal lines – have synthetic gauge fields and gravity, exotic topological defects, such as Alice strings, and Higgs modes. We discuss here some topics of the recent experimental and theoretical studies of these superfluids. This includes the Lifshitz transitions to antispacetime<sup>1</sup> and to type-II Weyl fermions behind the black hole horizon,<sup>2</sup> transition to Euclidean metric,<sup>3</sup> interplay of real-space and momentum-space topologies in fermionic glasses,<sup>4</sup> the flat band route to room temperature superconductivity,<sup>5</sup> etc.

1. Nissinen, J., Volovik, G. E. (2018). “Dimensional crossover of effective orbital dynamics in polar distorted  $^3\text{He}$ -A: Transitions to anti-spacetime”. *Phys. Rev. D* **97**, 025018.
2. Volovik, G. E. (2016). “Black hole and Hawking radiation by type-II Weyl fermions”. *JETP Lett.* **104**, 645.
3. Nissinen, J., Volovik, G. E. (2017). “Effective Minkowski-to-Euclidean signature change of the magnon BEC pseudo-Goldstone mode in polar  $^3\text{He}$ ”. *JETP Lett.* **106**, 234.
4. Volovik, G. E., Rysti, J., Mäkinen, J. T., Eltsov, V. B. (2018). “Spin, orbital, Weyl and other glasses in topological superfluids”. arXiv:1806.08177.
5. Volovik, G. E. (2018). “Graphite, graphene and flat band superconductivity”. *JETP Lett.* **107**, 516.

PLENARY TALK

## O28.2 Higgs mode in conventional and unconventional superconductors

R. Shimano

Cryogenic Research Center, The University of Tokyo, Tokyo, Japan

The study of collective modes is a fascinating issue as it provides deep insight into the properties of quantum fluids. In superconductors, two collective modes are expected to emerge associated with the spontaneous breaking of  $U(1)$  symmetry: the phase mode and the amplitude mode. The later one is recently referred to as the Higgs mode from its close relation to the Higgs boson in particle physics, where the particle-hole symmetry effectively plays a role of Lorentz invariance in the high energy physics. Although Higgs mode has long evaded the experimental observation because it does not couple to electromagnetic field, recently we have observed the Higgs mode-oscillation in a s-wave superconductor, NbN, by using the ultrafast terahertz spectroscopy technique.<sup>1,2</sup> The experiments are extended to a multiband superconductor,  $\text{MgB}_2$ , and unconventional d-wave high- $T_c$  cuprate superconductors.<sup>3</sup> The comprehensive studies of the Higgs mode will be reported in those conventional and unconventional superconductors.

1. R. Matsunaga, Y. I. Hamada, K. Makise, Y. Uzawa, H. Terai, Z. Wang, and R. Shimano, *Phys. Rev. Lett.* **111**, 057002 (2013).
2. R. Matsunaga, N. Tsuji, H. Fujita, A. Sugioka, K. Makise, Y. Uzawa, H. Terai, Z. Wang, H. Aoki, and R. Shimano, *Science* **345**, 1145 (2014).
3. K. Katsumi, N. Tsuji, Y. I. Hamada, R. Matsunaga, J. Schneeloch, R. D. Zhong, G. D. Gu, H. Aoki, Y. Gallais, and R. Shimano, *Phys. Rev. Lett.* **120**, 117001 (2018).

INVITED TALK

### O28.3 Collective excitations of a superfluid Fermi gas in the BEC-BCS crossover

J. Tempere, H. Kurkjian, and S. N. Klimin

TQC, Antwerp University, Antwerpen, Belgium

Experimental techniques such as Bragg spectroscopy have recently been applied to superfluid Fermi gases, and allowed to start mapping out the dispersion of the collective modes in superfluid Fermi gases. The low-energy collective mode that starts as a sound mode, and a theoretically predicted gapped collective mode often referred to as the Higgs mode, provide sensitive benchmarks for the various microscopic models of pairing used to describe fermionic superfluidity at finite temperatures in the crossover regime between a Bose condensate of molecules and a BCS state of weakly bound pairs. The fermionic superfluid also exhibits a pair-breaking continuum in its excitation spectrum, starting at twice the pair-breaking gap. As one crosses over from the BEC limit into the BCS regime, the onset of this continuum is lowered in energy and this affects the collective branch present below the continuum. Additionally a gapped collective mode develops inside the continuum. Theoretically, these collective modes can be related to the poles of the two-particle (or pair) propagator. Within the path-integral formalism this in turn corresponds to the zeroes of the fluctuation matrix. In this contribution, I review some recent experimental developments, and present our theoretical description of the collective modes, comparing them to experiment. We apply both the RPA formalism and the path-integral formalism and show that these lead to the same theoretical results. Applying Nozières' prescription for analytic continuation through a branch cut associated with the continuum, we identify the zeroes of the fluctuation matrix, taking the coupling between amplitude and phase fully into account. Besides the dispersion we also obtain the damping of the modes, study how the modes evolve along the BEC-BCS crossover, and investigate their temperature dependence.

INVITED TALK

### O28.4 Neutron Star Core: Densest State of Matter

Tetsuo Hatsuda

RIKEN Interdisciplinary Theoretical and Mathematical Sciences Program (iTHEMS), Japan

We review the equation of state of matter in neutron stars from the liquid nuclear matter to the quark regime at high density. We focus in detail on the question of how quark matter appears in neutron stars, and how it affects the equation of state. We describe equations of state useful for interpretation of both electromagnetic and gravitational observations, reviewing the emerging picture of hadron-quark continuity in which hadronic matter turns relatively smoothly, with at most only a weak first order transition, into quark matter with increasing density.<sup>1</sup>

Also, we discuss how vortices in dense superfluid hadronic matter can connect to vortices in superfluid quark matter, as in rotating neutron stars, focusing on the extent to which quark-hadron continuity can be maintained.<sup>2</sup>

1. G. Baym, T. Hatsuda, T. Kojo, P. D. Powell, Y. Song and T. Takatsuka, "From hadrons to quarks in neutron stars: a review," *Rept. Prog. Phys.* **81**, no. 5, 056902 (2018) [arXiv:1707.04966 [astro-ph.HE]].

2. M. G. Alford, G. Baym, K. Fukushima, T. Hatsuda and M. Tachibana, "Continuity of vortices from the hadronic to the color-flavor locked phase in dense matter," arXiv:1803.05115 [hep-ph].

PLENARY TALK

## O28.5 Neutron Star Crusts as Low Temperature Laboratories

Kei Iida

Department of Mathematics and Physics, Kochi University, Japan

Neutron stars, stellar remnants of core-collapse supernova explosions, were first discovered as radio pulsars. The salient features of the neutron star lie in its compactness and cooling, which give us an opportunity of “observing” matter at extremely high density and low temperature. In this talk, I would like to focus on the crustal part of the star, which contains a lattice of nuclei, superfluid neutrons, and possibly liquid crystalline structures of a nuclear matter liquid-gas mixture, and give implications for pulsar glitches and magnetar quasi-periodic oscillations.

INVITED TALK

## O28.6 Anomaly-Induced Transport in Weyl Superconductors and Neutron Stars

T. Mizushima

Department of Materials Engineering Science, Osaka University, Toyonaka, Osaka 560-8531, Japan

The Bogoliubov quasiparticles of Weyl superconductors and superfluids are a condensed matter realization of Weyl fermions that are considered as the fundamental building block of quantum field theory. In condensed matter, the chiral anomaly implies that parallel electric and magnetic fields give rise to the anomalous violation of the separate number conservation laws of Weyl fermions with different chiralities. Weyl fermions in Weyl semimetals bring about anomalous transport phenomena such as chiral magnetic effect and negative magnetoresistance. As the Weyl fermions in superconductors emerge in the particle-hole space, however, they are not responsible for real electromagnetic fields. Here I will present the anomalous transport due to chiral anomaly in Weyl superconductors and neutron stars, where the former includes  ${}^3\text{He-A}$ ,  $\text{UPt}_3$ ,  $\text{URu}_2\text{Si}_2$ , and  $\text{U}_{1-x}\text{Th}_x\text{Be}_{13}$ . In this talk, I will show that a nontrivial torsional field, which is an emergent magnetic field acting on Weyl fermions, can be generated by vortex texture and strain and leads to negative thermal magnetoresistivity and torsional chiral magnetic effect.<sup>1</sup> I will also discuss the topological aspect and Weyl superfluidity of  ${}^3P_2$  superfluids in the dense core of neutron stars.<sup>2,3</sup>

This work is in collaboration with T. Kobayashi, T. Matsushita, A. Tsuruta, S. Fujimoto, and M. Nitta.

1. T. Kobayashi, T. Matsushita, T. Mizushima, A. Tsuruta, and S. Fujimoto, arXiv:1806.00993.
2. T. Mizushima, K. Masuda, and M. Nitta, Phys. Rev. B **95**, 140503(R) (2017).
3. T. Mizushima and M. Nitta, Phys. Rev. B **97**, 024506 (2018).

INVITED TALK



## O28.7 Exploring superfluid $^3\text{He}$ universe with coherent bosons

V. B. Eltsov

Department of Applied Physics, Aalto University, Finland

Bose-Einstein condensation of quasiparticles brings new macroscopic quantum systems to laboratory. In such systems quasiparticles are externally pumped, but are sufficiently long-lived to form a coherent state. This talk presents an overview of recent findings made using BEC of quantized spin waves (magnons) in superfluid  $^3\text{He}$ . Experimentally such condensates are manifested via coherently precessing magnetization. Free precession breaks continuous time-translation symmetry and the magnon BEC is identified as a time crystal.<sup>1</sup> The discrete time-translation symmetry under pumping is also broken in incommensurate way, providing the first realization of time quasicrystals. Since magnon condensates possess spin superfluidity, they can be called time supersolids. Moreover, the magnon BEC in  $^3\text{He-B}$  is the first experimental demonstration of a Q-ball<sup>2</sup> – self-bound bosonic object from high-energy physics. Q-balls were speculatively used to explain e.g. baryogenesis and dark matter. Now they have been observed moving and interacting in a  $^3\text{He-B}$  sample at temperatures below  $200\ \mu\text{K}$ .

Magnon BEC and its Nambu-Goldstone (NG) mode, which is a phonon originating from breaking of time-translation symmetry in a time crystal, are also found<sup>3</sup> in the polar phase of  $^3\text{He}$ . By tilt of magnetic field, one can tune velocity of the NG bosons down to a complete stop.<sup>4</sup> This gives a possibility to simulate experimentally a black-hole horizon. These new features build on long coherence times, which have turned magnon condensates into ultra-sensitive probes of relaxation sources in studies of topological objects and various bosonic and fermionic excitations in topological superfluid  $^3\text{He}$ .

<sup>1</sup>Autti et al, PRL **120**, 215301 (2018).

<sup>3</sup>Autti et al, PRL in print (2018), arXiv:1711.02915.

<sup>2</sup>Autti et al, PRB **97**, 014518 (2018).

<sup>4</sup>Nissinen & Volovik, JETP Lett. **106**, 234 (2017).

PLENARY TALK

## O28.8 Phase diagram of superfluid $^3\text{He}$ in quasi-two-dimensional limit

P. J. Heikkinen<sup>a</sup>, A. Casey<sup>a</sup>, L. V. Levitin<sup>a</sup>, X. Rojas<sup>a</sup>, A. Vorontsov<sup>b</sup>, T. S. Abhilash<sup>c</sup>, N. Zhelev<sup>c</sup>, J. M. Parpia<sup>c</sup>, and J. Saunders<sup>a</sup>

<sup>a</sup>Royal Holloway, University of London, Department of Physics, Egham, United Kingdom

<sup>b</sup>Montana State University, Department of Physics, Bozeman, United States

<sup>c</sup>Cornell University, Department of Physics, Ithaca, United States

Order parameter of unconventional p-wave superfluid  $^3\text{He}$  is suppressed under high level of confinement due to the anisotropic surface pair-breaking dominating the superfluid properties. In our SQUID-NMR experiments we confine  $^3\text{He}$  in nanofabricated slab-shaped cavities of height  $D$  comparable to the pressure-tunable coherence length  $\xi_0$ . Well-controlled effective confinement  $D/\xi_0$  together with the boundary condition for surface scattering of quasiparticles define changes both in the superfluid transition temperature  $T_c$  and in the stability between various phases. In a cavity with  $D \sim 200\ \text{nm}$ , we have confirmed the stability of chiral A phase over time-reversal invariant B phase at all pressures down to zero pressure. Tuning the scattering boundary condition between diffuse and specular by adding a controlled amount of  $^4\text{He}$  impurities affects the suppression of  $T_c$  and superfluid energy gap in a good agreement with quasiclassical theory. The largest, unexpected, suppression observed in a sample of pure  $^3\text{He}$  likely indicates additional magnetic channel for scattering. In ongoing experiments, where  $D \sim 100\ \text{nm}$ , we have found the A phase to remain stable at  $D/\xi_0 > 2$  with both diffuse boundary condition and pure  $^3\text{He}$ . The ability to create specular boundary condition allows us to probe superfluidity down to  $D/\xi_0 \approx 1.5$ , thus helping to answer the still open question whether the chiral A phase remains stable approaching the quasi-two-dimensional limit or whether, for example, the time-reversal-invariant planar phase emerges. Any of these outcomes will open a new range of intriguing research possibilities.

INVITED TALK

## O28.9 Superfluidity beyond the Landau Velocity in $^3\text{He-B}$ and Dynamics of Surface States

S. Autti<sup>a</sup>, A.M. Guénault<sup>a</sup>, R.P. Haley<sup>a</sup>, A. Jennings<sup>a</sup>, S. Kafanov<sup>a</sup>, G.R. Pickett<sup>a</sup>, R. Schanen<sup>a</sup>, A.A. Soldatov<sup>b</sup>, V. Tsepelin<sup>a</sup>, and D.E. Zmeev<sup>a</sup>

<sup>a</sup>Department of Physics, Lancaster University, Lancaster, UK

<sup>b</sup>P.L. Kapitza Institute for Physical Problems of Russian Academy of Sciences, Moscow, Russia

Recently, it has been shown that superfluidity in  $^3\text{He-B}$  can survive in flows past objects at velocities far exceeding the critical Landau value. The model supporting this phenomenon suggests that the Andreev-bound states on the surface of the moving object are emitted into bulk, causing dissipation only during acceleration. Meanwhile, a mechanism for breaking bulk Cooper pairs does not appear to exist for arbitrarily fast uniform motion in our experimental configuration.

Our new experimental results imply that we can empty the most energetic bound states into bulk in a controllable manner and then observe as they are replenished. We were surprised to find the typical lifetime of the surface states to be around 6 milliseconds. Our measurements also suggest that this lifetime does not change significantly when the surface of the accelerated object is covered with 2.5 monolayers of  $^4\text{He}$ . The emission of the surface states into bulk stops below the critical Landau velocity, in accord with our model.

The experiments are performed in the temperature range of 150-230 microkelvin, where the bulk Bogoliubov excitations are ballistic. Our measurements provide insight into the dynamics of interaction between the gas of Bogoliubov excitations in a 3D topological superfluid and the corresponding gas of 2D edge states.

INVITED TALK

## O28.10 Novel Josephson and Proximity Effect using Triplet Superconductors

D. Manske

Max Planck Institute for Solid State Research, Heisenbergstrasse 1, 70569 Stuttgart, Germany

Max Planck – UBC – U Tokyo Center for Quantum Materials, 70569 Stuttgart, Germany

Josephson junctions with magnetic tunneling barriers provide an excellent opportunity to observe the interplay of ferromagnetism and superconductivity in a controlled setting. Using various approaches, we predict a universal  $0-\pi$  transition (sign reversal) of the charge current as the orientation of the barrier magnetic moment is varied. Furthermore, in the theoretical study of Josephson junctions, it is usually assumed that the properties of the tunneling barrier are fixed. This assumption breaks down when considering tunneling between two triplet superconductors with misaligned d-vectors in a TFT-junction (triplet-ferromagnet-triplet). Such a situation breaks time-reversal symmetry, which radically alters the behavior of the junction. A further consequence of the d-vector misalignment is the appearance of a Josephson spin current. In particular, we study the interplay of spin and orbital degrees of freedom in a triplet superconductor-ferromagnet junction [3]. Depending on the number of helical modes, the capacity of carrying spin and charge currents is shown to be directly related to the amplitude and orientation of the ferromagnetic magnetization with respect to the superconducting d-vector.

Recent experimental progress allows fabricating interfaces with the triplet superconductor  $\text{Sr}_2\text{RuO}_4$  and the ferromagnet  $\text{SrRuO}_3$  so that predictions for a long-range proximity effect could be verified. Since thin superconducting films, grown in a controlled way by MBE, of  $\text{Sr}_2\text{RuO}_4$  are now available, heterostructures such as TFT-junctions or triplet SQUIDS are now in reach. We compare our theoretical results with existing data and contrast them with junctions based on singlet superconductors.

INVITED TALK

## O28.11 Impurity Induced Anomalous Thermal Hall Effect in Chiral Superconductors

V. Ngampruetikorn and J. A. Sauls

Department of Physics and Astronomy and Center for Applied Physics and Superconducting Technology (CAPST), Northwestern University, Evanston, IL 60208, USA

We report theoretical results for the electronic contribution to thermal transport for chiral superconductors belonging to even or odd-parity  $E_1$  and  $E_2$  representations of the tetragonal and hexagonal point groups. Chiral superconductors exhibit novel transport properties that depend on the topology of the order parameter, topology of the Fermi surface, the spectrum of bulk Fermionic excitations, and – as we highlight – the structure of the impurity potential. The anomalous thermal Hall effect is shown to be sensitive to the structure of the electron-impurity t-matrix, as well as the winding number,  $\nu$ , of the chiral order parameter,  $\Delta(p) = |\Delta(p)| e^{i\nu\phi_p}$ . For heat transport in a chiral superconductor with isotropic impurity scattering, i.e., point-like impurities, a transverse heat current is obtained for  $\nu = \pm 1$ , but vanishes for  $|\nu| > 1$ . This is not a universal result. For finite-size impurities with radii of order or greater than the Fermi wavelength,  $R \geq \hbar/p_f$ , the thermal Hall conductivity is finite for chiral order with  $|\nu| \geq 2$ , and determined by a specific Fermi-surface average of the differential cross-section for electron-impurity scattering. Our results also provide quantitative formulae for interpreting heat transport experiments for superconductors predicted to exhibit broken time-reversal and mirror symmetries.

INVITED TALK

## O28.12 Parity-Time-Symmetric Optics, extraordinary momentum and spin in evanescent waves, and the quantum spin Hall effect of light

Franco Nori

RIKEN, Japan, and the University of Michigan, USA

Optical systems combining balanced loss and gain provide a unique platform to implement classical analogues of quantum systems described by non-Hermitian parity-time (PT)-symmetric Hamiltonians [1]. We report PT-symmetry breaking in coupled optical resonators. We observed non-reciprocity in the PT-symmetry-breaking phase due to strong field localization, which significantly enhances nonlinearity. Our results could lead to a new generation of synthetic optical systems enabling on-chip manipulation and control of light propagation. By analyzing fundamental spin properties of Maxwell waves, we show [2] that free-space light exhibits an intrinsic quantum spin Hall effect-surface modes with strong spin-momentum locking. Our findings illuminate the unusual transverse spin in evanescent waves and explain recent experiments that have demonstrated the transverse spin-direction locking in the excitation of surface optical modes. This reveals analogies with topological insulators for electrons. See also [3].

[1] B. Peng, et al., Parity-time-symmetric whispering-gallery microcavities, Nat. Phys. 10, 394 (2014).

[2] K.Y. Bliokh, D. Smirnova, F. Nori, Quantum spin Hall effect of light, Science 348, 1448(2015).

[3] Related work can be found in: <https://dml.riken.jp/pub/optics/>

INVITED TALK

# July 28 (Saturday) Poster Presentations

## P28.1 Superfluid $^3\text{He}$ in ultra dense nematic aerogel

V. V. Dmitriev<sup>a</sup>, A. A. Soldatov<sup>a,b</sup>, and A. N. Yudin<sup>a</sup>

<sup>a</sup>P.L. Kapitza Institute for Physical Problems of RAS, 119334, Moscow, Russia

<sup>b</sup>Moscow Institute of Physics and Technology, 141700, Dolgoprudny, Russia

A new superfluid phase of  $^3\text{He}$ , the polar phase, was discovered in nematic aerogel (nafen) [1]. Nafen consists of strands aligned along a specific direction. It leads to an anisotropic scattering of  $^3\text{He}$  quasiparticles that makes the polar phase favorable [2]. Commercial nafen has density  $72\text{ mg/cm}^3$  and porosity 98.2% which is close to that of silica aerogel mostly used to investigate impurity effects in superfluid  $^3\text{He}$ . We managed to obtain much denser nematic aerogel from this nafen by a simple technique described in Ref. [3] having in result density  $910\text{ mg/cm}^3$  and porosity 78%. Here we report results of NMR experiments with superfluid  $^3\text{He}$  in the sample of such aerogel. If we preplate nafen with complete  $^4\text{He}$  coverage to avoid any paramagnetic  $^3\text{He}$  on the nafen strands we observe only the polar phase with a rather high  $T_c$  suppression. However, in experiments with pure  $^3\text{He}$  no superfluidity of  $^3\text{He}$  is indicated. We point to a great importance of magnetic scattering in the observed phenomena and confirm it in experiments with smaller  $^4\text{He}$  coverages [4].

[1] V.V. Dmitriev, A.A. Senin, A.A. Soldatov, and A.N. Yudin, Phys. Rev. Lett. **115**, 165304 (2015).

[2] K. Aoyama and R. Ikeda, Phys. Rev. B **73**, 060504 (2006).

[3] V.V. Volkov, V.V. Dmitriev, D.V. Zolotukhin, A.A. Soldatov, and A.N. Yudin, Instrum. Exp. Tech. **60**, 737 (2017).

[4] V.V. Dmitriev, A.A. Soldatov, and A.N. Yudin, Phys. Rev. Lett. **120**, 075301 (2018).

## P28.2 Half-quantum vortices and Kibble walls in the polar-distorted phases of superfluid $^3\text{He}$

J. Rysti, V. B. Eltsov, J. T. Mäkinen, J. Nissinen, G. E. Volovik, and K. Zhang

Low Temperature Laboratory, Department of Applied Physics, Aalto University, Finland

When liquid  $^3\text{He}$  is placed in a nanostructured confinement, new superfluid phases are stabilized: the polar phase with a Dirac nodal line, the polar-distorted A phase with Weyl nodal points, and the fully gapped polar-distorted B phase. Topologically stable half-quantum vortices (HQVs) have been recently discovered in the polar phase [1]. In the distorted B phase the HQVs are no longer protected by topology. Remarkably, we have observed that HQVs created in the polar phase survive successive second- and first-order phase transitions from the polar phase to the A and then to the B phases. This is proven by the recovery of the NMR signature of HQVs upon returning to the polar phase.

When HQVs are taken through the phase transitions, new phenomena emerge. Walls bounded by strings can appear after two successive symmetry-breaking transitions, as was originally suggested in cosmology [2]: After the first transition, linear defects (strings or quantized vortices) are topologically stable, while after the second transition they become unstable and form boundaries of domain walls. We report the first observation of such Kibble walls. In our case they emerge between HQVs in the polar-distorted B phase of  $^3\text{He}$ . Kibble walls does not contract due to the strong pinning of HQVs in the confining medium and leave a characteristic signature in the NMR response of the B phase.

Stabilization of HQVs in the A phase can later be extended to 2D systems where  $p_x + ip_y$  order parameter allows core-bound states with non-Abelian statistics – an important ingredient of topological quantum computing.

1. Autti *et al*, Phys. Rev. Lett. **117**, 255301 (2016).

2. Kibble *et al*, Phys. Rev. D **26**, 435 (1982).

## P28.3 The Vortex-Core Phase Transition in Rotating Superfluid $^3\text{He-B}$

Robert C. Regan, J. J. Wiman, and J. A. Sauls

Department of Physics and Astronomy, Northwestern University, USA

Based on a strong-coupling Ginzburg-Landau (GL) theory that accurately accounts for the relative stability of the bulk A and B phases in  $^3\text{He}$ ,<sup>1</sup> we calculate the structure of vortices in rotating superfluid  $^3\text{He-B}$  and determine the pressure-temperature phase diagram for the regions of stability of the double-core and A-phase-core vortices. The equilibrium vortex phase at high pressure is the axi-symmetric A-phase-core vortex, while at low pressure the equilibrium state is the non-axi-symmetric double-core vortex. The vortex-core phase transition line in the pressure-temperature plane is calculated for both zero field and an applied field of  $\vec{H} = 300G\hat{\Omega}$  parallel to the axis of rotation. We compare our results with the experimentally determined vortex-core phase diagram.<sup>2</sup> We also compare our calculations for the order parameter, vortex-core magnetization, spin- and mass currents of these topological defects with earlier results reported by E. Thuneberg.<sup>3</sup>

1. *Strong-Coupling & the Stripe Phase of  $^3\text{He}$* , JLTP, 184, 1054 (2016), J. J. Wiman and J. A. Sauls.
2. *Magnetic Vortices in Superfluid  $^3\text{He-B}$* , PRL 51, 1362, (1983), P. J. Hakonen, et al.
3. *Ginzburg-Landau theory of vortices in superfluid  $^3\text{He-B}$* , PRB, 36, 3583, (1987), E. Thuneberg.

## P28.4 Capture of Xe and Ar atoms by quantised vortices in $^4\text{He}$ nanodroplets

François Coppens<sup>a</sup>, Francesco Ancilotto<sup>b</sup>, Manuel Barranco<sup>cd</sup>, Nadine Halberstadt<sup>a</sup>, and Martí Pi<sup>cd</sup>

<sup>a</sup>Université de Toulouse, UPS, CNRS UMR 5589, LCAR-IRSAMC, F-31062 Toulouse Cedex 09, France

<sup>b</sup>Dipartimento di Fisica e Astronomia ‘Galileo Galilei’, CNISM, Università di Padova, 35122 Padova; CNR-IOM Democritos, 34136 Trieste, Italy

<sup>c</sup>Departament FQA, Facultat de Física, Universitat de Barcelona, 08028 Barcelona, Spain

<sup>d</sup>Institute of Nanoscience and Nanotechnology (IN2UB), Universitat de Barcelona, Spain

We present a computational study<sup>[1]</sup>, based on time-dependent Density Functional theory, of the real-time interaction and trapping of Ar and Xe atoms in superfluid  $^4\text{He}$  nanodroplets, either pure or hosting quantised vortex lines. We investigate the phase-space trajectories of the impurities for different initial conditions and describe in detail the complex dynamics of the droplets during the capture of the impurities. We show that the interaction of the incoming atom with the vortex core induces large bending and twisting excitations of the vortex core lines, including the generation of helical Kelvin waves propagating along the vortex core. We have also calculated the stationary configurations for a  $^4\text{He}$  droplet hosting a 6-vortex array whose cores are filled with Ar atoms. As observed in recent experiments, we find that the doping adds substantial rigidity to the system; the doped vortex array remains stable, even at low values of the angular velocities. Moreover, we analysed the collision between a droplet hosting a linear vortex dipole and a Xe atom. Finally, we present preliminary results of ongoing work: an isotropic head-on collision between 6 Ar atoms and a vortex-free He droplet, and a droplet hosting a ring of 6 linear vortices.

[1] F. Coppens, F. Ancilotto, M. Barranco, N. Halberstadt, M. Pi, PCCP **19**, 24805 (2017)

## P28.5 Universal Drag Force Scaling in Oscillatory Flows of He II

D. Schmoranzler<sup>b</sup>, M. J. Jackson<sup>a</sup>, J. Bahyl<sup>a</sup>, S. Midlik<sup>a</sup>, and L. Skrbek<sup>a</sup>

<sup>a</sup>Faculty of Mathematics and Physics, Charles University, Prague, Czech Republic

<sup>b</sup>Institut Neel, CNRS Grenoble, France

We present a unified analysis of the drag forces acting on oscillating bodies submerged in superfluid <sup>4</sup>He: vibrating wire resonator, tuning fork, double-paddle, and torsionally oscillating disc. We find that in the two-fluid regime, for high Stokes number oscillatory flows, the drag forces originating from the normal component of He II exhibit a clearly defined universal scaling behavior with suitable dimensionless parameters. We use this approach to illustrate the transition from laminar to turbulent drag regime in oscillatory flow of He II. We show that, depending on the temperature and geometry of the flow, an instability may occur first either in the superfluid (production of quantized vorticity) or in the normal component (classical instability) and we demonstrate their crossover. Additionally, we develop a formalism describing the ballistic phonon gas at  $T < 0.6$  K, allowing direct comparison between measurements with resonators in He II and with NEMS devices in classical dilute gases. We verify that the ultra-relativistic gas of phonons shows the same asymptotic behavior as classical gases and thus provide support for the recently proposed universality scaling relation for high frequency oscillatory flows [1].

1. K. L. Ekinici, V. Yakhot, S. Rajauria, C. Colosquiac and D. M. Karabacak, *Lab Chip* **10**, 3013 (2010).

This research is funded by the Czech Science Foundation under project GACR 17-03572S.

## P28.6 Spinning superfluid <sup>4</sup>He nanodroplets

F. Ancilotto<sup>a</sup>, M. Barranco<sup>b</sup>, and M. Pi<sup>b</sup>

<sup>a</sup>Dipartimento di Fisica e Astronomia “Galileo Galilei” and CNISM, Universita’ di Padova, via Marzolo 8, 35122 Padova, Italy; CNR-IOM Democritos, via Bonomea, 265 - 34136 Trieste, Italy

<sup>b</sup>Departament FQA, Facultat de Física, Universitat de Barcelona. Diagonal 645, 08028 Barcelona, Spain; Institute of Nanoscience and Nanotechnology (IN2UB), Universitat de Barcelona, Barcelona, Spain.

The shape of spinning <sup>4</sup>He nanodroplets and the connection to superfluidity is a topic of great current interest: the transition from rigid body rotation to irrotational flow in superfluids, the conservation of angular momentum and its implications for the shape of superfluid droplets are fascinating and fundamental aspects of quantum physics. Recent experimental results<sup>1</sup> for fast spinning droplets showed remarkable similarities between the observed droplets shapes and those of classically rotating droplets made of normal, viscous fluid. We have studied<sup>2</sup> spinning superfluid <sup>4</sup>He nanodroplets using Density Functional theory. Due to the irrotational character of the superfluid flow, we find that the shapes of the spinning nanodroplets are very different from those of a viscous normal fluid drop in steady rotation. We show that when vortices are nucleated inside the superfluid droplets, their morphology, which evolves from axisymmetric oblate to triaxial prolate to two-lobed shapes, is in very good agreement with experiments. The presence of vortices in their interior confers to the superfluid droplets the rigid-body behavior of a normal fluid in steady rotation, and this is the ultimate reason for the surprising good agreement between experiments and the classical models used for their interpretation.

1. B. Langbehn et al, arXiv:1802.10584
2. F. Ancilotto, M. Barranco and M. Pi, arXiv:1711.03750

## P28.7 Dynamics of the free surface of superfluid $^4\text{He}$ probed by electrically charged tracer particles

P. Moroshkin<sup>a</sup>, P. Leiderer<sup>b</sup>, K. Kono<sup>c</sup>, S. Inui<sup>d</sup>, and M. Tsubota<sup>d</sup>

<sup>a</sup>Okinawa Institute of Science and Technology, Okinawa, Japan

<sup>b</sup>University of Konstanz, Konstanz, Germany

<sup>c</sup>National Chiao Tung University, Hsinchu, Taiwan

<sup>d</sup>Osaka City University, Osaka, Japan

We have developed a new experimental technique to study the dynamics of a free surface of superfluid helium. It relies on the imaging of electrically charged micron-sized particles trapped in a vertical electric field under a free surface of He II. The particles are free to move along the surface and can be used as tracers of the helium flow in 2D. We observe a collective particle motion driven by surface waves and by a thermally-induced counterflow which becomes turbulent at a large heating power. We can also induce the particle motion by applying a horizontal electric field and measure their mobility.

In the absence of external driving forces, most particles remain at rest and form a static 2D array similar to a disordered Wigner solid. However, some individual particles keep moving with a velocity in the range of 0.1–10 cm/s. We assign this anomalous behaviour to the particles trapped by quantized vortices and moving together with them. We distinguish two types of particle trajectories: (1) approximately circular loops 0.05–0.5 mm in diameter; (2) trajectories consisting of nearly straight segments with sharp turning points. The former are tentatively assigned to the particles bound to linear vortices which have their opposite ends pinned at the bottom. The latter probably represent vortex-antivortex pairs (vortex dipoles), or semicircular vortices with both ends terminating at the free surface.

## P28.8 Dynamics of fine particles due to quantized vortices on the surface of superfluid $^4\text{He}$

S. Inui<sup>a</sup>, M. Tsubota<sup>a</sup>, P. Moroshkin<sup>b</sup>, P. Leiderer<sup>c</sup>, and K. Kono<sup>d</sup>

<sup>a</sup>Osaka City University, Japan

<sup>b</sup>Okinawa Institute of Science and Technology, Japan

<sup>c</sup>University of Konstanz, Germany

<sup>d</sup>National Chiao Tung University, Taiwan

Peculiar dynamics of a free surface of the superfluid  $^4\text{He}$  has been observed experimentally with a newly established technique utilizing a number of electrically charged fine metal particles trapped electrically at the surface by Moroshkin et al. They have reported that some portion of the particles exhibit some irregular motions and suggested the existence of quantized vortices interacting with the metal particles. We have conducted preliminary calculations with the vortex filament model, which turns out to support the idea of the vortex-particle interactions. The observed anomalous metal particle motions are roughly categorized into two types; (1) circular motions with specific frequencies, and (2) quasi-linear oscillations. The former ones seem to be explained once we consider a vertical vortex filament whose edges are terminated at the bottom and at a particle trapped at the surface. Although it is not yet clear whether all the anomalous motions are due to the quantum vortices, the vortices seem to play important roles for the motions.

## P28.9 Characterization of Instabilities in Oscillatory Flows of Superfluid $^4\text{He}$

M.J. Jackson<sup>a</sup>, D. Schmoranzer<sup>a</sup>, Š. Midlik<sup>a</sup>, J. Bahyl<sup>b</sup>, and L. Skrbek<sup>a</sup>

<sup>a</sup>Faculty of Mathematics and Physics, Charles University, Ke Karlovu 3, 121 16, Prague 2, Czech Republic.

<sup>b</sup>Faculty of Mathematics, Physics and Informatics, Comenius University, Mlynská dolina F1, Bratislava, Slovak Republic.

We investigate high-Stokes number oscillatory flows of superfluid  $^4\text{He}$  due to an oscillating quartz tuning fork with a fundamental resonant mode of 6.5 kHz and an overtone mode at 40 kHz at various temperatures ranging from 1.35 to 2.15 K. The observed non-linear drag forces acting on the tuning fork are described in terms of classical-like instabilities in the normal fluid and/or quantized vorticity in the superfluid. The measured in-line drag forces determined directly from the response of the tuning fork are then compared with simultaneous measurements of the vortex line density determined by the attenuation of second sound. We demonstrate that the critical velocity of the fork at which quantized vorticity appears to set in (as deduced from the drag force) agrees with that inferred from the appearance of a measurable vortex line density in the vicinity of the fork, as detected by second sound attenuation; this critical velocity is independent of temperature. We show that classical or quantum instabilities can arise separately and we propose a flow phase diagram from which one can predict the nature of flow instabilities in the two-fluid regime of  $^4\text{He}$ .

This research is supported by the Czech Science Foundation project GAČR 17-03572S. M.J.J. acknowledges personal support from Vakuum Praha spol. s r.o.

## P28.10 Real-time monitoring of vortex dynamics in a superfluid helium thin film

S. Forstner<sup>a</sup>, C.G. Baker<sup>a</sup>, X. He<sup>a</sup>, Y. Sfondla<sup>a</sup>, A. Sawadsky<sup>a</sup>, G.I. Harris<sup>a</sup>, D. McAuslan<sup>a</sup>, M. Davis<sup>a</sup>, M. Reeves<sup>a</sup>, O. Stockdale<sup>a</sup>, X. Yu<sup>b</sup>, A. Bradley<sup>b</sup>, and W.P. Bowen<sup>a</sup>

<sup>a</sup>School of Mathematics and Physics, University of Queensland, St Lucia, Queensland 4072, Australia

<sup>b</sup>Department of Physics, The University of Otago, Dunedin, New Zealand

Two-dimensional superfluids exhibit a rich range of thermodynamical and quantum behavior, from quantum vortices and turbulence to two dimensional phase transitions. We experimentally probe this physics through the evanescent interaction between a two-dimensional superfluid helium thin film and an optical whispering gallery mode microcavity. The resonator geometry enables both sound waves and vortices to be confined to areas four orders of magnitude smaller than has been previously possible, as well as precision optical read-out of the superfluid motion [1,2]. The increased confinement results in enhanced interactions between the sound waves and both light and vortices, allowing for real-time read-out and control of these excitations. We initialize an ensemble of about 16 vortices in the center of a microtoroidal resonator. This vortex ensemble creates a spectral splitting of surface excitations on this film, so called 'third-sound' waves. We track these splittings simultaneously for a number of modes over a time of six minutes, which allows us to infer the time dynamics of the vortex ensemble. Our data shows diffusive vortex motion and suggests a crossover between the ballistic and diffusive regime, as predicted recently [3].

1. Harris G. I. et al. (2016). "Laser cooling and control of excitations in superfluid helium", Nat. Phys. 12, 788
2. McAuslan D. et al. (2016). "Microphotonic Forces from Superfluid Flow", Phys. Rev. X 6, 021012
3. E. Rickinson et al. (2018) "Diffusion of quantum vortices", arxiv: 1805.09187v1



## P28.11 Looking for Quantum Vortex Production in Oscillatory Motion

R. P. Haley, S. Kafanov, M. T. Noble, G. R. Pickett, V. Tsepelin, T. Wilcox, and D. E. Zmееv

Department of Physics, Lancaster University, Lancaster, UK

We are pioneering the intermodulation multi-frequency technique, developed by the atomic force microscopy community<sup>1</sup>, to study the creation and growth of vortices in superfluid helium. Vortex nucleation and growth around a vibrating object should result in the effective mass or inertial force of the oscillator increasing, while vortex shedding will enhance the dissipative force as energy is lost to bulk. The commonly used lock-in amplifier technique allows us to measure the force-velocity characteristic to deduce the average response of the oscillator for a single driving force. With a multi-frequency technique we can measure the non-linear intermodulation products created by the interactions of the oscillator with the fluid, vortices and turbulence. The intermodulation products are the result of frequency mixing of two driving tones. They yield the inertial and dissipative forces felt by the oscillator as a function of its velocity.

1. D. Platz, E. A. Tholén, D. Pesen and D. B. Haviland (2008), Intermodulation atomic force microscopy, *Applied Physics Letters* **92** (15), 153106.

## P28.12 Turbulent statistics and intermittency enhancement in coflowing superfluid <sup>4</sup>He

L. Biferale<sup>a</sup>, D. Khomenko<sup>b</sup>, V.S. L'vov<sup>c</sup>, A. Pomyalov<sup>c</sup>, I. Procaccia<sup>c</sup>, and G. Sahoo<sup>d</sup>

<sup>a</sup>Department of Physics, University of Tor Vergata, Rome, Italy

<sup>b</sup>Laboratoire de physique théorique, Département de physique de l'ENS, École normale supérieure, PSL University, Sorbonne Université, CNRS, Paris, France

<sup>c</sup>Department of Chemical and Biological Physics, Weizmann Institute of Science, Rehovot, Israel

<sup>d</sup>Dept. of Mathematics and Statistics and Dept. of Physics, University of Helsinki, Finland

The large scale turbulent statistics of mechanically driven superfluid <sup>4</sup>He (a coflow) was shown experimentally to follow the classical counterpart. However, at smaller scales of the order of the intervortex distance, the superfluid and normal fluid components are not fully coupled and therefore can have different statistics. In this work we present results of direct numerical simulations study of the <sup>4</sup>He coflow in a wide range of temperatures. The numerics employs HVBK model with self-consistently and non-linearly coupled normal and superfluid components. The main results are that (i) the velocity fluctuations of normal and super components are well-correlated in the inertial range of scales, but decorrelate at small scales. (ii) The energy transfer by mutual friction between components is particularly efficient in the temperature range between 1.8 K and 2 K, leading to enhancement of small scales intermittency for these temperatures. (iii) At low  $T$  and close to  $T_\lambda$  the scaling properties of the energy spectra and structure functions of the two components are approaching those of classical hydrodynamic turbulence.

### P28.13 **The Effect of Remnant Vortices in He II on Multiple Modes of a Micro-electromechanical Resonator**

Y. Lee<sup>a</sup>, C.S. Barquist<sup>a</sup>, W.G. Jiang<sup>a</sup>, P. Zheng<sup>a</sup>, and H.B. Chan<sup>b</sup>

<sup>a</sup>Department of Physics, University of Florida, Gainesville, USA

<sup>b</sup>Department of Physics, The Hong Kong University of Science and Technology, Kowloon, Hong Kong

A micro-electromechanical plate resonator suspended  $2\ \mu\text{m}$  above a substrate was immersed in  $^4\text{He}$  below 20 mK at saturated vapor pressure. A similar device has been used in the study of surface Andreev bound states in superfluid  $^3\text{He-B}$ <sup>1,2</sup>. At these temperatures four vibrational modes of the device are observed. The corresponding motion of these modes is identified by comparing the observed modes with computer simulation. Due to its large surface area and small mass, the resonator is sensitive to remnant vortices. Because of their unique motions, the different vibrational modes exhibit different sensitivities to vortices present near the device. The behavior of the different modes is studied in the presence of remnant vortices attached to the device and also in the presence of fully developed turbulence generated by a quartz tuning fork.

This work is supported by the National Science Foundation through DMR-1708818.

1. P. Zheng *et al.* (2016). “Anomalous Damping of a Micro-electro-mechanical Oscillator in Superfluid  $^3\text{He-B}$ ”. *Phys. Rev. Lett.* **111**, 195301.
2. P. Zheng *et al.* (2017). “Critical Velocity in the Presence of Surface Bound States in Superfluid  $^3\text{He-B}$ ”. *Phys. Rev. Lett.* **118**, 065301.

### P28.14 **The Role of Substrate Roughness on the Superfluid Film Flow Rate of $^4\text{He}$**

J. Usami<sup>a</sup>, T. Matsui<sup>a</sup>, and Hiroshi Fukuyama<sup>a,b</sup>

<sup>a</sup>Department of Physics, The University of Tokyo, Japan

<sup>b</sup>Cryogenic Research Center, The University of Tokyo, Japan

It has long been known that the film flow rate ( $j$ ) of superfluid  $^4\text{He}$  increases dramatically when the wall of a liquid container is contaminated by solid air.<sup>1</sup> For this phenomenon, two different explanations can be considered. One is the increase of the effective perimeter of the container  $L_{\text{eff}}$  (the geometrical effect) and the other is the enhancement of the superfluid critical velocity  $v_c$  due to stronger pinning of vortices (the vortex pinning effect). As far as we know, the true mechanism has not been clarified yet. Recently, we have measured  $j$  for the container with largely different conditions in terms of the surface area ( $0.77 \sim 6.15\ \text{m}^2$ ) and the surface morphology (channel size:  $0.1 \sim 1.0\ \mu\text{m}$ ) using sintered silver powders and porous glasses. We were able to observe an increase of  $j$  by more than two orders of magnitude compared to non-treated glass containers. We found that measured  $j$  is roughly proportional to  $L_{\text{eff}}$  which was estimated by imaging the surface morphology with scanning electron microscope. This indicates that the geometrical effect is predominantly important and  $v_c$  is nearly constant regardless of the different surface conditions. If we estimate the size ( $b$ ) of microscopic surface roughness from our data based on the vortex depinning model,<sup>2</sup> we obtain  $b \approx 2\ \text{nm}$ . The  $T$ -dependence of measured  $j$  at  $1.4 \leq T \leq 2.1\ \text{K}$ , where the superfluid healing length changes appreciably, is consistent with the vortex depinning model rather than the vortex nucleation one.

1. R. Bowers and K. Mendelssohn, *Proc. Phys. Soc.* **A63**, 1318 (1950).
2. K. W. Schwarz, *Phys. Rev. B* **31**, 5782 (1985).

## P28.15 Nanomechanical Wire Resonator for Probing Quantum Vortex in Superfluid He

Y. Nago<sup>a</sup>, Y. Morikawa<sup>a</sup>, Y. Tanaka<sup>a</sup>, K. Kato<sup>b</sup>, T. Takagi<sup>b</sup>, H. Maki<sup>b,c</sup>, S. Murakawa<sup>d</sup>, and K. Shirahama<sup>a</sup>

<sup>a</sup>Department of Physics, Keio University, Japan

<sup>b</sup>Department of Applied Physics and Physico-informatics, Keio University, Japan

<sup>c</sup>JST-PRESTO, Japan

<sup>d</sup>Cryogenic Research Center, The University of Tokyo, Japan

Mechanical oscillating objects can generate quantum vortices and turbulence in superfluid He via the intrinsic process related to the Landau critical velocity or the extrinsic process attributed to remanent vortices pinned on the object surfaces [1]. Quantum turbulence created by object oscillation decays following the Kolmogorov energy-cascade process, which has been experimentally revealed by vortex probes such as second sound [2] or vibrating wires [3]. However, clarification of microscopic dynamics of vortex lines in turbulent generation and decay processes requires sensitive measurements using much smaller probes like NEMS. We have been recently developing nanomechanical wire resonators consisting of the bridged carbon nanotube and the thin superconducting film deposited on it [4]. This fabrication process enables to tune the wire size down to nm, close to the vortex core scale ( $\sim$  nm for  $^4\text{He}$  and  $\sim$  100 nm for  $^3\text{He}$ ). We will present the preliminary measurements at low temperatures and our future plans for investigation of quantum vortex and turbulence.

1. W.F. Vinen and L. Skrbek, PNAS **111**, 4699(2014). 2. Steven R. Stalp *et al*, PRL **82**, 4831(1999). 3. D. I. Bradley *et al*, PRL **96**, 0358301(2006). 4. K. Masuda, H. Maki *et al*, APL **108**, 222601(2016).

## P28.16 Instability of a Doubly Quantized Vortex in Uniform Superfluids at Zero Temperature

Hiromitsu Takeuchi<sup>a</sup>, Michikazu Kobayashi<sup>b</sup>, and Kenichi Kasamatsu<sup>c</sup>

<sup>a</sup>Department of Physics, Osaka City University, Osaka 558-8585, Japan

<sup>b</sup>Department of Physics, Kyoto University, Kyoto 606-8502, Japan

<sup>c</sup>Department of Physics, Kindai University, Higashi-Osaka, Osaka 577-8502, Japan

We provide an answer to the long-standing question whether a doubly quantized vortex (DQV) is stable or not against splitting into two singly-quantized vortices (SQVs) in uniform single-component superfluids at zero temperature.<sup>1</sup> This problem is of fundamental importance to non-equilibrium dynamics in superfluids at very low temperature since its analysis becomes quite complicated if we allow the presence of DQVs. Nevertheless, no thorough investigation had been done for this problem because of theoretical and computational difficulties. We investigated the system-size dependence of the excitation frequency of a DQV through large-scale numerical simulations of the Bogoliubov–de Gennes equation, and found that the imaginary part of the frequency is asymptotic to a small finite value in the infinite-system-size limit; a DQV is dynamically unstable in uniform systems. The perturbation and semi-classical theories of a Bogoliubov quasi-particle, extended to the case of complex eigenvalue in Bose–Einstein condensates, reveals that the splitting instability accompanies phonon radiation due to the *growing* quasi-normal mode by the precession of two SQVs.

1. Hiromitsu Takeuchi, Michikazu Kobayashi, and Kenichi Kasamatsu (2018). “Is a Doubly Quantized Vortex Dynamically Unstable in Uniform Superfluids?”. J. Phys. Soc. Jpn. **87**, 023601; arXiv:1710.10810.

## P28.17 A theory of energy spectra in superfluid He-4 counterflow turbulence

V.S. L'vov and A. Pomyalov

Department of Chemical and Biological Physics, Weizmann Institute of Science, Israel

During last few years the statistical properties of the counterflow turbulence in superfluid He-4 have become a subject of intensive research. The most recent developments include experimental measurements [1] of the normal velocity component's transversal structure functions in a wide range of flow parameters and an analytical theory [2], predicting the energy spectra for both normal and superfluid components. We present in details the theory [2], which accounts for the physical mechanisms, defining the energy spectra: i) the scale-dependent competition between the turbulent velocity coupling by the mutual friction and the counterflow velocity-induced turbulent velocity decoupling and ii) the turbulent energy dissipation by mutual friction enhanced by the velocity decoupling. The energy spectra were found to be non-scale-invariant and to depend on flow parameters. The mean exponents of the normal fluid energy spectra  $\langle m \rangle_{10}$ , found without fitting parameters, qualitatively agree with the observed [1] exponents  $n_{\text{exp}} + 1$  for  $T > 1.85$  K. We discuss possible effects of the spectral anisotropy on the velocity energy spectra scaling behavior in the He-4 counterflow.

1. J. Gao, E. Varga, W. Guo and W. F. Vinen, *Energy spectrum of thermal counterflow turbulence in superfluid helium-4*, Phys. Rev. B 96, 094511 (2017).
2. V. L'vov and A. Pomyalov. *A theory of energy spectra in superfluid He-4 counterflow turbulence*, Arxiv:1804.02208.

## P28.18 Visualization study of thermal counterflow in the heater proximity

P. Švančara, P. Hrubcová, and M. La Mantia

Faculty of Mathematics and Physics, Charles University, Prague, Czech Republic

The motions of micrometer-sized particles, suspended in He II, are investigated by flow visualization. We capture the particle time-dependent positions inside our experimental channel, of square cross section, with a planar heater placed at its bottom. We confirm that, in steady-state thermal counterflow, the statistical distributions of the particle velocities display, at scales smaller than the mean distance between quantized vortices, power-law tails.<sup>1</sup> We estimate the vortex line density (VLD) from the scale-dependent shape of these distributions. When solid deuterium particles are used, the obtained VLD is, close to the heater, approximately two orders of magnitude larger than that expected in the bulk, at the same temperature and heat flux.<sup>2</sup> Additionally, we show that the estimated VLD appears to be in the flow source proximity even larger when one employs lighter particles, made of solid deuterium hydride. The result supports the idea that heavy particles tend to interact less with quantized vortices than light ones.<sup>3</sup>

We thank D. Duda, L. Skrbek, and M. Rotter for fruitful discussions and valuable help. We acknowledge the support of the Czech Science Foundation (GAČR) under grant 16-00580S.

1. La Mantia, M., Švančara, P., Duda, D., Skrbek, L. (2016). “Small-scale universality of particle dynamics in quantum turbulence”. Physical Review B.
2. Hrubcová, P., Švančara, P., La Mantia, M. (2018). “Vorticity enhancement in thermal counterflow of superfluid helium”. Physical Review B.
3. La Mantia, M., Skrbek, L. (2014). “Quantum turbulence visualized by particle dynamics”. Physical Review B.

## P28.19 Numerical Study on Entrance Length in Thermal Counterflow of Superfluid $^4\text{He}$

H. Kobayashi<sup>a</sup>, S. Yui<sup>b</sup>, and M. Tsubota<sup>b</sup>

<sup>a</sup>Department of Physics, Hiyoshi Campus, Keio University, Yokohama 223-8521, Japan

<sup>b</sup>Department of Physics, Osaka City University, Osaka 558-8585, Japan

Three-dimensional numerical simulation in a square duct was conducted to investigate entrance lengths of normal fluid and superfluid flows in a thermal counterflow of Superfluid  $^4\text{He}$ . The two fluids were coarse-grained by using the Hall-Vinen-Bekharevich-Khalatnikov (HVBK) model and were coupled through a mutual friction. Our simulation showed that the entrance length of the normal fluid from a hot end becomes shorter than that of a single normal fluid flow due to the mutual friction with the parabolically developed superfluid flow near the hot end. As the mutual friction increases, the entrance length decreases. Same as that, the entrance length of the superfluid from a cold end is affected by the strength of the mutual friction due to the parabolically developed normal fluid flow near the cold end. The deformations of the normal fluid and superfluid are consistent with our recent results.<sup>1</sup> The differences from Ref. 2 are the inlet condition for both fluids and the formulation of the mutual friction which is a simplified model tested in Ref. 2.

1. Yui, S., Tsubota, M., and Kobayashi, H. (2018). “Three-Dimensional Coupled Dynamics of the Two-Fluid Model in Superfluid  $^4\text{He}$ : Deformed Velocity Profile of Normal Fluid in Thermal Counter Flow”. *Physical Review Letters* 120, 155301.
2. Bertolaccini, J., L ev eque, E., and Roche, P.-E. (2017). “Disproportionate entrance length in superfluid flows and the puzzle of counterflow instabilities”. *Physical Review Fluids* 2, 123902.

## P28.20 Generation of $^4\text{He}_2^*$ Clusters via Neutron- $^3\text{He}$ Absorption Reaction towards Visualization of Full Velocity Field in Quantum Turbulence

T. Matsushita<sup>a</sup>, S. Kokuryu<sup>b</sup>, W. Kubo<sup>b</sup>, Y. Tsuji<sup>b</sup>, S. Suzuki<sup>b</sup>, V. Sonnenschein<sup>b</sup>, K. Hirota<sup>a</sup>, T. Shinohara<sup>c</sup>, K. Hiroi<sup>c</sup>, H. Hayashida<sup>d</sup>, W. Guo<sup>e</sup>, H. Tomita<sup>b</sup>, T. Iguchi<sup>b</sup>, N. Wada<sup>a</sup>, M. Kitaguchi<sup>a</sup>, Y. Kiyonagi<sup>b</sup>, H. M. Shimizu<sup>a</sup>, D. Ito<sup>f</sup>, and Y. Saito<sup>f</sup>

<sup>a</sup>Department of Physics, Nagoya University, Nagoya, Japan

<sup>b</sup>Department of Energy Engineering, Nagoya University, Nagoya, Japan

<sup>c</sup>J-PARC Center, Japan Atomic Energy Agency, Tokai, Ibaraki, Japan

<sup>d</sup>Comprehensive Research Organization for Science and Society, Tokai, Ibaraki, Japan

<sup>e</sup>National High Magnetic Field Laboratory/Florida State University, Tallahassee, Florida, USA

<sup>f</sup>Research Reactor Institute, Kyoto University, Kumatori, Osaka, Japan

To visualize quantum turbulence,  $^4\text{He}_2^*$  excimers are unique tracers which affect vortices minimally and follow only normal-component flow above 1 K. Recently the normal-component turbulence onset has been successfully observed by a  $^4\text{He}_2^*$  line generated with femtosecond laser. However, in order to observe full velocity field, particle tracking using localized clouds of  $^4\text{He}_2^*$  is strongly desired. To generate these, we propose to use the neutron absorption reaction of  $^3\text{He}$  impurities in  $^4\text{He}$ , and the proof-of-principle experiments have been conducted using neutron beams of J-PARC/MLF and KU Reactor.  $^4\text{He}_2^*$  generated in superfluid  $^4\text{He}$  were detected by the laser-induced fluorescence using photomultiplier tubes. Fluorescence increased proportionally to the neutron flux, indicating that the  $^4\text{He}_2^*$  were generated by neutrons. The ratio of  $^4\text{He}_2^*$  generated by  $\gamma$ -ray accompanying neutrons was experimentally estimated to be less than 40%. Thus, a sufficient amount of  $^4\text{He}_2^*$  clusters for flow visualization were confirmed to be generated by the n- $^3\text{He}$  absorption reaction. This is the first observation of neutron-generated excimers by fluorescence.

## P28.21 Peculiarities of a spherically symmetric thermal counterflow

E. Varga

Faculty of Mathematics and Physics, Charles University, Czech Republic

Superfluid  $^4\text{He}$  (He II) flows as if composed of two semi-independent fluids – the normal and superfluid component. This two-fluid behaviour allows for greater freedom for the motion of He II than in classical liquids. One such non-classical flow can be activated using a heat flux – so called thermal counterflow – in which the two components flow in opposite directions with zero net mass transport. Thermal counterflow has been studied extensively both experimentally and numerically in rectilinear flows. Other geometries so far received scant attention. Of particular interest, however, is a spherically symmetric flow where a slight anisotropy naturally present in a rectilinear counterflow cannot be globally present.

This work presents a series of numerical simulations of a tangle of quantized vortices using the vortex filament method in the vicinity of a point heat source, with the singularity near the origin removed. The flow of the normal fluid is assumed to be laminar. The numerical experiments performed for temperatures ranging from 1.3 K to 2.16 K indicate a strong temperature dependence of a critical counterflow velocity for the appearance of turbulence, possibly hinting at an existence of critical temperature above which a statistically steady turbulent tangle does not develop. Specifically, random initial seed loops quickly dissipate for sufficiently high temperatures and realistic heat inputs. Moreover, for the range of temperatures where a stable turbulence is observed, the vortex line density increases with decreasing temperature for a fixed counterflow velocity, i.e., an opposite trend to what is observed in a rectilinear counterflow.

This work is supported by the Charles University under GAUK 368217.

## P28.22 Vortex Emission from Quantum Turbulence Generated in Superfluid $^4\text{He}$

H. Yano, K. Sato, R. Mushiake, K. Obara, and O. Ishikawa

Graduate School of Science, Osaka City University, Japan

Vortex rings are produced by reconnection between vortex lines constituting a quantum turbulence, moving away from a turbulence region in a superfluid. To investigate the growth and formation of quantum turbulence in superfluid  $^4\text{He}$ , we have studied the vortex emission from a turbulence region generated by a vibrating wire by detecting a vortex ring at a distance. Although vortex rings are emitted randomly, an averaged emission rate can be estimated as a function of time from the beginning of a turbulence generation. The emission rate of vortex rings remains low until the beginning of high-rate emissions, suggesting that some of the vortex lines produced by the wire combine to form a vortex tangle, until an equilibrium is established between the rate of vortex line combination with the tangle and dissociation. By setting the limit on the detection diameter of a vortex ring, we find that the emission rate reveals a power law behavior with ring diameter in an equilibrium state. Since the diameter of a vortex ring is associated with a vortex line spacing when reconnection occurs, the distribution of vortex line spaces in a turbulence is considered to be reflected in the size distribution of emission rings. Therefore, the power law dependence of the vortex emission suggests the fractal structure of vortex lines in a turbulence.

## P28.23 Vorticity of suction vortex observed by second sound in superfluid $^4\text{He}$

I. [Matsumura](#), K. Sato, Y. Kimura, K. Obara, H. Yano, and O. Ishikawa

Graduate School of Science, Osaka City University, Japan

Superfluid under rotation has been attracted academic interests for a long time because it shows a simple and direct quantum nature of condensed matter. Until recently, most of the experiments were carried out in the rotating vessels or the rotating cryostats, so that the vortex lines arranged so as to form a regular triangular lattice, and their meniscus were parabolic. Recently, we succeeded in generating a new type of the vortex, which was called the suction vortex, by rotating a centrifugal pump directly driven by a cryogenic motor. The meniscus of this giant vortex was the funnel-shaped that were commonly appeared in the classical rotating fluid with a vertical flow. Yano et al experimentally revealed the net circulation from the shape by the classical fluid-dynamics, and showed surprisingly high values<sup>1</sup>. It means that the quantum vortex lines are centralized by the suction flow and, plausibly, forming a vortex sheet around the hollow core. Our motivation is to clarify the distribution of the quantum vortex line density by means of the attenuation of the second sound. Up to now, we have succeeded in measuring the attenuation of the second sound as a function of the rotation speed at 1.6 K. We found that the attenuation due to the vortex line across the giant vortex were approximately proportional to the rotation speed. Since the theory that can reveal the vortex line density in the inhomogeneously distributing vortex lines is not established yet, we simply calculated the vortex line density by assuming the homogeneous distribution in a proper area near the hollow core. We will evaluate the vortex line density distribution and discuss the validity of our model in the conference.

1. H. Yano, K. Ohshima, K. Obara and O. Ishikawa, *J. Phys.: Conf. Ser.* **969** (2018) 012002

## P28.24 Vortex Emission from Turbulence Produced by Counterflow in Superfluid $^4\text{He}$

K. [Hamazaki](#), K. Sato, Y. Kimura, K. Obara, H. Yano, and O. Ishikawa

Graduate School of Science, Osaka City University, Japan

We report vortex emissions from quantum turbulence produced by counter flow in superfluid  $^4\text{He}$ . In a circular channel, vortex lines emerge due to a thermal counter flow above a critical velocity. We generated turbulence in a circular channel with an inner diameter of 0.2 mm by thermal counter flow and detected emitted vortices by a vibrating wire located in front of the outlet of the channel. Since vortex rings shrink during flying due to a normal fluid component, the diameters of detected vortex rings are larger than 94  $\mu\text{m}$  in our setup. By measuring the time between the beginning of counter flow generation and detection of a vortex ring, we found that vortex rings are rarely emitted from a dilute turbulence (T1) emerging below the second critical velocity, but are released well from a dense turbulence (T2) above the second critical velocity. The mean emission rate from T2 is considerably higher than that from T1. These results denote that the emission rate reflects the vortex line density and the distribution of turbulence in the channel.

[1] K.P. Martin and J.T. Tough, *Phys. Rev. B* **27**, 2788 (1983)

## P28.25 Power dependence of vortex emission generated by vibrating wire in HeII

K. Sato, R. Mushiake, K. Obara, H. Yano, and O. Ishikawa

Graduate School of Science, Osaka City University, Japan

An oscillating object can generate quantum turbulence in the path of the oscillation in superfluid  $^4\text{He}$ . Vortex rings are emitted by reconnection between vortex lines constituting quantum turbulence. To investigate the growth and formation of quantum turbulence in superfluid  $^4\text{He}$ , we have studied the power dependence of vortex emissions from turbulence by using a set of vibrating wires as a generator and detector.

The detection rate of vortex rings from a turbulent region remains low until the beginning of high-rate detections at a generation power of 150 pW for the emission rings larger than 60  $\mu\text{m}$  in diameter. At a lower power of 40 pW, however, the detection rate becomes high at the beginning of turbulence generation, followed by a low detection rate.

We suggest the emission rate of vortex rings is low until a turbulent become an equilibrium at 150 pW. On the other hand, the emission rate is high until following by a low detection rate at 40 pW. It may imply that vortex rings emitted from the generator form a vortex tangle, which emits a large vortex ring. We will evaluate the power dependence of vortex emission and discuss in the conference.

## P28.26 Induced Fractional Electric Charge in a Boojum on the Interface between Superfluid $^3\text{He-A}$ and $^3\text{He-B}$

I. Kanazawa, M. Nakajima, R. Maeda, and Shun Nakamura

Department of Physics, Tokyo Gakugei University

A nexus with fractional magnetic charge can be constructed by using geometry with several condensates [1]. The nexus pinned by the interface between superfluid  $^3\text{He-A}$  and the nonchiral superfluid  $^3\text{He-B}$ . For the superconducting analogs, such a nexus represents the monopole with  $1/2$  of the elementary flux. A monopole, which is topologically pinned by a surface or interface, is a boojum. Recently one (I. K) of the present authors [2,3] has proposed exotic quasiparticles with fractional charge in semiconductor-dot and domain walls. In this study, we propose that exotic quasiparticles with fractional charge might be induced on a boojum between superfluid  $^3\text{He-A}$  and superfluid  $^3\text{He-B}$ , using the previous formula [2,3]. [1] G.E.Volovik, PNAS, 97,2431(2000) [2]I.Kanazawa, J.Phys.Conf.Ser. 807,102004(2017) [3]I. Kanazawa, R.Maeda, J.Low.Temp.Phys. 191,84(2018)



## P28.27 Pairing Phenomena from Cold Gases to Neutron Stars

H.-H. Fan<sup>ab</sup> and E. Krotscheck<sup>ab</sup>

<sup>a</sup>Department of Physics, University at Buffalo, SUNY Buffalo NY 14260

<sup>b</sup>Institut für Theoretische Physik, Johannes Kepler Universität, A 4040 Linz, Austria

We develop the full variational and correlated basis functions/parquet–diagram theory of strongly interacting superfluid systems. Starting with a Jastrow–Feenberg (or, in a more recent language “fixed–node”) wave function for the superfluid state, we derive the fully optimized Fermi–Hypernetted Chain (FHNC–EL) equations which sum a local approximation of the parquet–diagrams. Close examination of the procedure reveals that it is essential to go *beyond* the usual Jastrow–Feenberg approximation and to include the exact particle–hole propagator to guarantee the correct stability range. We implement this method and apply it to neutron matter and low density Fermi liquids interacting via the Lennard–Jones model interaction. In all cases, we find a lowering in superfluid gap and — in the Lennard–Jones liquid — a significant change of the stability range compared to earlier purely variational calculations [1,2]. The consequences to “fixed–node” Monte Carlo calculations are discussed.

1. H.-H. Fan, E. Krotscheck, T. Lichtenegger, D. Mateo, R. E. Zillich; Phys. Rev. **A 92** 023640 (2015).
2. H.-H. Fan, E. Krotscheck, J. W. Clark; J. Low Temp. Phys. **189** 470 (2017).

## P28.28 Hidden charge-conjugation, parity, time-reversal symmetries and Higgs modes in superconductors

S. Tsuchiya<sup>a</sup>, D. Yamamoto<sup>b</sup>, R. Yoshii<sup>a</sup>, and M. Nitta<sup>c</sup>

<sup>a</sup>Department of Physics, Chuo University, 1-13-27 Kasuga, Bunkyo-ku, Tokyo 112-8551, Japan

<sup>b</sup>Department of Physics and Mathematics, Aoyama Gakuin University, 5-10-1 Fuchinobe, Chuo-ku, Sagami-hara, Kanagawa 252-5258, Japan

<sup>c</sup>Department of Physics, Keio University, Hiyoshi 4-1-1, Yokohama, Kanagawa 223-8521, Japan

A gapful Higgs mode is a collective excitation that arises in a system involving spontaneous breaking of a continuous symmetry, along with a gapless Nambu–Goldstone mode. Here we construct a new framework to explain the appearance of a Higgs mode as a pure amplitude mode in fermionic systems with a particle–hole (p–h) symmetric dispersion. To this end, we introduce nontrivial charge-conjugation ( $\mathcal{C}$ ), parity ( $\mathcal{P}$ ), and time-reversal ( $\mathcal{T}$ ) operations involving the swapping of pairs of the wave vectors symmetrical with respect to the Fermi surface. It is shown that a fermionic Hamiltonian with a p–h symmetric dispersion exhibits the discrete symmetries under  $\mathcal{C}$ ,  $\mathcal{P}$ ,  $\mathcal{T}$ , and  $\mathcal{CPT}$ . We find that in the superconducting ground state,  $\mathcal{T}$  and  $\mathcal{P}$  are spontaneously broken simultaneously with the U(1) symmetry. The spontaneous breaking of  $\mathcal{T}$  is responsible for the emergence of a gapful Higgs mode that induces pure amplitude oscillation of the gap function due to the unbroken  $\mathcal{C}$ . Moreover, we demonstrate that the broken  $\mathcal{T}$  is restored in the excited state with a Higgs mode.

## P28.29 Infrared-active Higgs mode in an s-wave superconductor NbN under DC current injection

S. Nakamura<sup>a</sup>, Y. Iida<sup>b</sup>, R. Matsunaga<sup>c</sup>, H. Terai<sup>d</sup>, and R. Shimano<sup>a,b</sup>

<sup>a</sup>Cryogenic Research Center, The University of Tokyo, Japan

<sup>b</sup>Department of Physics, The University of Tokyo, Japan

<sup>c</sup>The Institute for Solid State Physics, The University of Tokyo, Japan

<sup>d</sup>National Institute of Information and Communications Technology, Japan

Superconducting transition is associated with the spontaneous breaking of U(1) rotational symmetry in terms of the phase of wave function. Then, two collective modes appear that correspond to the fluctuation of amplitude and phase of the complex order parameter, respectively. The amplitude mode is recently referred to as Higgs mode from an analogy to the Higgs boson in elementary particle physics. It has been difficult to excite or observe the Higgs mode as it does not involve either electric or magnetic polarizations, and only recently it was observed in a time-resolved manner by using ultrafast laser spectroscopy technique with the photon energy close to the superconducting gap energy,  $2\Delta$ , in the terahertz frequency range<sup>1</sup>. Alternatively, here we demonstrate that the Higgs mode can be detected in the linear optical conductivity measurement if the dc supercurrent is introduced into the superconductor. We observed a sharp resonant peak at  $\omega \approx 2\Delta$  in the optical conductivity spectrum of a thin-film NbN with applying current of  $2.5 \text{ MA/cm}^2$ . The peak is observed only when the probe THz electric field is in parallel to the current direction, which is consistent with the recent theoretical prediction<sup>2</sup>.

1. R. Matsunaga, H. Terai, R. Shimano *et al.*, Phys. Rev. Lett. **111**, 057002 (2013).
2. A. Moor, A. F. Volkov, and K. B. Efetov, Phys. Rev. Lett. **118**, 047001 (2017).

## P28.30 Influence of the intersite Coulomb repulsion on the superconducting gap of the spin-polaron quasiparticles in cuprate superconductors

V. V. Val'kov<sup>a</sup>, M. M. Korovushkin<sup>a</sup>, and A. F. Barabanov<sup>b</sup>

<sup>a</sup>Kirensky Institute of Physics, Federal Research Center KSC SB RAS, 660036 Krasnoyarsk, Russia

<sup>b</sup>Vereshchagin Institute for High Pressure Physics, 108840 Troitsk, Moscow, Russia

With an account for the real crystalline structure of the  $\text{CuO}_2$  plane and the strong spin-fermion coupling, the influence of the intersite Coulomb repulsion between holes on the superconducting  $d$ -wave pairing of the spin-polaron quasiparticles in cuprate superconductors is studied. It is shown that the intersite Coulomb interaction  $V_1$  between the holes located at the nearest oxygen ions does not affect the Cooper pairing, because its Fourier transform  $V_q$  vanishes in the kernel of the corresponding integral equation. It is shown that an account for the intersite Coulomb interaction  $V_2$  of fermions located at the next-nearest oxygen ions leads to the decrease in the superconducting transition temperature, but this temperature remains within the limits that are observed experimentally. It is established that the formation of resulting superconducting gap with the  $d$ -wave symmetry of the order parameter in the spin-fermion model is caused by three components. On the basis of the self-consistent solution of four integral equations, the dependence of the superconducting gap width on the intersite interaction  $V_2$  is studied.

The work is supported by the Russian Foundation for Basic Research (RFBR) (projects nos. 16-02-00304 and 18-02-00837) and partly by the Government of Krasnoyarsk Region and the Krasnoyarsk Region Science and Technology Support Fund (projects nos. 18-42-243002 and 18-42-243018), as well as the grant of the President of the Russian Federation (project MK-1398.2017.2).

## P28.31 Magnetic Response of Critical Current in Junctions using Ion-gated MoS<sub>2</sub> and Conventional Superconductor

Y. Aikawa<sup>a</sup>, K. Tsumura<sup>b</sup>, T. Narita<sup>a</sup>, H. Takayanagi<sup>c</sup>, and R. Ishiguro<sup>a</sup>

<sup>a</sup>Division of Mathematical and Physical Science, Japan Women's University, Japan

<sup>b</sup>Department of Applied Physics, Tokyo University of Science, Japan

<sup>c</sup>Research Institute for Science and Technology, Tokyo University of Science, Japan

Realization of unconventional superconductivity with exotic pairing symmetry is theoretically predicted in monolayer transition metal dichalcogenides (mTMDCs) [1]. Molybdenum disulphide (MoS<sub>2</sub>) is a typical example of the mTMDCs, and the electric-field-induced superconductivity was demonstrated by using ion-gated MoS<sub>2</sub> [2]. Moreover, the two-dimensional superconductivity is protected by spin-valley locking due to broken-inversion symmetry and strong orbit interaction [3]. However, there has been no experimental reports about the pairing symmetry. In order to study the pairing symmetry in atomically thin MoS<sub>2</sub>, we have fabricated junctions between ion-gated MoS<sub>2</sub> and conventional superconductor Al [4, 5]. Here, we report an unconventional magnetic fields response of critical current, which flows through the junction between the ion-gated MoS<sub>2</sub> and the Al electrode. We observed a very small critical current, and the magnetic response was asymmetric with respect to magnetic field and current direction. We will discuss the results from the point of view of Josephson penetration depth.

[1] Yuan, N. F. Q. *et al.* (2014). *Phys. Rev. Lett.* **113**, 097001. [2] Ye, J. T. *et al.* (2012). *Science* **338**, 1193-1196. [3] Saito, Y. *et al.* (2016). *Nat. Phys.* **12**, 144. [4] Aikawa, Y. *et al.* (2018). *J. Phys.: Conf. Ser.* **969**, 012058. [5] Aikawa, Y. *et al.* (2018). *J. Phys.: Conf. Ser.* **969**, 012057.

## P28.32 Local electronic structure around a nonmagnetic impurity in multiband superconductor CeCu<sub>2</sub>Si<sub>2</sub>

Dongdong Wang and Bin Liu

Department of Physics, Beijing Jiaotong University, Beijing 100044, China

As the first discovered unconventional superconductor, CeCu<sub>2</sub>Si<sub>2</sub> has always been regarded as a single band nodal *d*-wave superconductor and been indirectly evidenced by many experiments in the past decades. But direct experimental detection of the pairing symmetry are still lacking. Recent experiments on CeCu<sub>2</sub>Si<sub>2</sub> have found that multiband superconductivity with dominant two-gap features may be more appropriate, such as nodeless *s*<sup>±</sup>-wave or loop-nodal *s*-wave. In this paper, we study the problem within an effective model with two hybridization bands obtained from the first principle calculations. Our calculations which based on T-matrix approximation reveal that both the loop-nodal *s*-wave and *d*-wave pairing can give rise to impurity-induced bound states. The intra-gap state for loop-nodal *s*-wave pairing has emerged far away from the Fermi energy regardless of the impurity scattering strength. However, when we consider the *d*-wave one, a nearly zero-energy impurity induced bound state appears for weak impurity scattering. Furthermore, we also find that in the case of nodeless *s*<sup>±</sup>-wave, there are NO intra-gap impurity states. These features can be readily verified by high-resolution scanning tunneling microscopy/spectroscopy and are proposed to shed light on the gap symmetry of CeCu<sub>2</sub>Si<sub>2</sub>.

**P28.33 Impurity-induced resonance states and their spatial modulation in heavy-fermion superconductor CeCoIn<sub>5</sub>**

Bin Liu

Department of Physics, Beijing Jiaotong University, Beijing 100044, China

Superconducting gap symmetry reflects the nature of the underlying attractive interactions that give rise to the Cooper pairs in unconventional superconductors. Very recently, new spectroscopic technique was developed based on high-resolution scanning tunneling microscopy (STM/STS), which has been successfully applied into study the unconventional superconductivity in heavy-fermion superconductor CeCoIn<sub>5</sub>. In this work, we extend this idea and use the T-matrix approach to investigate the spatial modulation of the local electronic structures around a unitary nonmagnetic impurity in superconducting CeCoIn<sub>5</sub>. We obtain a sharp nearly zero-energy resonance state (ZERS) in the strong impurity potential scattering, and find qualitative differences in the spatial pattern of the tunneling conductance modulated by the nodal structure of the superconducting gap with  $d_{x^2-y^2}$  or  $d_{xy}$  pairing symmetry, which is in agreement with the experiment measurement, and thus proposed an alternative way to identify the pairing state in superconducting CeCoIn<sub>5</sub>.

**P28.34 Quantum Nonlinear Optics without Photons, how to excite two or more atoms simultaneously with a single photon, and other unusual properties of ultra-strongly-coupled QED systems including superconducting circuit QED.**

Franco Nori

RIKEN, Japan, and the University of Michigan, USA

We consider two separate atoms interacting with a single-mode optical or microwave resonator [1]. When the frequency of the resonator field is twice the atomic transition frequency, we show that there exists a resonant coupling between one photon and two atoms, via intermediate virtual states connected by counterrotating processes. If the resonator is prepared in its one-photon state, the photon can be jointly absorbed by the two atoms in their ground state which will both reach their excited state with a probability close to one. Spontaneous parametric down-conversion is a well-known process in quantum nonlinear optics in which a photon incident on a nonlinear crystal spontaneously splits into two photons. We have studied an analogous physical process where one excited atom directly transfers its excitation to a pair of spatially separated atoms with probability approaching 1. The interaction is mediated by the exchange of virtual rather than real photons [2,3]. This nonlinear atomic process is coherent and reversible, so the pair of excited atoms can transfer the excitation back to the first one: the atomic analog of sum-frequency generation of light.

[1] L. Garziano, et al., One Photon Can Simultaneously Excite Two or More Atoms, Phys. Rev. Lett. 117, 043601 (2016).

[2] R. Stassi, et al., Quantum Nonlinear Optics without Photons, Phys. Rev. A 96, 023818 (2017).

[3] Related work can be found in: <https://dml.riken.jp/pub/Ultra-strong/>

## P28.35 Probing Quantum Fluids with Nanomechanical Systems

A. Guthrie<sup>a</sup>, A. Guénault<sup>a</sup>, R.P. Haley<sup>a</sup>, S. Kafanov<sup>a</sup>, Yu. A Pashkin<sup>a</sup>, G. R. Pickett<sup>a</sup>, V. Tsepelin<sup>a</sup>, E. Collin<sup>b</sup>, O. Maillet<sup>b</sup>, and R. Gazizulin<sup>b</sup>

<sup>a</sup>Lancaster University, United Kingdom

<sup>b</sup>Université Grenoble Alpes, CNRS Institut NÉEL, BP 166, 38042, Grenoble Cedex 9, France

Nanoelectromechanical systems (NEMS) have great potential for sensing applications due to their unparalleled mass and force sensitivity. Here we present our experiments using doubly clamped, composite nano-beams of extremely high quality factor operating in superfluid <sup>4</sup>He at mK temperatures. We demonstrate the nano-beams' sensitivity to the thermal excitations, phonons and rotons, as well as the role of acoustics in the damping at the lowest temperatures. We present the unique ability to drive the nano-beams using the momentum transfer of phonons generated by a nearby heater. This so-called “phonon wind” is a thermomechanical effect that until now has never been demonstrated. Our work paves the way towards future low-temperature experiments using NEMS, such as probing the complex properties of superfluid <sup>3</sup>He at the lowest temperatures.

## P28.36 Optomechanics with Acoustic Modes in Helium

A. B. Shkarin<sup>a</sup>, A. D. Kashkanova<sup>a</sup>, C. D. Brown<sup>a</sup>, N. E. Flowers-Jacobs<sup>a</sup>, L. Childress<sup>a</sup>, S. W. Hoch<sup>a</sup>, L. Hohmann<sup>b</sup>, K. Ott<sup>b</sup>, S. Garcia<sup>b</sup>, J. Reichel<sup>b</sup>, and J. G. E. Harris<sup>a</sup>

<sup>a</sup>Department of Physics, Yale University, New Haven, CT 06511, USA

<sup>b</sup>Laboratoire Kastler Brossel, ENS, UPMC, CNRS, 24 rue Lhomond, 75005 Paris, France

Optomechanics is a useful tool for studying properties of mechanical objects. It can combine high sensitivity (on the level of thermal or even quantum fluctuations), small probing volume, and ability to drive mechanical motion and manipulate its properties *in situ*.

Here we describe experiments in a compact ( $\sim (100\mu\text{m})^3$ ) optomechanical device which couples infrared optical mode and acoustic modes in superfluid helium<sup>1</sup>. We observe three distinct families of acoustic modes<sup>2</sup>, which have different mode shapes and optomechanical coupling mechanisms and range in frequency from 20 kHz to 300 MHz.

We investigate in detail the highest-frequency modes, which are best suited for quantum optomechanics experiments. Their high quality factor of  $10^5$  and large optomechanical coupling allowed us to coherently excite their mechanical motion, manipulate their frequency and linewidth through dynamic back-action effect, and measure their average energy with precision better than their single energy quantum. This high precision enabled observations of quantum signatures in the motion of the acoustic waves and in their interaction with light.

1. Kashkanova, A. D., et al. *Nat. Phys.* **13**, 74–79 (2016)

2. Kashkanova, A. D., et al. *J. Opt.* **19**, 034001 (2017)

## P28.37 Statistical property of small particle trajectories in fully developed turbulent state of HeII

W. Kubo and Y. Tsuji

Energy Engineering and Sciences, Nagoya University, Japan

Lagrange trajectories of small particle in fully developed turbulent state are studied in small rectangular duct ( $10 \times 10\text{mm}^2$  in cross section). The plate heater is attached on the bottom to generate the thermal counter flow. The bath temperature is changed from 1.9K to 2.17K, and it is controlled within 1mK. The small particles made of solid hydrogen are visualized by high-speed camera and their trajectories are recorded. Not only depending on bath temperature and heater power, but also depending on their particle sizes<sup>1</sup>, their motions indicate complicated features. In this study, the Hurst exponent defined by  $|\vec{x}(t + \tau) - \vec{x}(t)| \propto \tau^H$ , where  $\vec{x}(t)$  denotes the particle position at time  $t$ . It was found that there is a typical time scale  $\tau_0$ . In small time separation ( $\tau \leq \tau_0$ ), the exponent  $H$  is small however for large time separation ( $\tau_0 \ll \tau$ ),  $H$  is nearly 1. The intermittent features are also discussed in the poster.

1. W. Kubo and Y. Tsuji, (2017). "Lagrangian Trajectory of Small Particles in Superfluid He II". Journal of Low Temperature Physics, June 2017, Volume 187, pp 611-617.

## P28.38 Periodic Oscillation of Liquid Helium Boiling in Narrow Rectangular Duct

K. Ishida<sup>a</sup>, Y. Eikoku<sup>a</sup>, A. Iwamoto<sup>b</sup>, and Y. Tsuji<sup>a</sup>

<sup>a</sup>Energy Engineering and Sciences, Nagoya University, Japan

<sup>b</sup>National Institute for Fusion Science, Japan

Temperature fluctuations in saturated super fluid He II (at 1.9K) was measured by using the small thermistors operated by a lock-in amplifier. The experiments were performed in a rectangular channel ( $13 \times 13 \times 200$  mm) in which the heater was set at the bottom. We found that the periodic temperature oscillation and the pulsive boiling sound appear. They are synchronizing and the oscillating frequencies strongly depend on the helium pressure and the heat flux. When the He pressure decreases, the oscillation frequency decreases. However, the decay rate is independent of the heat flux. This physical mechanism will be discussed in the poster. Increasing the heat flux, we observed the film boiling in He II. In the boiling process, the pressure above lambda pressure (5kPa) is a decisive factor which boiling mode appears. Above the lambda pressure, the film boiling is related with the co-existence of three phases, that is He II, He I and helium vapor. Below the lambda pressure, the film boiling should be accompanied with only two phases; He II and helium vapor. The boiling curve for He II may be different from that of classical fluid, but the detailed things are not clarified. In He II boiling, the detached vapor bubbles cannot be seen due to extremely large effective thermal conductivity, and the nucleate boiling is only observed in a transition state at the beginning of film boiling.

## P28.39 **Superradiant phase transition in the open Dicke model with local and collective driven-dissipative effects**

N. Shammah<sup>a</sup>, S. Ahmed<sup>a</sup>, N. Lambert<sup>a</sup>, S. De Liberato<sup>b</sup>, and F. Nori<sup>a</sup>

<sup>a</sup>Theoretical Quantum Physics Laboratory, RIKEN Cluster for Pioneering Research, Saitama, Japan

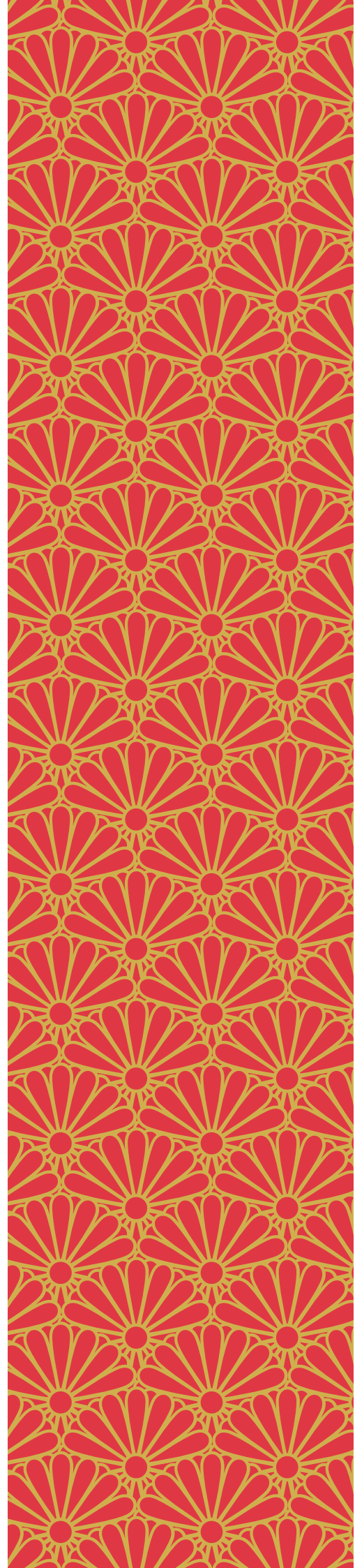
<sup>b</sup>School of Physics and Astronomy, University of Southampton, Southampton, United Kingdom

We study the Dicke model in the open setting, in the presence of collective and local incoherent processes. Each degree of freedom can couple to its own local reservoir, while there are also collective incoherent processes coupling to a common reservoir. Such local processes, although often unavoidable, are seldom considered in standard open quantum systems approaches. We have developed an open-source library in Python, the Permutational-Invariant Quantum Solver (PIQS), which we have used to study a variety of phenomena in driven-dissipative open quantum systems, including the open Dicke model. We consider both local and collective incoherent processes in the weak, strong, and ultrastrong-coupling regimes.

1. Shammah, N., Lambert, N., Nori F., and De Liberato, S., (2017). “Superradiance with local phase breaking effects”. *Phys. Rev. A*, 96, 023863, 2017
2. Shammah, N., Ahmed, S., Lambert, N., De Liberato, S., and Nori F., (2018). “Open quantum systems with both local and collective dissipation”. Submitted
3. Shammah, N., Ahmed, S., (2018). <https://github.com/nathanshammah/piqs/>
4. Dalla Torre, E.G., Shchadilova, Y., Wilner, E.Y., Lukin, M.D., Demler, E., (2018). “Dicke phase transition without total spin conservation”, *Phys. Rev. A* 94, 061802(R) (2016)
5. Kirton, P., Keeling, J., (2017). “Suppressing and restoring the Dicke superradiance transition by dephasing and decay”. *Phys. Rev. Lett.* 118, 123602 (2017)



**July 30 (Monday)**





## July 30 (Monday) Oral Presentations

### O30.1 Visualization study of quantum turbulence in superfluid helium-4: progress and future development

W. Guo<sup>a,b</sup>

<sup>a</sup>National High Magnetic Field Laboratory, 1800 East Paul Dirac Drive, Tallahassee, FL 32310, USA

<sup>b</sup>Mechanical Engineering Department, Florida State University, Tallahassee, FL 32310, USA

Helium-4 in the superfluid phase (He II) is a two-fluid system that exhibits fascinating quantum hydrodynamics with important scientific and engineering applications. It supports the most efficient heat-transfer mechanism (i.e. thermal counterflow), and it also allows the generation of flows with extremely high Reynolds numbers for turbulence modelling. However, the lack of high-precision flow measurement tools in He II has impeded the progress in understanding and utilizing its hydrodynamics. In recent years, there have been extensive efforts in developing quantitative flow visualization techniques applicable to He II. Two types of techniques based on the use of either particle tracers (i.e. micron-sized frozen particles) or molecular tracers (i.e. He<sub>2</sub> excimer molecules) have been developed. We will discuss the advantages and issues associated with these visualization techniques and will highlight some recent progress in our visualization study of counterflow and grid turbulence in He II. We will also briefly introduce our on-going work on developing the next generation flow visualization techniques and our effort on imaging quantized vortices in pure superfluid helium at low temperatures.

PLENARY TALK

### O30.2 Probing quantum turbulence using mechanical oscillators

A.M. Guènault, R.P. Haley, S. Kafanov, M.T. Noble, G.R. Pickett, M. Poole, V. Tsepelin, D.E. Zmeev, and T. Wilcox

Department of Physics, Lancaster University, LA1 4YB, United Kingdom

We present studies of quantum turbulence in superfluid <sup>3</sup>He-B and <sup>4</sup>He using mechanical oscillators. Quantum turbulence comprises single quantised vortices and is expected to differ from its classical counterpart. We use a wide range of high quality-factor resonators (superconducting wires, quartz tuning forks and nano-electromechanical beams) to generate and probe quantum turbulence. Measurements of their force-velocity characteristics allow one to probe the creation of vortices and other excitations in both superfluids. In superfluid <sup>4</sup>He the appearance of turbulence can be confirmed using the second sound attenuation in the two fluid regime or more sophisticated techniques at low temperatures. In superfluid <sup>3</sup>He, despite the stringent requirements to reach one ten-thousandth of a degree, turbulence imaging and visualisation is more straightforward since we do not need to add tracer particles and can instead exploit the properties of its inherent ballistic quasiparticles. Our measurements combined with numerical simulations of realistic 3D vortex tangles suggest that quantum turbulence produced by uni-directional injection of energy is polarised. We attribute the latter to the observed similarities between quantum and classical turbulence at ultra low temperatures. We propose experiments to create non-polarised tangles and discuss other finding.

INVITED TALK

### O30.3 Numerical Study of Coupled Dynamics in the Two-Fluid Model for Superfluid $^4\text{He}$

S. Yui<sup>a</sup>, M. Tsubota<sup>a</sup>, and H. Kobayashi<sup>b</sup>

<sup>a</sup>Department of Physics, Osaka City University, Osaka 558-8585, Japan

<sup>b</sup>Department of Physics, Hiyoshi Campus, Keio University, Yokohama 223-8521, Japan

We studied the three-dimensional coupled dynamics in the two-fluid model for superfluid  $^4\text{He}$ . We investigated quantum turbulence in a thermal counterflow with laminar normal fluid. In this numerical simulation, we combined the vortex filament model of the superfluid and the Navier–Stokes equations of the normal fluid. Our simulation showed that the velocity profile of the normal fluid is deformed significantly as quantum turbulence becomes strong. This result is consistent with the recent visualization experiments.<sup>1</sup> We investigated how the velocity profiles of the two fluids cooperatively develop. Furthermore, we introduced two parameters to characterize the normal fluid dynamics, namely Reynolds number and a mutual friction parameter. More details are shown in Ref. 2.

1. Marakov, A. *et al.* (2015). “Visualization of the normal-fluid turbulence in counterflowing superfluid  $^4\text{He}$ ”. *Physical Review B* **91**, 094503.

2. Yui, S., Tsubota, M., and Kobayashi, H. (2018). “Three-Dimensional Coupled Dynamics of the Two-Fluid Model in Superfluid  $^4\text{He}$ : Deformed Velocity Profile of Normal Fluid in Thermal Counterflow”. *Physical Review Letters* **120**, 155301.

INVITED TALK

### O30.4 Superfluid $^3\text{He}$ in Planar Aerogel

V. V. Dmitriev<sup>a</sup>, M. S. Kutuzov<sup>b</sup>, V. N. Morozov<sup>c,d</sup>, A. Y. Mikheev<sup>c</sup>, A. A. Soldatov<sup>a,e</sup>, and A. N. Yudin<sup>a</sup>

<sup>a</sup>P.L. Kapitza Institute for Physical Problems of RAS, 119334, Moscow, Russia<sup>b</sup>Metallurg Engineering Ltd., 11415, Tallinn, Estonia<sup>c</sup>Institute of Theoretical and Experimental Biophysics of RAS, 142290, Pushchino, Russia<sup>d</sup>George Mason University, Manassas, VA 20110, USA

<sup>e</sup>Moscow Institute of Physics and Technology, 141700, Dolgoprudny, Russia

We report results of experiments with liquid  $^3\text{He}$  confined in a high porosity anisotropic nanostructure which we call planar aerogel. This aerogel consists of nanofibers (with diameters  $\sim 10$  nm) which are randomly oriented in the plane normal to the specific axis. We used two samples of planar aerogel prepared using different techniques. We have found that at all used pressures (s.v.p – 29.3 bar) on cooling from the normal phase of  $^3\text{He}$  the superfluid transition in both samples occurs into an Equal Spin Pairing superfluid phase. NMR properties of this phase qualitatively agree with the properties of the ABM superfluid state but there are essential quantitative differences. Possible reasons of that will be discussed in the talk. The obtained superfluid phase diagrams will be also presented.

INVITED TALK

## O30.5 Influence of Exchange Scattering on Superfluid $^3\text{He}$ states in Nematic Aerogel

V.P. Mineev

Univ. Grenoble Alpes, CEA, INAC, PHELIQS, GT, F-38000 Grenoble, France

Superfluid state in bulk liquid  $^3\text{He}$  is realized in form of A or B phases. Uniaxially anisotropic aerogel (nafen) stabilizes transition from the normal to the polar superfluid state that on further cooling transfers by the second order phase transition to the axipolar orbital glass state. This is the case in nafen aerogel preplated by several atomic layers of  $^4\text{He}$ .<sup>1</sup> When the pure liquid  $^3\text{He}$  fills the same nafen aerogel a solid-like layer of  $^3\text{He}$  atoms coats the aerogel structure. The polar state is not formed anymore and phase transition occurs directly to the axipolar phase.<sup>2</sup> The calculation taking into account the exchange scattering shows that it can decrease the degree of anisotropy that was in its absence. The derived anisotropy of spin diffusion coefficient in globally anisotropic aerogel is determined by the same parameter which controls the polar state emergence that allows to check the effect of anisotropy suppression by the exchange scattering.

1. V. V. Dmitriev, A. A. Senin, A. A. Soldatov, and A. N. Yudin, Phys. Rev. Lett. **115**, 165304 (2015).
2. V. V. Dmitriev, A. A. Soldatov, and A. N. Yudin, Phys. Rev. Lett. **120**, 075301 (2018).

INVITED TALK

## O30.6 Stability of Half-Quantum Vortices in Polar Phase in Anisotropic Aerogel

Ryusuke Ikeda and Natsuo Nagamura

Department of Physics, Kyoto University, Japan

Recent experiment on superfluid  $^3\text{He}$  in globally anisotropic aerogels have shown realization of the half-quantum vortices (HQVs) in the polar phase [1,2] under a rotation [3]. It has been unclear why the HQVs, which had not been detected clearly in the A phase of the bulk liquid, were realized in the polar phase. We theoretically examine [4] the relative stability of a HQV-pair against a single phase vortex in both the bulk A-phase and the polar phase in an aerogel by microscopically deriving a higher order gradient term which assists the stability of HQVs but has never been taken into account so far in the Ginzburg-Landau approach. We conclude that the detected HQVs in the polar phase are not metastable objects supported by the strong pinning to the aerogel, and that the extension of the polar phase at lower pressures in the phase diagram is one of the main origins for stabilizing the HQVs in the phase.

1. K. Aoyama and R. Ikeda, Phys. Rev. B **73**, 060504(R) (2006).
2. V. V. Dmitriev et al., Phys. Rev. Lett. **115**, 165304 (2015).
3. S. Autti et al., Phys. Rev. Lett. **117**, 255301 (2016).
4. N. Nagamura and R. Ikeda, arxiv:1804.10460, v.3.

INVITED TALK

## O30.7 Rotating superfluid wave turbulence

J. T. Mäkinen<sup>a</sup>, S. Autti<sup>a</sup>, P. J. Heikkinen<sup>a</sup>, V. S. L'vov<sup>b</sup>, V. V. Zavjalov<sup>a</sup>, and V. B. Eltsov<sup>a</sup>

<sup>a</sup>Low Temperature Laboratory, Department of Applied Physics, Aalto University, Finland

<sup>b</sup>Department of Chemical and Biological Physics, Weizmann Institute of Science, Israel

Turbulence of rotating classical fluids in the limit of large Reynolds and small Rossby numbers is manifested as a wave turbulence (WT) of inertial waves (IW) [1]. In superfluids, spectrum of general vortex waves [2] extends beyond the IW cutoff frequency of  $2\Omega$  towards larger frequencies and smaller length scales as Kelvin waves, posing a question of interplay of classical and quantum features in rotating turbulence. Dynamics at the crossover length scales is important for many superfluid systems in non-stationary rotation, such as neutron stars. We suggest that rotating superfluid wave turbulence provides an experimental platform to study nonlinear vortex interactions and energy transfer at all length scales, simplified by the absence of reconnections and of hydrodynamic energy cascade.

We have experimentally studied WT on an array of vortex lines in rotating superfluid  $^3\text{He-B}$ . We create a steady WT state by periodically modulating the rotation velocity  $\Omega$  at temperatures below  $0.2T_c$ . The IW propagation velocity at the beginning of the modulation and the turbulent buildup time agree with theoretical predictions for WT. We demonstrate that the kinetic energy stored in the motion at large length scales cascades to scales smaller than the intervortex distance. As a result, the energy dissipation at large length scales is independent of the details of the dissipation at microscopic scales. Furthermore, the dissipation rate at small length scales also becomes temperature-independent at values of the mutual friction [3] where the onset of the Kelvin-wave cascade is expected [4].

[1] Yarom *et al*, Phys. Rev. Fluids **2**, 122601 (2017)[2] Henderson *et al*, Europhys. Lett. **67**, 56 (2004)

[3] Mäkinen *et al*, Phys. Rev. B **97**, 014527 (2018) [4] Boué *et al*, Phys. Rev. B **91**, 144501 (2015)

INVITED TALK

## O30.8 Quantum Vortex Shedding in Atomic Superfluid Gases

Y. Shin

Department of Physics and Astronomy, Seoul National University, Seoul, Korea

The wake behind a moving obstacle is a classic problem in fluid dynamics. I will present our recent vortex-shedding experiments with weakly interacting atomic Bose-Einstein condensates and strongly interacting fermionic superfluid gases. Highly oblate large atomic samples were prepared and perturbed by translating a repulsive optical obstacle formed by a focused laser beam, and their responses in terms of vortex nucleation were investigated for various sweeping conditions. We observed a regular-to-turbulent transition of vortex shedding pattern as the obstacle velocity increases, resembling the universal behavior of classical fluids<sup>1</sup>. We observed development of spatial pair correlations of vortices and antivortices in the turbulent superfluid containing many vortices<sup>2</sup>. In the experiments with strongly interacting atomic Fermi gases, we investigated the critical vortex shedding across the BEC-BCS crossover and observed a qualitative change of the dependence of  $v_c$  on the sweeping distance, which is attributed to the participation of pair breaking in the vortex shedding dynamics<sup>3</sup>. Finally, I will discuss the extension of the vortex-shedding experiment to a spinor superfluid which has mass and spin superfluidities simultaneously<sup>4</sup>.

1. W. J. Kwon, J. H. Kim, S. W. Seo, and Y. Shin, Phys. Rev. Lett. **117**, 245301 (2016).

2. S. W. Seo, B. Ko, J. H. Kim, and Y. Shin, Sci. Rep. **7**, 4587 (2017).

3. J. W. Park, B. Ko, and Y. Shin, arXiv:1805.08950.

4. J. H. Kim, S. W. Seo, and Y. Shin, Phys. Rev. Lett. **119**, 185302 (2017).

PLENARY TALK

## O30.9 Turbulence in a Quantum Gas

Nir Navon

Department of Physics, Yale University, New Haven, CT 06511, USA

The recent production of box-trapped Bose gases has offered new exciting possibilities to study turbulence in simple, uniform quantum fluids. We observe the emergence of a turbulent cascade in a homogeneous Bose fluid forced on a large scale using a spatially-uniform force. In contrast to classical fluids where the dissipation scale is set by the viscosity of the fluid, the turbulent cascade of our quantum gas stops when the particles kinetic energy exceeds the laser-trap depth. This mechanism allows us to effectively tune the dissipation scale where particles (and energy) are lost, and measure the particle flux in the cascade at the dissipation scale. Our measurements are in good agreement with simulations of the Gross-Pitaevskii equation that include dissipation.

[1] N. Navon et. al. *Nature* **539**, 72 (2016).

INVITED TALK

## O30.10 Quantum turbulence cascades in the Gross–Pitaevskii model

D. Proment<sup>a</sup>, M. Onorato<sup>c</sup>, and S. Nazarenko<sup>b</sup>

<sup>a</sup>School of Mathematics, University of East Anglia, Norwich Research Park, NR4 7TJ Norwich, United Kingdom

<sup>b</sup>Dipartimento di Fisica Generale, Università di Torino, Via Pietro Giuria 1, 10125 Torino, Italy

<sup>c</sup>Institut de Physique de Nice, Université Nice-Sophia Antipolis, Parc Valrose, 06108 Nice, France

I will present a numerical and theoretical study of the quantum turbulence regimes arising within in the three-dimensional Gross–Pitaevskii equation [1]. Specifically, I will focus on the direct energy cascade in the case of an open (forced-dissipated) system modelled using the wave turbulence theory. I will show that the behaviour of the system is very sensitive to the properties of the model at the scales greater than the forcing scale, identifying three different regimes: (1) a non-stationary regime characterised by a condensation process and a transition from a four-wave to a three-wave interaction process when the largest scales are not dissipated; (2) a steady weak wave turbulence regime when largest scales are dissipated with a friction-type dissipation; and (3) a state with a scale-by-scale balance of the linear and the nonlinear time scales when the large-scale dissipation is modelled using a hypo-viscous term. Those results turn out to be particularly interesting when interpreting recent experiments of out-of-equilibrium Bose–Einstein condensates [2].

1. Proment, D., Nazarenko, S., & Onorato, M. (2009). Quantum turbulence cascades in the Gross–Pitaevskii model. *Physical Review A*, 80(5), 051603.

2. Navon, N., Gaunt, A. L., Smith, R. P., & Hadzibabic, Z. (2016). Emergence of a turbulent cascade in a quantum gas. *Nature*, 539(7627), 72.

INVITED TALK

## O30.11 Vortex line density dynamics and temperature profile in thermal counterflow

E. Varga and L. Skrbek

Faculty of Mathematics and Physics, Charles University, Prague, Czech Republic

Although thermal counterflow of superfluid  $^4\text{He}$  represents the first and most extensively studied form of quantum turbulence, a number of open problems remain. Recently an intense theoretical debate about what form, if any, of the so-called Vinen equation accurately captures the dynamics of vortex line density,  $L$ , prompted us to study this problem experimentally in a 21 cm long channel of square  $7 \times 7 \text{ mm}^2$  cross section. Based on large statistics of second-sound data measured in non-equilibrium square-wave modulated thermally induced counterflow, we found that for sparse tangles all proposed forms of Vinen equation provide equally adequate descriptions of the growth of  $L$ , while for dense tangles ( $L > 10^5 \text{ cm}^{-2}$ ) none of them is satisfactory<sup>1</sup>. More recently, experimental observation<sup>2</sup> of the motion of small hydrogen and deuterium particles in the close vicinity of the heat source in thermal counterflow revealed significantly higher  $L$  than in the bulk. This ought to mean higher thermal impedance and thus a steeper temperature gradient near the heat source. For accessible heat inputs (higher than in Ref.<sup>2</sup>), we have measured the distribution of temperature directly inside the channel with six static and one movable thermometer, allowing us to approach a flat uniform heater within  $\simeq 100 \mu\text{m}$ , with a thermometer  $\simeq 1 \text{ mm}$  in size. So far, we observe no deviation from a linear temperature gradient along the channel, even close to the heater. Thus, at least from the temperature perspective, the boundary effects in thermal counterflow near the heat source for sufficiently high heat flux do not appear to play a significant role. This research is funded by the Czech Science Foundation under project GAČR 17-03572S.

1. E. Varga, L. Skrbek, (2018) Phys. Rev. B **97**, 064507

2. P. Hrubcová, P. Švančara, M. La Mantia (2018) Phys. Rev. B **97**, 064512

INVITED TALK

## July 30 (Monday) Poster Presentations

### P30.1 Spin diffusion in liquid $^3\text{He}$ confined in planar aerogel

V. V. Dmitriev<sup>a</sup>, M. S. Kutuzov<sup>b</sup>, L. A. Melnikovsky<sup>a</sup>, B. D. Slavov<sup>a,c</sup>, A. A. Soldatov<sup>a,c</sup>, and A. N. Yudin<sup>a</sup>

<sup>a</sup>P.L. Kapitza Institute for Physical Problems of RAS, 119334, Moscow, Russia<sup>b</sup>Metallurg Engineering Ltd, 11415, Tallinn, Estonia

<sup>c</sup>Moscow Institute of Physics and Technology, 141700, Dolgoprudny, Russia

We report results of both theoretical and experimental investigation of a spin diffusion in the normal phase of liquid  $^3\text{He}$  in an aerogel-like material consisting of nano-strands parallel to a specific plane (originally used for producing of filtration membranes [1]). This material corresponds to the infinite squeezing of an initially anisotropic aerogel, the opposite case of a nematic aerogel [2]. So we call it a planar aerogel. Using standart spin echo techniques we measure a spin diffusion coefficient in directions perpendicular and parallel to the plane. We see a very good agreement of the experimental results with a developed theory.

[1] V.M.T. Su, M. Terehov, and T.W. Clyne, *Adv. Eng. Mater.* **14**, 1088 (2012).

[2] V.E. Asadchikov, et al., *JETP Letters* **101**, 556 (2015).

### P30.2 Second-order Transition between the Polar and the Polar-distorted B Phases of Superfluid $^3\text{He}$

J. Rysti<sup>a</sup>, A.N. Yudin<sup>b</sup>, J. T. Mäkinen<sup>a</sup>, V.V. Dmitriev<sup>b</sup>, and V.B. Eltsov<sup>a</sup>

<sup>a</sup>Department of Applied Physics, Aalto University, 00076 AALTO, Finland

<sup>b</sup>P.L. Kapitza Institute for Physical Problems, Moscow 119334, Russia

New superfluid phases of  $^3\text{He}$  were observed in recent experiments with  $^3\text{He}$  in nafen [1], namely the polar, polar-distorted A (PdA) and polar-distorted B (PdB) phases. Here we report transitions between these phases measured at temperatures down to  $0.2 T_c$ . A new finding is a direct second-order transition between the polar and the PdB phases. Nafen is a high-porosity material consisting of nearly parallel nanofibers. Strong anisotropy of nafen makes the polar phase favorable on cooling from the normal state. On further cooling of  $^3\text{He}$  in nafen-90 (density  $90 \text{ mg/cm}^3$ , porosity 98%) the polar phase changes via a 2nd order transition into the PdA phase and then via a 1st order transition into the PdB phase, as was observed at pressures  $P > 10 \text{ bar}$  [1]. At lower pressures and essentially lower temperatures we have found that the polar-PdA phase transitions line in nafen-90 ends on the line of transitions into the PdB phase at  $P \approx 1 \text{ bar}$ . Below this pressure the PdA phase does not exist and on cooling from the polar phase we observe a 2nd order transition into the PdB phase. At very low temperatures the same transition is also found in  $^3\text{He}$  in nafen-243 (porosity 94%). These observations confirm the identification of the high-temperature superfluid phase as the polar phase. Since phase boundaries in  $^3\text{He}$  preserve macroscopic superfluid coherence, the discovered transitions provide a unique possibility to study transformation of various topological structures, like half-quantum vortices (HQVs) [2], between different phases [3].

[1] V.V. Dmitriev *et al.*, *PRL* **115**, 165304 (2015).

[2] S. Autti *et al.*, *PRL* **117**, 255301 (2016).

[3] Rysti *et al.*, HQVs and Kibble walls in the polar-distorted phases of superfluid  $^3\text{He}$ , This conference.

### P30.3 Anisotropic Aerogel on a Floppy Wire in $^3\text{He}$

S. Autti, A.M. Guénault, R.P. Haley, A. Jennings, S. Kafanov, G.R. Pickett, R. Schanen, V. Tsepelin, and D.E. Zmeev

Department of Physics, Lancaster University, UK

Recently it has been shown that a wire driven at quasi-uniform velocity can exceed the predicted Landau velocity in  $^3\text{He-B}$  at very low temperatures without a large increase in damping.<sup>1</sup> Here we present plans for a further experiment in which the goalpost-shaped “floppy” wire has a nafen aerogel sample encased in an NMR coil attached to the crossbar. The presence of anisotropic aerogels in  $^3\text{He}$  allows the creation of the polar phase as well as polar-distorted A phase and B phase below the transition temperature.<sup>2</sup>

This experiment will allow the probing of properties of several superfluid phases and a larger investigation into the dissipation mechanisms associated with both accelerating and uniform motion, and pinpoint critical velocities of all known possible  $^3\text{He}$  superfluids.

1. D. I. Bradley *et al.*, Nat. Phys. **12**, 1017 (2016).
2. V.V. Dmitriev *et al.*, Phys. Rev. Lett. **115**, 165304 (2015).

### P30.4 Spin Waves in Disordered Superfluid $^3\text{He}$

A. M. Zimmerman, M. D. Nguyen, and W. P. Halperin

Department of Physics and Astronomy, Northwestern University, Evanston, IL 60208, USA

Spin waves in superfluid  $^3\text{He}$  have been reported from continuous wave NMR measurements in a uniform magnetic field, appearing as sharp periodic resonances that separate from the main NMR spectra.<sup>1,2</sup> These modes have only been observed in the B-phase of the pure superfluid, and are induced by order parameter textures<sup>3</sup> created by parallel plate geometries,<sup>1</sup> or the flare out texture in a cylinder.<sup>2</sup>

We have observed a new spin wave phenomenon in disordered superfluid  $^3\text{He}$  confined within anisotropic silica aerogel with negative uniaxial strain,<sup>4</sup> in this case in both the A and B-phases. With a high-resolution, pulsed NMR technique, the resulting peaks are extremely well resolved, with up to six distinct spin resonances. In contrast to the bulk measurements,<sup>1,2</sup> the spin waves in silica aerogel occur only once the spin has been tipped by a comparably large angle of the nuclear magnetization,  $50^\circ$  to  $270^\circ$ . The frequency and line width of the resulting spin resonances are both tip angle and temperature dependent, disappearing at the critical temperature of the aerogel superfluid and changing at the A to B transition. Here, we report the experimental properties of this new class of spin waves. This work is supported by the National Science Foundation, DMR-1602542.

1. D.D. Osheroff, Physica, 90B, 20 (1977).
2. P.J. Hakonen *et al.* JLTP, **76**, 3-4, 225 (1989).
3. H. Smith *et al.*, Phys. Rev. B **15**, 1, 199 (1977).
4. J.I.A. Li *et al.*, Phys. REv. Lett. 112, 115303 (2014); *ibid* 114, 105302 (2015).



### P30.5 The Polar-phase of Superfluid $^3\text{He}$ Stabilized in Anisotropic Silica Aerogel

Man D. Nguyen, A.M. Zimmerman, and W.P. Halperin

Department of Physics and Astronomy, Northwestern University, Evanston, USA

Silica aerogel can be used to introduce disorder into superfluid  $^3\text{He}$ , stabilizing new phases and order parameter textures that do not occur in the pure superfluid<sup>1,2,3</sup>. In particular, aerogel can be processed to have anisotropic disorder by either stretching (positive strain) or compressing (negative strain) the samples. Using NMR spectroscopy, we observe evidence at low pressure for a new superfluid phase in 20% negatively strained aerogel. The magnetic susceptibility of this new phase is consistent with an equal-spin pairing state. In addition, the frequency shift of this new phase is greater than the A-phase frequency shift in isotropic (zero strain) aerogel. Thirdly, there is a continuous phase transition into a polar distorted B-phase at lower temperatures. These three observations indicate that the polar phase of superfluid  $^3\text{He}$  has been stabilized at low pressure by the anisotropic disorder of the aerogel. This work is supported by the National Science Foundation, DMR-1602542.

- [1] J. Pollanen *et al*, Nature Physics **8**, 317-320 (2012).
- [2] J.I.A. Li *et al*, Phys. Rev. Lett. **114**, 105302 (2015).
- [3] V.V. Dmitriev *et al*, Phys. Rev. Lett. **115**, 165304 (2015).

### P30.6 Phase Diagram of Superfluid $^3\text{He}$ in Nematic Aerogel in Strong Magnetic Field (Ginzburg-Landau Theory)

E. Surovtsev

P.L. Kapitza Institute for Physical Problems of Russian Academy of Science, Russia

All components of the order parameter of bulk superfluid  $^3\text{He}$  have the same transition temperature. Global anisotropy introduced into the system lifts the given degeneracy. For nematic aerogels this leads to the splitting of transition temperature for different projections of orbital momentum of Cooper pairs:  $T_{c_0}$  for  $l = 0$  and  $T_{c_1}$  for  $l = \pm 1$ ,  $T_{c_0} > T_{c_1}$ .<sup>1</sup> Magnetic field, in its turn, makes transition temperature different for each component of spin part of the order parameter.<sup>2</sup> Here we present analysis of the simultaneous effect of the orbital and spin global anisotropies on the phase diagram of superfluid  $^3\text{He}$ . Calculations are made in the framework of Ginzburg-Landau theory. The sequence of four second-order transitions is found. The first transition occurs into the  $\beta$ -phase with the order parameter of the form  $\frac{\Delta}{\sqrt{2}}(d_\mu + ie_\mu)m_j$ . NMR properties of new phases are presented.

1. K. Aoyama and R. Ikeda, Phys. Rev. B, **73**, 060504 (2006).
2. V. Ambegaokar and N. D. Mermin, Phys. Rev. Lett., **30**, 81 (1973).

### P30.7 NMR Shifts in Pure $^3\text{He}$ in Anisotropic Aerogels Induced by Demagnetizing Fields

V. V. Dmitriev<sup>a</sup>, A. A. Soldatov<sup>a,b</sup>, and A. N. Yudin<sup>a</sup>

<sup>a</sup>P.L. Kapitza Institute for Physical Problems RAS, Moscow, Russia

<sup>b</sup>Moscow Institute of Physics and Technology, Dolgoprudny, Russia

It is known that strands of aerogel immersed in liquid pure  $^3\text{He}$  are covered by  $\sim 2$  atomic layers of solid  $^3\text{He}$ . The magnetic moment of these layers follows the Curie-Weiss law and near the  $^3\text{He}$  superfluid transition temperature ( $T_c$ ) can exceed that of liquid  $^3\text{He}$  inside the aerogel sample. The magnetic properties of these layers can be described by demagnetizing factors of a system of cylindrical surfaces resulting in NMR shift [1]. In globally isotropic aerogel the influence of the demagnetizing field produced by randomly oriented cylindrical surfaces is averaged and the NMR shift is absent. Here we report the results of NMR experiments with pure  $^3\text{He}$  in anisotropic aerogels with different types of anisotropy (nematic and planar aerogels). In this case the NMR shift is clearly seen and depends on value and orientation of the magnetic field. The obtained results are well described by a model of the system of non-interacting paramagnetic cylinders. The shift is proportional to the magnetization of solid  $^3\text{He}$  and at  $T \sim T_c$  can be large that complicates NMR experiments in superfluid  $^3\text{He}$  in aerogel.

[1] C. Kittel, Phys. Rev. **73**, 155 (1948).

### P30.8 Spectrum in the strong turbulence region of Gross-Pitaevskii turbulence

K. Yoshida<sup>a</sup>, Y. Tsuji<sup>b</sup>, and H. Miura<sup>c</sup>

<sup>a</sup>Faculty of Pure and Applied Sciences, University of Tsukuba, Tsukuba, Japan

<sup>b</sup>Graduate School of Engineering, Nagoya University, Nagoya, Japan

<sup>c</sup>National Institute for Fusion Science, Toki, Japan

Dynamics of quantum fluids such as superfluid  $^4\text{He}$  or Bose-Einstein condensates (BECs) of ultracold atoms are approximately described by the Gross-Pitaevskii (GP) equations under a certain condition. Turbulent states of quantum fluids have been studied from various aspects including theoretical analysis, numerical simulations, and experiments. The statistical properties such as spectrum seems to depend on situations and the comprehensive understanding of the spectrum has not been established yet. In the present study, we performed the numerical simulation of GP equation in a three-dimensional box with periodic boundary conditions, focusing on the strong turbulence region, i.e., the wavenumber region where the nonlinearity in the GP equation is strong. Pumping and dissipation of the mass are applied in small- and large-wavenumber regions, respectively, in order to maintain a turbulent state. It is found that the mass is transferred with a constant flux from a small wavenumber range to a large wavenumber range and the spectrum approximately obeys the  $k^{-1}$  law, where  $k$  is the wavenumber, predicted from a spectral closure approximation<sup>1</sup>.

1. Yoshida, K. and Arimitsu, T. (2013). "Inertial-range structure of Gross-Pitaevskii turbulence within a spectral closure approximation". J. Phys. A: Math. Theor., **46**, 35501.

### P30.9 Visualization of a Coflow Jet in Superfluid $^4\text{He}$ Using Tracer Particles

M.J. Jackson<sup>a</sup>, D. Schmoranzer<sup>a</sup>, and J. Luzuriaga<sup>b</sup>

<sup>a</sup>Faculty of Mathematics and Physics, Charles University, Ke Karlovu 3, 121 16, Prague 2, Czech Republic.

<sup>b</sup>Centro Atómico Bariloche, (8400) S.C. Bariloche, CNEA, Inst. Balseiro, UNC, Argentina.

We present preliminary results of the visualization of a submerged coflow jet of liquid helium propagating inside the bulk superfluid. The apparatus is based on a fountain effect pump producing a jet when power is applied to its heater. The volume in front of the pump's orifice is illuminated by a green laser light cone. We introduce small particles of solid hydrogen to visualize the flow. We report on the statistics of the velocities inferred from the particle trajectories recorded by a high speed camera at 1.68 and 1.95 K, for jet velocities ranging from 47 to 4500 mm/s. We compare the characteristics of such a coflow jet with those of a classical submerged fluid jet and we comment on the efficiency of the jet at dragging the particles along with it.

This research is supported by the Czech Science Foundation project GAČR 17-03572S and by the grant 7AMB15AR026 under the EU-7AMB Czech-Argentine MOBILITY scheme.

### P30.10 Nanomechanical probes of the quantum fluids with single-vortex sensitivity

T. Kamppinen, V. B. Eltsov, and J. Mäkinen

Low Temperature Laboratory, Department of Applied Physics, Aalto University, Finland

Modern nanofabrication techniques enable creation of extremely sensitive force and mass detectors, which have many potential applications in the quantum fluids like  $^3\text{He}$  and  $^4\text{He}$ . We have fabricated suspended aluminium nanomechanical resonators with beam cross section  $150\text{ nm} \times 1.1\text{ }\mu\text{m}$ , size  $\sim 10\text{ }\mu\text{m}$ , and resonance frequency between 300 – 500 kHz. The response of these magnetomotively driven devices has been measured in vacuum and superfluid  $^4\text{He}$  at temperatures down to 16 mK, where Q values up to 35000 are reached. In vacuum at  $T < 0.7\text{ K}$ , the resonance line width (damping) depends on temperature as  $\Delta f \propto T^{0.4}$  and the resonance frequency increases logarithmically with temperature. We attribute these properties to tunneling two-level systems present in the native aluminium oxide layer. In superfluid  $^4\text{He}$  at  $T < 1\text{ K}$ , damping increases further due to momentum exchange with phonon and roton quasiparticles, while acoustic emission is not observed. At large oscillation amplitudes the response becomes Duffing-like nonlinear and bistable. In superfluid  $^4\text{He}$  at  $T = 18\text{ mK}$ , when oscillation velocity reaches  $v_c = 0.17\text{ m/s}$ , a sudden collapse of oscillations is observed independently of the driving force. We attribute this collapse to emission of a vortex ring. The force resolution of these devices  $\sim 1\text{ fN}$  is sufficient for detecting a single quantized vortex attached to the device, which allows in future to study experimentally the cascade of Kelvin waves on a single quantized vortex in superfluid  $^3\text{He}$  and  $^4\text{He}$ ; the role of vortex-core-bound fermions in vortex dynamics in  $^3\text{He-B}$ ; vortex friction due to the chiral anomaly, and the synthetic electromagnetic fields created by vortex motion in Weyl superfluid  $^3\text{He-A}$ .

### P30.11 Picturing Quantum Turbulence with a Quasiparticle Camera

R. P. Haley, S. Kafanov, M. T. Noble, G. R. Pickett, M. Poole, R. Schanen, V. Tsepelin, T. Wilcox, and D. E. Zmeev

Department of Physics, Lancaster University, Lancaster LA1 4YB, UK

We present measurements of quantum turbulence in  $^3\text{He-B}$  using a quasiparticle camera<sup>1</sup> at ultra-low temperatures. A black body radiator creates a beam of thermal quasiparticles towards a  $5 \times 5$  array of quartz tuning forks that can measure the local quasiparticle flux. By creating a quantum turbulent vortex tangle in-between the black box and the camera we can image turbulence by observing the decrease in quasiparticle flux due to the Andreev reflection of a fraction of quasiparticles off the vortices in the tangle. In recent measurements we explore the dynamics and development of quantum turbulence produced by a vibrating wire resonator on front of the camera.

1. S. L. Ahlstrom, D. I. Bradley, S. N. Fisher and et al (2014), A Quasiparticle Detector for Imaging Quantum Turbulence in Superfluid  $^3\text{He-B}$ , *Journal of Low Temperature Physics*, **175** 5-6, 725.

### P30.12 Vortex reconnections in superfluids: universal properties and sound emission

A. Villois<sup>a</sup>, D. Proment<sup>a</sup>, and G. Krstulovic<sup>b</sup>

<sup>a</sup>School of Mathematics, University of East Anglia, Norwich Research Park, NR4 7TJ Norwich, United Kingdom

<sup>b</sup>Laboratoire Lagrange, Observatoire de la Côte d'Azur, CNRS, Université de la Côte d'Azur, 06304 Nice, France

I will present numerical and theoretical investigations of vortex reconnections in superfluids modelled by the Gross–Pitaevskii equation. Firstly, I will explain what are the universal and nonuniversal aspects of the reconnection process, by mentioning the rate of approach and separation and the geometrical properties of the filaments about the reconnection event [1]. Specifically, I will show how the ratio between the rate of approach and separation identifies uniquely a local reconnecting angle. I will then report on a recent statistical study on the decay of a quantum vortex (Hopf) link into ring(s), obtained by varying the initial relative position of the vortices forming the link. In this respect, I will analyse how the emission of phonons is linked to the distribution of the local reconnecting angle and speculate about the statistical irreversibility of the flow occurring due the reconnection events.

1. Villois, A., Proment, D., & Krstulovic, G. (2017). Universal and nonuniversal aspects of vortex reconnections in superfluids. *Physical Review Fluids*, 2(4), 044701.

### P30.13 Vortex phase separation in two-component Bose-Einstein condensates

J. Han and M. Tsubota

Department of Physics, Osaka City University, Osaka, Japan

Three-dimensional classical turbulence shows the energy cascade from large to small spatial scales. Three-dimensional quantum turbulence also shows the similar energy cascade.<sup>1</sup> On the other hand, Kraichnan predicted that two-dimensional classical turbulence shows the inverse energy cascade from small to large spatial scales.<sup>2</sup> Onsager predicted the emergence of large-scale vortex structures for two-dimensional system.<sup>3</sup> In two-dimensional quantum turbulence, like-sign vortices are expected to cluster and form a large-scale Onsager vortices. Groszek et al. studied numerically the dynamics of quantized vortices in two-dimensional one-component Bose-Einstein condensate (BECs) by the Gross-Pitaevskii equation, thus showing formation of a Onsager vortices.<sup>4</sup> Multicomponent BECs are related to superfluid <sup>3</sup>He, unconventional superconductors, and so on, and show some different dynamics from one-component BECs.<sup>5</sup> Thus we study numerically the dynamics of quantized vortices in two-dimensional two-component BECs. We confirm that the vortices of the two-components spatially separate from each other, even for miscible two-component BECs, suppressing the formation of Onsager vortices.<sup>6</sup> This phenomenon, which we call vortex phase separation, is caused by the repulsive interaction between vortices belonging to different components. We discuss the dependence of vortex phase separation on the interaction.

1. M. Kobayashi and M. Tsubota, *Pays. Rev. Lett.* **94**, 065302 (2005). 2. R. H. Kraichnan, *Phys.Fluids* **10**, 1417 (1967). 3. L. Onsager, *Nuovo Cimento* **6**, 279 (1949). 4. A. J. Groszek et al., *Phys. Rev. A* **93**, 043614 (2016). 5. K. Kasamatsu, M. Tsubota and M. Ueda, *Int. J. Mod.Phys. B*, **19**, 1835 (2005). 6. J. Han and M. Tsubota, *J. Phys. Soc. Jpn* **87**, 063601 (2018).

### P30.14 Collective modes of vortex lattices in two-component Bose-Einstein condensates in synthetic gauge fields

T. Yoshino<sup>a</sup>, S. Furukawa<sup>a</sup>, S. Higashikawa<sup>a</sup>, and M. Ueda<sup>a,b</sup>

<sup>a</sup>Department of Physics, University of Tokyo, Japan

<sup>b</sup>RIKEN Center for Emergent Matter Science (CEMS)

There has been an ever-growing interest in artificially created gauge fields in ultracold atomic gases, which are induced by either rotating gases or optically dressing atoms. When the gas is composed of two components, the former (latter) method induces mutually parallel (antiparallel) synthetic magnetic fields in the two components. Two-component Bose-Einstein condensates (BECs) in parallel and antiparallel fields are known to show the same vortex-lattice phase diagram with five different lattice structures determined by the ratio of the intercomponent interaction  $g_{\uparrow\downarrow}$  to the intracomponent one  $g$  within the mean-field theory. Therefore it is interesting to ask whether and in what way the difference between the cases of parallel and antiparallel fields occurs. Here we study collective modes of vortex lattices in two-component BECs by means of the Bogoliubov theory and an effective field theory as a consequence of quantum fluctuations. We find that two modes with linear and quadratic dispersion relations appear in both the types of synthetic fields. While the excitation spectra are significantly different between the two types of synthetic fields, their low-energy parts are found to be related to each other by simple rescaling for intercomponent attraction  $g_{\uparrow\downarrow} < 0$ . However, contrary to the effective theory prediction, this relation is violated for intercomponent repulsion  $g_{\uparrow\downarrow} > 0$  with a greater degree of violation for larger repulsion. We also analyze the anisotropy of the Bogoliubov excitation spectra at low energies and find that it is well described by the effective theory for all vortex lattice phases.

P30.15 **Anomalous hierarchy in domain coarsening dynamics of two-component Bose–Einstein condensates**

Hiromitsu Takeuchi

Department of Physics, Osaka City University, Osaka 558-8585, Japan

Non-equilibrium time evolution of phase ordering due to spontaneous symmetry breaking (SSB) occurs universally in systems ranging from condensed matter to cosmology and high-energy physics. We can predict nothing more than a small part of the whole story of the SSB time evolution, such as the number of topological defects nucleated in early stage according to the Kibble–Zureck mechanism and the power-law decay of the defect density in the late stage according to the dynamic scaling law of phase ordering kinetics, even for the simplest case of domain coarsening dynamics induced by  $Z_2$  symmetry breaking in two dimensions. It is important to develop an understanding of the evolution in multi-component superfluids like superfluid  $^3\text{He}$  and binary/spinor Bose–Einstein condensates (BECs) since they can display the most diverse phenomena of SSB in condensed matter owing to their multi-degree of freedom and quantum effects. The prediction of the non-equilibrium dynamics is improved substantially by combining percolation theory with phase ordering kinetics. The combined theory suggests that there is a hierarchy with the two scaling regimes, called the microscopic and macroscopic regimes, during the dynamic scaling regime of the SSB time evolution. In the SSB time evolution of two-dimensional domain coarsening dynamics, the hierarchy is highlighted due to *quantum-fluid effect*; that is, the number of smaller domains is maximized in the presence of vortex sheets.<sup>1</sup>

1. Hiromitsu Takeuchi (2018). “Domain-area distribution anomaly in segregating multi-component superfluids”. Phys. Rev. A **97**, 013617; arXiv:1703.10581.

P30.16 **Thermalization of a weakly interacting Bose gas in a disordered trap**

Che-Hsiu Hsueh<sup>a</sup>, Makoto Tsubota<sup>b,c</sup>, and Wen-Chin Wu<sup>a</sup>

<sup>a</sup>Department of Physics, National Taiwan Normal University, Taipei 11677, Taiwan

<sup>b</sup>Department of Physics, Osaka City University, Sugimoto 3-3-138, Sumiyoshi-ku, Osaka 558-8585, Japan

<sup>c</sup>The OCU Advanced Research Institute for Natural Science and Technology (OCARINA), Osaka, Japan

Previously we numerically showed that thermalization can occur in an oscillating Bose-Einstein condensate (BEC) with a disordered harmonic trap when healing length  $\xi$  of the condensate is shorter than the correlation length  $\sigma_D$  of the disorder [see, for example, the experiment reported in Phys. Rev. A **82**, 033603 (2010)]. In this work, we investigate the weakly interacting regime  $\xi > \sigma_D$  and show that the oscillating BEC can also exhibit a relaxation process from nonequilibrium to equilibrium. In such an isolated quantum system, energy and particle number are conserved and the irreversible evolution towards thermodynamic equilibrium is induced by the disorder. The thermodynamic equilibrium is evidenced by the maximum entropy  $S[n_k]$  in which the waveaction spectrum  $n_k$  follows the Rayleigh-Jeans distribution. Besides, unlike a monotonic irreversible process of thermalization to equilibrium, the Fermi-Pasta-Ulam-Tsingou recurrence arises in this system manifested by the oscillation of the non-equilibrium entropy.

### P30.17 Can the truncated-Wigner approximation correctly describe thermal and quantum phase slips in one-dimensional Bose gases?

M. Kunimi<sup>a</sup> and I. Danshita<sup>b</sup>

<sup>a</sup>Yukawa Institute for Theoretical Physics, Kyoto University, Japan

<sup>b</sup>Department of Physics, Kindai University, Japan

Thermal or quantum phase slips are a main mechanism of superflow decay in low-dimensional systems. The recent experiment [1] and the subsequent theoretical study [2] have revealed that the damping of dipole oscillations of one-dimensional Bose gases in an optical lattice is due to thermal phase slips when the flow velocity is small. However, the damping mechanism in the large-velocity regime remains unclear. One difficulty is that one must calculate finite temperature quantum dynamics quantitatively to compare the experimental and the theoretical results. While the truncated-Wigner approximation (TWA) [3,4] is one of the candidates for describing such dynamics, there has been no evidence that the TWA can describe the phase slips quantitatively. We calculate the flux quench dynamics in one-dimensional Bose-Hubbard model and compare the TWA results with the Kramers formula for thermal phase slips [2] and the instanton method for the quantum phase slip [5], respectively. We show that the TWA with the Bogoliubov-type initial condition fails to describe the phase slips quantitatively.

1. L. Tanzi, *et al.*, *Sci. Rep.* **6**, 25965 (2016).
2. MK and ID, *Phys. Rev. A* **95**, 033637 (2017).
3. P. B. Blakie, *et al.*, *Adv. Phys.* **57**, 363 (2008).
4. A. Polkovnikov, *Ann. Phys.* **325**, 1790 (2010).
5. ID and A. Polkovnikov, *Phys. Rev. B* **82**, 094304 (2010).

### P30.18 Impurities in a Bose-Einstein Condensate: from Yukawa to Efimov

P. Naidon

RIKEN Nishina Centre, Wako, Japan

The Yukawa attraction (screened  $1/r$  interaction) is known to arise between two particles exchanging bosons, such as nucleons exchanging mesons in nuclear physics, or helium-3 atoms exchanging bosonic excitations of a helium-4 liquid in low-temperature physics<sup>1</sup>. On the other hand, at the three-body level, the Efimov attraction ( $1/r^2$  three-body interaction) can emerge from resonant two-body interactions, leading to the existence of the famous Efimov three-body bound states<sup>2</sup>.

In this work<sup>3</sup>, I look into how the mediated interaction between two particles immersed in a Bose-Einstein condensate can go from a Yukawa attraction to an Efimov attraction, as the strength of the particle-boson interaction is increased.

This has implications for the many-body physics of Bose polarons, which are currently being realised in ultra-cold mixtures of atoms. My results show that in the intermediate regime between Yukawa and Efimov, the mediated interaction can bind two polarons to form bipolarons that correlate in the limit of resonant particle-boson interaction to Efimov three-body states of two impurities and one boson.

1. Bardeen, Baym, Pines (1967). “Effective Interaction of He<sup>3</sup> Atoms in Dilute Solutions of He<sup>3</sup> in He<sup>4</sup> at Low Temperatures” *Phys Rev* 156, 207.
2. Efimov, V. (1970) “Weakly-bound states of three resonantly-interacting particles” *Yad. Fiz.* 12 1080. Naidon, P. and Endo, S. (2017) “Efimov physics: a review” *Rep. Prog. Phys.* 80 056001.
3. Naidon, P. (2018) “Two impurities in a Bose-Einstein condensate: from Yukawa to Efimov attracted polarons” *J. Phys. Soc. Jpn.* 87, 043002

### P30.19 Minimum of the ratio of shear viscosity to entropy density in an ultracold Fermi gas

D. Kagamihara, D. Inotani, and Y. Ohashi

Department of Physics, Keio University, Japan

We theoretically investigate hydrodynamic properties of an ultracold Fermi gas in the BCS-BEC crossover region. Among various hydrodynamic quantities, the shear viscosity  $\eta$  in a strongly-interacting fluid has attracted much attention, because Kovtun, Son, and Starinets conjectured the presence of lower bound of the ratio  $\eta/s$  of the shear viscosity to the entropy density  $s$  (KSS conjecture)[1]. Since this ratio is known to become small when fluctuations are strong, the unitary regime of an ultracold Fermi gas is considered as a good testing ground to assess this conjecture.

In this work, including pairing fluctuations within the framework of a self-consistent  $T$ -matrix approximation[2], we numerically evaluate the shear viscosity  $\eta$ , the entropy density  $s$ , as well as the ratio  $\eta/s$ , in the BCS-BEC crossover region. We find that the minimum of the ratio  $\eta/s$  is obtained in the strong-coupling BEC side,  $(k_F a_s)^{-1} \simeq 0.4$ , not at the superfluid phase transition temperature  $T_c$ , but slightly above  $T_c$ ,  $T \simeq 0.25T_F$ . The minimum value is about 5 times larger than the conjectured lower bound,  $\hbar/4\pi k_B$ . We also point out that, to properly describe  $\eta$ , one should carefully take into account an effective interaction between preformed Cooper pairs, especially in the strong-coupling BEC side.

1. P. K. Kovtun, D. T. Son, and A. O. Starinets, Phys. Rev. Lett. **94**, 111601 (2005).
2. R. Haussmann, Z. Phys. B **91**, 291 (1993); T. Enss, R. Haussmann, and W. Zwerger, Ann. Phys. **326**, 770 (2011)
3. E. Elliott, J. A. Joseph, and J. E. Thomas, Phys. Rev. Lett. **113**, 020406 (2014).

### P30.20 Isothermal Compressibility of an Ultracold Fermi Gas in the BCS-BEC Crossover

R. Sato, D. Kagamihara, K. Manabe, D. Inotani, and Y. Ohashi

Department of Physics, Keio University, 3-4-1 Hiyoshi, Kohoku-ku, Yokohama 223-8522, Japan

We theoretically investigate the isothermal compressibility  $\kappa$  in an ultracold Fermi gas with a contact-type attractive interactions in the normal state. It has been known that  $\kappa$  calculated within a conventional non-self-consistent  $T$ -matrix approximation shows an artificial divergence at the superfluid transition temperature  $T_c$  because the repulsive inter-pair interaction is not considered<sup>1</sup>. In this presentation, by including pairing fluctuations within the self-consistent  $T$ -matrix approximation<sup>2</sup>, in which the repulsive molecular interaction is taken into account, we successfully calculate  $\kappa$  in the entire BCS-BEC crossover region in the normal phase without the divergence at  $T_c$ . We find that the calculated  $\kappa$  quantitatively describes the recent experiment on a <sup>6</sup>Li Fermi gas at the unitarity limit.<sup>3</sup> We also show that  $\kappa$  is sensitive to the interaction between the preformed Cooper pairs above  $T_c$ . This result indicates that the observation of  $\kappa$  might be useful for understanding the effects of the repulsive inter-pair interactions in the BCS-BEC crossover phenomenon.

1. A. Perali, P. Pieri, G. C. Strinati, and C. Castellani, Phys. Rev. B **66**, 024510 (2002)
2. R. Hausmann, Z. Phys. B. **91**, 291 (1993)
3. M. J. H. Ku, A. T. Sommer, L. W. Cheuk, and M. W. Zwierlein, Science **335**, 563 (2012)



### P30.21 Strong coupling effects on specific heat in the BCS-BEC crossover

D. Inotani, P. van Wyk, and Y. Ohashi

Department of Physics, Keio University, Yokohama, Japan

We investigate strong-coupling effects on specific heat at constant volume  $C_V$  of a superfluid Fermi gas with a tunable attractive interaction associated with Feshbach resonance. Including strong fluctuations of the superfluid order parameter within a Gaussian approximation<sup>1,2</sup>, we calculate  $C_V$ , by numerically evaluating the temperature derivative of the internal energy, in the entire BCS-BEC crossover regime below the superfluid transition temperature  $T_c$ . We show that the temperature dependence of  $C_V$  is useful to clarify which kind of low-energy excitation dominates the thermodynamic properties of the system. We also determine a characteristic temperature below which the contribution from the Anderson-Bogoliubov mode to the thermodynamic quantities is dominant.

We find that our numerical result quantitatively describes an experimental result on  $^6\text{Li}$  Fermi gas<sup>3</sup>. Since the low-energy excitations, such as the Anderson-Bogoliubov mode and the Higgs mode, are fundamental physical phenomenon in the Fermionic superfluidity, our results indicate that the observation of  $C_V$  is useful for further understanding the BCS-BEC crossover physics.

1. Y. Ohashi and A. Griffin, Phys. Rev. A **67**, 063612 (2003).
2. H. Hu, X. J. Liu, and P. D. Drummond, Phys. Rev. A **77**, 061605R (2008).
3. M. J. H. Ku, A. T. Sommer, L. W. Cheuk, and M. W. Zwierlein, Science. **335**. 563-567 (2012).

### P30.22 Photoemission Spectra in the BCS-BEC Crossover Regime of a Rare-Earth $^{173}\text{Yb}$ Fermi Gas in a Harmonic Trap

S. Mondal, D. Inotani, and Y. Ohashi

Faculty of Science and Technology, Department of Physics, Keio University (Japan)

We theoretically investigate photoemission spectra (PES) in a  $^{173}\text{Yb}$  Fermi gas with an orbital Feshbach resonance (OFR). This novel Feshbach resonance has been discovered very recently, and is now expected as a promising pairing mechanism of the superfluid phase transition in this rare-earth Fermi gas. All including (1) the two-band nature of this gas system, (2) effects of strong-pairing fluctuations originating from a tunable pairing interaction associated with OFR within the framework of a strong-coupling  $T$ -matrix approximation, as well as (3) effects of spatial inhomogeneity coming from the trapped geometry in the local density approximation, we evaluate PES in the BCS-BEC crossover region. We clarify strong-coupling corrections to PES in both the open and closed channel. We also discuss similarity and difference between the present two-channel system with OFR and the single-channel case with a broad magnetic Feshbach resonance that has been extensively discussed in alkali-metal  $^{40}\text{K}$  Fermi gases.

### P30.23 **Photoemission Spectrum in the Normal State of a Strongly Interacting Bose-Fermi Mixture**

K. Manabe, D. Kagamihara, D. Inotani, and Y. Ohashi

Department of Physics, Keio University, Japan

We theoretically investigate strong-coupling effects on single-particle properties of a Bose-Fermi mixture with a realistic mass-imbalance between two atomic species, by extending some of the authors' previous work for the mass-balanced case. Including the effects of an attractive hetero-pairing interaction within the theoretical framework of an improved  $T$ -matrix approximation<sup>1</sup>, we calculate single-particle spectral weight (SW), as well as photoemission spectrum(PES) in existing  $^{23}\text{Na}$ - $^{40}\text{K}$  and  $^{87}\text{Rb}$ - $^{40}\text{K}$  mixture. We find that while a three-peak structure in SW associated with strong pairing fluctuations, as shown in the mass-balanced case<sup>1</sup>, remains even when mass imbalance exists, it is sensitive to the mass difference between Bose and Fermi atoms which peak structure is clearly seen in SW. We also clarify that these strong-coupling phenomena can be seen in PES, which is experimentally accessible in cold atom physics. Since the effects of pairing fluctuations on the single-particle properties of a Bose-Fermi mixture are qualitatively different from those of a two-component Fermi gas, our results would help to understand how the quantum statistics affects pairing phenomena in a two-component gas mixture.

1. D. Kharga, D. Inotani, R. Hanai, Y. Ohashi, J. Phys. Soc. Jpn. **86**, 084301 (2017).

### P30.24 **Collective excitations in Bose-Fermi mixtures**

Y. Asano, Y. Narushima, S. Watabe, and T. Nikuni

Department of Physics , Tokyo University of Science, Japan

Properties of collective excitations in a normal Bose-Fermi mixture are studied. We investigate a collective excitation of density fluctuations and the dynamic density structure factor by changing population and mass imbalance parameters as well as interaction strength. Our work shows that although the frequency of the collective excitation at the low temperature deviates from that of the hydrodynamic mode, this frequency is also different from that in the collisionless regime, which has been studied in the context of the zero-sound in the Fermi liquids. We discuss the effect of the Bose statistics in the collective excitation.

### P30.25 Higgs mode in a superfluid Fermi gas in the BCS-BEC crossover

J. Tokimoto<sup>a</sup>, S. Tsuchiya<sup>b</sup>, and T. Nikuni<sup>a</sup>

<sup>a</sup>Department of Physics, Tokyo University of Science, Japan

<sup>b</sup>Department of Physics, Chuo University, Japan

In quantum many-body systems with spontaneous breaking of a continuous symmetry, Higgs modes emerge as collective amplitude oscillations of order parameters. Recently, Higgs modes have been observed in superconductors and in Bose gases in optical lattices. However, it has yet to be observed in Fermi gases. We use the time-dependent Bogoliubov-de Gennes equations to investigate Higgs amplitude oscillations of the superfluid order parameter in a trapped Fermi gas induced by a sudden change of the s-wave scattering length. In particular, we investigate the Higgs mode with different values of the initial scattering length and discuss how the frequency and damping of the Higgs mode changes in the BCS-BEC crossover.

### P30.26 Comparative study of many-body $t$ -matrix theories for a Fermi gas through the BCS-BEC crossover

M. Pini<sup>a</sup>, P. Pieri<sup>a,b</sup>, and G. Calvanese Strinati<sup>a,b</sup>

<sup>a</sup>School of Science and Technology, Physics Division, University of Camerino, Italy

<sup>b</sup>INFN, Sezione di Perugia, 06123 Perugia, Italy

In the latest several years, diagrammatic theories based on the  $t$ -matrix approximation with different degrees of self-consistency have been developed to describe a Fermi gas through the BCS-BEC crossover (see Ref.<sup>1</sup> for a review). A comprehensive comparison between the results obtained by the different approaches for both thermodynamical and dynamical quantities is, however, still lacking. In the present work, we consider all the possible ways of implementing self-consistency in the  $t$ -matrix approximation and compare the outcomes of the different approaches between each other (and with the available experimental and Quantum Monte Carlo data) through the whole BCS-BEC crossover. In this way, we expect to provide a guideline on the virtues and the drawbacks of each scheme that can help future research in this field.

1. Calvanese Strinati, G., Pieri, P., Röpke, G., Schuck, P., and Urban, M. (2018) “The BCS-BEC crossover: From ultra-cold Fermi gases to nuclear systems”. *Physics Reports* **738**, 1.

### P30.27 Multi-body correlations in SU(3) Fermi gases

H. Tajima and P. Naidon

Quantum Hadron Physics Laboratory, RIKEN Nishina Center, Saitama, Japan

We theoretically investigate strong-coupling effects in a three-component Fermi gas. This system is experimentally realized in a gas of  ${}^6\text{Li}$  atoms<sup>1</sup> and expected to be a simulator of quantum chromodynamics (QCD) where quarks with three colors strongly interact with each other<sup>2</sup>. Within the framework of a many-body  $T$ -matrix approximation for the two-channel model<sup>3</sup>, we incorporate two-body correlations associated with strong pairing fluctuations and determine medium properties such as the critical temperature of Cooper-pair-condensation at various scattering lengths and effective ranges. In addition, we also discuss how trimer properties are affected by effects of finite temperature and chemical potential by solving a Skorniakov-Ter-Martirosian (STM) equation with medium corrections, where the STM equation is known to exactly describe Efimov states in vacuum<sup>4</sup>. Our study would be an important milestone for the unified understanding of strong-coupling physics underlying multi-component Fermi gases as well as dense QCD matter.

1. T. B. Ottenstein, T. Lompe, M. Kohnen, A. N. Wenz, and S. Jochim, “Collisional Stability of a Three-Component Degenerate Fermi Gas” *Phys. Rev. Lett.* **101**, 203202 (2008).
2. Y. Nishida, “New Type of Crossover Physics in Three-Component Fermi Gases”, *Phys. Rev. Lett.* **109**, 240401 (2012).
3. H. Tajima, “Precursor of superfluidity in a strongly interacting Fermi gas with negative effective range”, *Phys. Rev. A* **97**, 043613 (2018).
4. P. Naidon and M. Ueda, “The Efimov effect in lithium 6”, *C. R. Physique* **12**, 13 (2011).

### P30.28 A mobile soliton-impurity system in an attractive binary quantum gas

M. J. Edmonds<sup>a</sup>, J. L. Helm<sup>b</sup>, and Th. Busch<sup>c</sup>

<sup>a</sup>Quantum Systems Unit, Okinawa Institute of Science and Technology Graduate University, Okinawa 904-0495, Japan

<sup>b</sup>Department of Physics, University of Otago, Dunedin, New Zealand

<sup>c</sup>Quantum Systems Unit, Okinawa Institute of Science and Technology Graduate University, Okinawa 904-0495, Japan

We study the dynamics of a bright soliton-impurity system modeled in terms of a binary Bose-Einstein condensate. This is achieved by ‘switching off’ one of the two self-interaction scattering lengths, giving a two component system where the second component is trapped entirely by the presence of the first component. It is shown that this system possesses rich dynamics, including the identification of unusual ‘weak’ dimers that appear close to the zero inter-component scattering length. It is further found that this system supports quasi-stable trimers in regimes where the equivalent single-component gas does not, which is attributed to the presence of the impurity which can dynamically tunnel between the solitons, and maintain the required phase difference that support the trimer state.

M. J. Edmonds, J. L. Helm, Th. Busch, In preparation (2018).

### P30.29 3/2-body correlations in the ground state of Bose–Einstein condensates

W. Kohno, A. Kirikoshi, and T. Kita

Department of Physics, Hokkaido University, Japan

Recently, a variational wave function has been constructed,<sup>1</sup> which describes weakly interacting Bose–Einstein condensates (BECs) with dynamical 3/2-body correlations, where one of the two colliding non-condensates drops into the condensate and visa versa. According to the study, (i) 3/2-body correlations suppress the unphysical energy gap caused by interactions between non-condensates and (ii) the one-particle excitation is a bubbling mode with a finite lifetime. In this presentation, to investigate the properties of 3/2-body correlations in BECs more qualitatively, we develop the variational method as follows.

First, we constructed a variational ground-state wave function of  $M$ -component BECs.<sup>2</sup> From our numerical calculations with various masses and particle numbers, we find that the 3/2-body correlations between different particles contribute to lowering the ground-state energy. We also consider the stability condition for 2-component miscible states using the new ground-state wave function. Through this calculation, we obtain the relation  $U_{AB}^2 = U_{AA}U_{BB} < 1 + \alpha$ , where  $U_{ij}$  is the effective contact potential between particles  $i$  and  $j$  and  $\alpha$  is the correction due to the many-body effect.

Next, we construct a variational wave function for a general trap potential and apply the formulation to a system in a one-dimensional harmonic potential. From our numerical results, the 3/2-body correlations lower the ground-state energy in an amount comparable to the mean-field contribution.

1. T. Kita, J. Phys. Soc. Jpn. 86, 044003 (2017).
2. W. Kohno, A. Kirikoshi, and T. Kita, J. Phys. Soc. Jpn. 87, 34002 (2018).

### P30.30 Many-Body Effects in the Bose-Einstein Condensates at Finite Temperature

A. Kirikoshi, W. Kohno, and T. Kita

Department of Physics, Hokkaido University, Japan

The variational wave function was constructed for the ground state of weakly interacting bosons incorporating dynamical 3/2-body correlations, where one of two colliding non-condensed particles drops into the condensate and vice versa.<sup>1</sup> It was found that unphysical energy gap of the one-particle excitation arising in the Hartree-Fock-Bogoliubov theory tends to close and the one-particle excitation seems to have a finite lifetime even in the long-wavelength limit. These results are different from the widely accepted results where the single-particle excitation is identified with the collective mode in the Bose-Einstein condensed phase.

To investigate the properties of many-body effects, we try to extend the variational method to finite temperatures. First, we construct a variational density matrix incorporating 3/2-body correlations, and then evaluate the grand potential using Green's function. This method makes it possible to investigate the temperature dependence of the many-body effects in the Bose-Einstein condensed phase. We apply this method to a low temperature system and find that the 3/2-body correlations contribute to lowering the free energy as in the case of zero temperature system and suppress thermal excitations. We also calculate the one-particle spectral function.

1. T. Kita, J. Phys. Soc. Jpn. **86**, 044003 (2017).

**P30.31 Decay of phase-imprinted dark soliton in Bose–Einstein condensate at non-zero temperature**

H. Ohya, S. Watabe, and T. Nikuni

Department of Physics, Tokyo University of Science, Japan

We study relaxation dynamics of dark soliton, created by a phase-imprinted method, in a two-dimensional trapped Bose–Einstein condensate at non-zero temperatures by using the projected Gross-Pitaevskii equation. At absolute zero temperature, a dark soliton is known to decay with a snake instability. At non-zero temperature, as we expected, we find that this snake instability cannot be clearly seen as in the absolute zero temperature case because of the presence of thermal fluctuations. However, we find that the decay rate, the half width of the overlap integral with respect to the phase-imprinted initial state, shows a power law decay as a function of the energy and finally remains a non-zero value.

**P30.32 Transferring angular momentum of non-resonant lights onto exciton-polariton condensation**

Byoung Yong Oh<sup>†a</sup>, Min-Sik Kwon<sup>†a</sup>, Su-Hyun Gong<sup>a</sup>, Je-Hyung Kim<sup>a</sup>, Hang Kyu Kang<sup>b</sup>, Sooseok Kang<sup>b</sup>, Jin Dong Song<sup>b</sup>, Yong-Hoon Cho<sup>\*a</sup>, and Hyoungsoon Choi<sup>\*b</sup>

<sup>a</sup>Department of Physics, Korea Advanced Institute Science and Technology (KAIST), Republic of Korea

<sup>b</sup>Center for Opto-Electronic Convergence Systems, Korea Institute of Science and Technology (KIST), Republic of Korea

Exciton-polariton condensates are bosonic condensates / superfluids in a semiconductor microcavity. Photon leaking out of the microcavity gives exciton-polaritons a finite lifetime and the system must be pumped by the laser, making it an intrinsically non-equilibrium system. For the first time, we have experimentally demonstrated that orbital angular momentum of non-resonant pump beam can be transferred to exciton-polariton condensates, which makes it a very effective method to create quantized vortices in exciton-polariton superfluid. Vortex number and chirality matches that of the incident pump laser, despite long standing belief that states of non-resonant pump beams cannot be preserved in the resulting polariton quantum fluids. This could be related to a unique multistate superfluidity not found in conventional superfluids. A ground state with zero angular momentum and excited vortex carrying states are found to coexist. The multistate superfluidity is thought to be a consequence of non-equilibrium dynamics and requires future investigation.

<sup>†</sup> These authors contributed equally to this work.

\* These authors are corresponding author who contributed equally.

### P30.33 Robustness of anomaly-related transport phenomena in Weyl semimetals

Hiroaki Ishizuka<sup>a</sup> and Naoto Nagaosa<sup>b</sup>

<sup>a</sup>Department of Applied Physics, University of Tokyo, Japan

<sup>b</sup>Center for Emergent Matter Science, RIKEN, Japan

Weyl semimetals, a realization of Weyl fermions in condensed-matter setup, have recently attracted interest due to its experimental discovery. While they are expected to be a realization of the Weyl fermions, they also have several distinct features from the Weyl Hamiltonian, e.g., the effective theory for the Weyl semimetals have several terms beside the Weyl Hamiltonian; in fact, the realistic effective theory is often somewhat different from the Weyl Hamiltonian and the Fermi level can be far from the nodes so that multiple nodes are enclosed in a Fermi surface. These features provide new directions in the studies of Weyl semimetals, such as chiral anomaly and related phenomena. However, it also raises fundamental questions on the relation to Weyl fermions, namely, how much of the physics of Weyl fermions survives in Weyl semimetals. Nevertheless, such problems have not been investigated carefully.

In this work, we theoretically study the robustness of the anomaly-related magnetotransport, which is often considered as an evidence for the chiral anomaly in Weyl semimetals. By deriving a general formula for the anomaly-related current in the semiclassical limit, we discuss that the anomaly-related current remains robust even when the Fermi level is above the arc in the dispersion connecting different Weyl nodes<sup>1</sup>. This is further demonstrated by considering a model with two Weyl nodes, where the magnitude of anomaly-related current decays with a power of chemical potential even above the arc. The results show that the anomaly-related current remains robust in the Weyl semimetals even if the effective model deviates from the Weyl Hamiltonian. The results potentially contribute to a better understanding of chiral anomaly and further studies on them in Weyl semimetals.

### P30.34 Microscopic Theory for the Sign Change of the Hall Coefficient in Type-II Superconductors

H. Ueki<sup>a</sup>, M. Ohuchi<sup>b</sup>, and T. Kita<sup>b</sup>

<sup>a</sup>Department of Mathematics and Physics, Hirosaki University, Hirosaki, Japan

<sup>b</sup>Department of Physics, Hokkaido University, Sapporo, Japan

The sign reversal of the the Hall conductivity was found in the vortex state of a wide variety of materials,<sup>1</sup> and intensive studies have been performed on the Hall effect in type-II superconductors theoretically and experimentally. Despite these efforts, a microscopic understanding of the sign change of the Hall coefficient in type-II superconductors is still missing. This is because all the force terms used to describe the Hall effect in superconductors are missing from the standard Eilenberger equations (i.e., the quasiclassical equations of superconductivity).<sup>2</sup> Recently, we derived the augmented Eilenberger equations in the Matsubara formalism with the Lorentz force, the force caused by the pair-potential gradient, and the pressure due to the slope in the DOS by incorporating the first order of the quasiclassical parameter  $\delta$ . Using it, we calculated the core charge in an isolated vortex of an *s*-wave superconductor with a spherical Fermi surface and study which of the three forces dominantly contributes to the charging.<sup>3</sup> We derive augmented quasiclassical equations in the Keldysh formalism incorporating the three force terms. Using it, we calculate the temperature dependence of the Hall electric field induced by a motion of an isolated vortex by transforming the energy variable of the augmented quasiclassical equations in Keldysh formalism into the Matsubara energy on the imaginary axis to explore the possibility of its sign change.

1. See, e.g., S. J. Hagen *et al.*, Phys. Rev. B. **41**, 11630 (1990). 2. G. Eilenberger, Z. Phys. **214**, 195 (1968). 3. H. Ueki, M. Ohuchi, T. Kita, J. Phys. Soc. Jpn. **87**, 044704 (2018).

### P30.35 Development of superconducting electronic cooling with controlled Schottky barrier by using electric double layer transistor structure

Y. Aikawa, E. Hagimoto, and R. Ishiguro

Division of Mathematical and Physical Science, Japan Woman's University, Japan

Superconducting electronic cooling methods with normal/insulator/Superconductor(NIS) junctions have been studied for a long time[1,2,3]. The superconducting electronic cooling has been demonstrated to work effectively in the temperature range below 300 mK, because aluminum electrode with a superconducting critical temperature of 1 K was used[1,2,3]. If it is possible to use a superconductor with a high superconducting transition temperature, it can be expected that its superconducting electron cooling will operate in a higher temperature range. However, with materials other than aluminum, it has not succeeded in forming a tunnel junction that realizes the superconducting electronic cooling. Therefore, we are planning to utilize an electric field controlled Schottky barrier in an electric double layer transistor(EDLT) structure to realize a suitable tunnel junction. In this presentation, we will present sample structure and basic experiment results of the transport measurements with the EDLT structures[4,5,6].

- [1] M. Nahum, *et al.* Applied Physics Letters, **65** (1994) 3123-3125.
- [2] F. Giazotto, *et al.*, Reviews of Modern Physics, **78** (2006) 217-274.
- [3] X. Zhang, *et al.*, Physical Review Applied, **4** (2015).
- [4] T. Narita, *et al.*, Journal of Physics: Conference Series, **969** (2018) 012030.
- [5] Y. Aikawa, *et al.*, Journal of Physics: Conference Series, **969** (2018) 012058.
- [6] Y. Aikawa, *et al.*, Journal of Physics: Conference Series, **969** (2018) 012057.

### P30.36 Operating a MEMS Gyroscope on a Dilution Refrigerator

HeeSu Byun<sup>a</sup>, Jinhoon Jeong<sup>a</sup>, Kitak Kim<sup>a</sup>, Sang Goon Kim<sup>c</sup>, Seung-Bo Shim<sup>b</sup>, Junho Suh<sup>b</sup>, and Hyoungsoon Choi<sup>\*a</sup>

<sup>a</sup>Department of Physics, KAIST, Daejeon 34141, South Korea

<sup>b</sup>Korea Research Institute of Standards and Science, Daejeon 34113, South Korea

<sup>c</sup>IBS, Daejeon, 34126, South Korea

The angular momentum paradox is one of the oldest controversies surrounding an unconventional superconductor, more specifically, a  $p_x + ip_y$  chiral superconductor. Theoretical debate seems to be settling more recently, as numerous new calculations of the intrinsic orbital angular momentum of a  $p_x + ip_y$  chiral superconductor agrees upon the value of  $N\hbar/2$  [1,2]. An experimental confirmation is still yet to come and there was a recent proposal which claims that a micro-electro-mechanical systems (MEMS) gyroscope would have a sufficient signal sensitivity to measure the effect [3]. Here we report low temperature characteristics of such a MEMS gyroscopic device built upon the proposal and results of preliminary test runs using such devices are also presented.

- [1] T. Ojanen, Phys. Rev. B **93**, 174505 (2016).
- [2] A. Shitade and Y. Nagai, Phys. Rev. B **93**, 174517 (2016).
- [3] HeeSu Byun et al., arXiv:1609.07641.

\* These authors are corresponding author who contributed equally.



### P30.37 **Study of the non-linear dynamics of micro-resonators based on a Sn-whisker in vacuum and at mK temperatures**

M. Človečko, P. Skyba, and F. Vavrek

Centre of Low Temperature Physics, Institute of Experimental Physics, Slovak Academy of Sciences and P. J. Šafárik University, Košice, Watsonova 47, 040 041 Košice, Slovakia

The dynamics of micro-resonators (or any mechanical resonators) can be studied by two complementary methods allowing the measurements in two different domains: (i) in the frequency domain - by the frequency sweeps using cw-excitation, and (ii) in the time domain - by the pulse techniques<sup>1</sup>, when the free-decay oscillations are investigated. To broaden the knowledge about the intrinsic mechanical properties of micro-resonators based on a Sn-whisker<sup>2</sup> we used both methods. We show that the dynamics of the Sn-whisker can be described by a phenomenological theory of the Duffing oscillator. Furthermore, we present the results of theoretical analysis based on the Duffing's model provided in the time and frequency domains, and we show that these results are qualitatively the same with those measured experimentally.

1. M. Človečko, M. Grajcar, M. Kupka, P. Neilinger, M. Reháč, P. Skyba, F. Vavrek, "High Q value Quartz Tuning Fork in Vacuum as a Potential Thermometer in Millikelvin Temperature Range", *J. Low Temp. Phys.*(2017) 187, 573

2. M. Človečko, E. Gažo, S. Longauer, E. Múdra, P. Skyba, F. Vavrek, M. Vojtko, "Vacuum Measurements of a Novel Micro-resonator Based on Tin Whiskers Performed at mK Temperatures", *J. Low Temp. Phys.* (2014) 175, 449

### P30.38 **Thermal coupling of silicon oscillators in cryogen-free dilution refrigerators**

D. Schmoranzler<sup>a</sup>, S. Kumar<sup>a</sup>, A. Luck<sup>a</sup>, E. Collin<sup>a</sup>, A. Fefferman<sup>a</sup>, X. Liu<sup>b</sup>, T. Metcal<sup>b</sup>, and G. Jernigan<sup>b</sup>

<sup>a</sup>Institut Néel/CNRS & Univ. Grenoble Alpes

<sup>b</sup>US Naval Research Lab

Silicon double paddle oscillators (DPOs) have been successfully used for measuring the elastic properties of amorphous films down to 10 mK (see for example [1,2]). Until now, our group has used a wet dilution refrigerator for the lowest temperature measurements. We present measurements carried out on a Bluefors cryogen-free dilution refrigerator that demonstrate an extreme sensitivity of the thermal coupling of the DPO to its environment. These measurements show that it is necessary to enclose the DPO in a shield at the mixing chamber temperature. Any gaps in the shield limit its effectiveness, even if there is no line-of-sight path to the DPO. In the absence of a hermetic shield at MXC temperature, turning off the pulse tube while maintaining the MXC and still temperatures leads to heating of the DPO. This demonstrates that any heating of the sample due to pulse tube vibrations is a less important effect.

We acknowledge support from the ERC StG grant UNIGLASS No. 714692 and ERC CoG grant ULT-NEMS No. 647917 and from the US Office of Naval Research.

1. X. Liu *et al.*, *Phys. Rev. Lett.* **113**, 025503 (2014).

2. A. Fefferman *et al.*, *J. Low Temp. Phys.* **187**, 654 (2017).



**July 31 (Tuesday)**



## July 31 (Tuesday) Oral Presentations

### O31.1 Spectroscopy and dynamics of molecules in quantum fluids and solids: *Towards molecular superfluidity and ultracold chemistry*

T. Momose

Department of Chemistry, The University of British Columbia, Vancouver, CANADA

Spectroscopy of molecules embedded in quantum fluids and solids, such as superfluid helium droplets and parahydrogen crystals, has revealed various unique properties of atoms and molecules at temperatures around 4 K or below.<sup>1</sup> We have been using these quantum fluids and solids to the study of dynamics of cold molecules, such as quantum tunneling reactions and quantum diffusion as well as an investigation of a possible superfluid phase of molecular hydrogen. To further reduce the temperature of molecules below 100 mK, we have also been working on the development of a technique to create quantum gases of molecules in vacuum. Recently, we were successful in trapping reactive free radicals in a magnetic trap at a temperature of < 200 mK.<sup>2</sup> The study of reactive scattering with the trapped free radicals will provide an opportunity to investigate chemical reactions at ultracold temperatures. In this talk, we will discuss a couple of topics related to the unique nature of cold molecules. They include (1) a possible superfluid phase of hydrogen molecules at 0.4 K, and (2) the creation of quantum gases of reactive molecules.

1. T. Momose, and T. Shida, “Matrix Isolation Spectroscopy Using Solid Parahydrogen as the Matrix: Application to High-resolution Spectroscopy, Photochemistry and Cryochemistry” *Bull. Chem. Soc. Jpn.*, **71**, 1 (1998).
2. Y. Liu et. al. “Magnetic Trapping of Cold Methyl Radicals”, *Phys. Rev. Lett.*, **118**, 093201 (2017).

PLENARY TALK

### O31.2 Efimov resonances in an ultracold mixture

S. Inouye and K. Kato

Graduate School of Science, Osaka City University, Japan

Efimov states, an infinite series of three-body bound states with discrete scale invariance when a two-body scattering length diverges, provided us a unique opportunity to investigate the properties of few-body physics both theoretically and experimentally. We studied multichannel Efimov physics using ultracold heteronuclear admixtures of K and Rb atoms. We observe a shift in the scattering length where the first atom-dimer resonance appears in the 41K-87Rb system<sup>1</sup> relative to the position of the previously observed atom-dimer resonance in the 40K-87Rb system.<sup>2</sup> This shift is well explained by our calculations with a three-body model including van der Waals interactions, and, more importantly, multichannel spinor physics.<sup>1</sup> With only minor differences in the atomic masses of the admixtures, the shift in the atom-dimer resonance positions can be cleanly ascribed to the isolated and overlapping Feshbach resonances in the 40K-87Rb and 41K-87Rb systems, respectively. Our study demonstrates the role of multichannel Feshbach physics in determining Efimov resonances in heteronuclear three-body systems.

1. Kato, K. (2017). “Isotopic Shift of Atom-Dimer Efimov Resonances in K-Rb Mixtures: Critical Effect of Multichannel Feshbach Physics”. *Phys. Rev. Lett.*, **118**, 163401.
2. Bloom, R.S., Hu, M.-G., Cumby, T.D., and Jin, D.S., (2013). “Tests of Universal Three-Body Physics in an Ultracold Bose-Fermi Mixture”. *Phys. Rev. Lett.* **111**, 105301.

INVITED TALK

### O31.3 Screening corrections on the critical temperature and gap parameter throughout the BCS-BEC crossover

L. Pisani<sup>a</sup>, P. Pieri<sup>a,b</sup>, and G. Calvanese Strinati<sup>a,b</sup>

<sup>a</sup>School of Science and Technology, Physics Division, University of Camerino, Italy

<sup>b</sup>INFN, Sezione di Perugia, 06123 Perugia, Italy

It has long been known that the critical temperature and gap parameter of a BCS weak-coupling superfluid are considerably reduced by the inclusion of the Gorkov-Melik-Barkhudarov (G-MB) correction, whereby particle-hole excitations screen the two-fermion effective interaction in the medium. We have extended the effects of the G-MB correction throughout the whole BCS-BEC crossover by identifying the Feynman diagrams responsible for the G-MB correction in both the normal<sup>1</sup> and superfluid phases<sup>2</sup>, and by modifying accordingly a T-matrix formalism previously extensively used for the study of the BCS-BEC crossover<sup>3</sup>. The numerical solution of the resulting equations yields results for the critical temperature and gap parameter which agree well with Quantum Monte Carlo and experimental data in the crossover region.

1. Pisani, L., Perali, A., Pieri P., and Calvanese Strinati, G. (2018). “Entanglement between pairing and screening in the Gorkov-Melik-Barkhudarov correction to the critical temperature throughout the BCS-BEC crossover”. *Physical Review B* **97**, 014528.
2. Pisani, L., Pieri, P., and Calvanese Strinati, G. (2018). “Gap equation with pairing correlations beyond mean field and its equivalence to a Hugenholtz-Pines condition for fermion pairs”. Preprint.
3. Calvanese Strinati, G., Pieri, P., Röpke, G., Schuck, P., and Urban, M. (2018) “The BCS-BEC crossover: From ultra-cold Fermi gases to nuclear systems”. *Physics Reports* **738**, 1.

INVITED TALK

### O31.4 Nano structures and Devices to Study Quantum Fluids and Solids

K. Kono<sup>ab</sup>

<sup>a</sup>Department of Electrophysics, NCTU, Taiwan

<sup>b</sup>RIKEN CEMS, Japan

In the recent years there have been a lot of interests in the application of nano structures and devices to study properties of quantum fluids and solids. In the field of electrons on liquid He the theoretical proposal by Dykman and Platzman<sup>1</sup>, initiated a break of developing nano devices towards single electron manipulation and detection<sup>2,3</sup>. Micrometer thick liquid helium is prepared by capillary action in a geometrically defined channel as a substrate to support electrons. Together with a nano-gapped electrode assembly, versatile devices are developed to study a quasi-one-dimensional electron transport on liquid He. Curious dynamical properties of the Wigner solid is one of the most prominent outcomes<sup>4</sup>. In this talk, the use of nano structures and devices is reviewed to discuss possibilities of further interesting applications.

1. Platzman, P. M. and Dykman, M. I. (1999). “Quantum Computing with Electrons Floating on Liquid Helium”. *Science* **284**, 1967.
2. Bradbury, F. R. *et al.* (2011). “Efficient Clocked Electron Transfer on Superfluid Helium”. *Phys. Rev. Lett.* **107**, 266803.
3. Papageorgiou, G. *et al.* (2005). “Counting Individual Trapped Electrons on Liquid Helium”. *App. Phys. Lett.* **86**, 153106.
4. Rees D. G. *et al.* (2016). “Stick-Slip Motion of the Wigner Solid on Liquid Helium”. *Phys. Rev. Lett.* **116**, 206801.

INVITED TALK

## O31.5 Microfabricated Fourth-Sound Resonators for Confined Quantum Liquids

A. Shook, F. Souris, P.H. Kim, and J.P Davis

Department of Physics, University of Alberta, Edmonton, Alberta, Canada T6G 2E9

The past few years has seen a significant interest in the use of superfluids as the medium for mechanical resonators, based on the fact that they can not only have ultralow mechanical loss,<sup>1</sup> but also ultralow dielectric loss<sup>2</sup> for optomechanics and electromechanics. Of potential interest to the quantum fluids community is that such superfluid mechanical resonators can also be used to explore the properties of the superfluids themselves, with extraordinary sensitivity or in unusual superfluid regimes. As an example, we have developed superfluid mechanical resonators to study superfluid <sup>4</sup>He and <sup>3</sup>He in quasi-2D confined geometries – specifically where the third dimension is below the viscous penetration depth and therefore the normal fluid is clamped, making these fourth-sound Helmholtz resonators.<sup>3</sup> Here I will review our current progress with these devices, and our planned explorations of topological physics in superfluid <sup>3</sup>He.<sup>4</sup>

1. L. A. De Lorenzo and K. C. Schwab, “Superfluid optomechanics: Coupling of a superfluid to a superconducting condensate,” *New J. Phys.* 16, 113020 (2014).
2. F. Souris, H. Christiani and J.P Davis, “Tuning a 3D Microwave Cavity via Superfluid Helium at MilliKelvin Temperatures,” *Appl. Phys. Lett.* 111, 172601 (2017)
3. F. Souris, X. Rojas, P.H. Kim and J.P Davis, “Ultra-Low Dissipation Superfluid Micromechanical Resonator,” *Phys. Rev. Applied* 7, 044008 (2017).
4. H. Wu and J. A. Sauls, “Majorana excitations, spin and mass currents on the surface of topological superfluid <sup>3</sup>He B,” *Phys. Rev. B* 88, 184506 (2013).

INVITED TALK

## O31.6 Quantum Optomechanics with Superfluid Helium Density Waves

A. B. Shkarin<sup>a</sup>, A. D. Kashkanova<sup>a</sup>, C. D. Brown<sup>a</sup>, N. E. Flowers-Jacobs<sup>a</sup>, S. Garcia<sup>b</sup>, K. Ott<sup>b</sup>, J. Reichel<sup>b</sup>, and J. G. E. Harris<sup>a</sup>

<sup>a</sup>Department of Physics, Yale University, New Haven, CT 06511, USA

<sup>b</sup>Laboratoire Kastler Brossel, ENS, UPMC, CNRS, 24 rue Lhomond, 75005 Paris, France

The field of quantum optomechanics seeks to measure and coherently manipulate mechanical states with single-quantum precision and to interface these states with electromagnetic radiation without loss. To accomplish that, one generally aims to create a system with strong optomechanical coupling, while maintaining low optical and mechanical losses and low temperature. Superfluid helium is a liquid which is uniquely well-suited to meet these requirements due to its low acoustic dissipation, negligible optical absorption, low temperature, and absence of impurities.

In this talk I describe our cavity optomechanics systems in which infrared light is coupled to a standing acoustic wave in superfluid helium. With this system, we used light to coherently excite acoustic vibrations and manipulate their frequency and damping rate using the dynamic back-action effect. In addition, we measured mechanical mode fluctuations with sufficient precision to reveal quantum signatures in the motion of the acoustic waves and in their interaction with light. Specifically, we observed the expected one-phonon difference between the Stokes and anti-Stokes mechanical sidebands, and indirectly measured the action of the optical shot noise on the mechanical object by investigating the correlations between these sidebands.

INVITED TALK

## O31.7 A New Spin of Non-equilibrium Disordered Quantum Systems

A. Luck, A. Reiser, A. Fleischmann, and C. Enss

Kirchhoff Institute for Physics, Heidelberg University, INF 227, D-69120 Heidelberg, Germany

The investigation of non-equilibrium disordered quantum systems with novel experimental techniques have resulted in fundamentally new insights of their dynamics. In particular, the importance of nuclear spins as surprisingly active degrees of freedom at ultra-low temperatures has been revealed in recent measurements on amorphous solids. These new findings are potentially of high relevance to many quantum devices, like quantum dots, qubits, SQUIDs, nano-mechanical systems and quantum limited amplifiers. They also show that the universality of glasses is limited to certain temperatures and properties. We present the experimental evidence for a nuclear spin driven dynamics in non-equilibrium disordered quantum systems and discuss a possible theoretical framework for such a mechanism.

INVITED TALK

# Author Index

|                       |                                 |
|-----------------------|---------------------------------|
| Abe S.                | P27.16                          |
| Abhilash T. S.        | P26.17 O28.8                    |
| Adams J.              | P26.9                           |
| Ahmed S.              | P28.39                          |
| Ahokas J.             | P26.12                          |
| Aikawa Y.             | P28.31 P30.35                   |
| Amaike K.             | P26.3                           |
| Amelio I.             | O27.10                          |
| Amrit J.              | P26.11                          |
| Ancilotto F.          | P27.9 P28.4 P28.6               |
| Aoki T.               | P26.36                          |
| Arnold F.             | O27.6                           |
| Arrayás M.            | O26.3                           |
| Asano Y.              | P30.24                          |
| Autti S.              | P26.33 P26.34 O28.9 O30.7 P30.3 |
| Badrutdinov A. O.     | P27.4 P27.5                     |
| Bahyl J.              | P28.5 P28.9                     |
| Baidyanath S.         | P27.25                          |
| Baker C. G.           | P27.27 P28.10                   |
| Bakkers E.            | O26.4                           |
| Balk S.               | O26.4                           |
| Barabanov A. F.       | P27.23 P28.30                   |
| Barquist C. S.        | P26.32 P28.13                   |
| Barranco M.           | P28.4 P28.6                     |
| Beamish J.            | O26.10 P26.13                   |
| Beauvois K.           | O27.9                           |
| Beekman A. J.         | O27.7                           |
| Biferale L.           | P28.12                          |
| Borsoi F.             | O26.4                           |
| Böttcher H.           | P26.4                           |
| Bowen W. P.           | P27.27 P28.10                   |
| Bradley A.            | P28.10                          |
| Bradley D. I.         | P26.33                          |
| Brazhnikov M. Yu.     | O26.11                          |
| Britz D.              | P26.26                          |
| Brown C. D.           | P28.36 O31.6                    |
| Budrin K. S.          | P27.22                          |
| Bunkov Yu. M.         | O26.8 P27.15                    |
| Busch Th.             | P30.28                          |
| Byun H. S.            | P26.35 P30.36                   |
| Cagnon L.             | P26.4                           |
| Calvanese Strinati G. | P30.26 O31.3                    |
| Candela D.            | P26.9                           |
| Casey A.              | O27.6 O28.8                     |
| Chan H. B.            | P28.13                          |
| Chan M. H. W.         | O26.9                           |
| Cheng Z. G.           | O26.10 P26.13                   |

|                      |  |
|----------------------|--|
| Chikov A. A.         | P27.22                                 |
| Childress L.         | P28.36                                 |
| Chishko K. A.        | P27.26                                 |
| Chizaki Y.           | P26.36                                 |
| Cho Y. H.            | P30.32                                 |
| Choi H.              | P26.35 P30.32 P30.36                   |
| Choi J.              | P26.10 O27.8                           |
| Človečko M. M.       | P30.37                                 |
| Collin E.            | P27.31 P28.35 P30.38                   |
| Coppens F.           | P28.4                                  |
| Cowan B.             | O27.6                                  |
| Danshita I.          | P30.17                                 |
| Davis J. P           | O31.5                                  |
| Davis M.             | P28.10                                 |
| de Jong N.           | O26.4                                  |
| De Liberato S.       | P28.39                                 |
| de Moor M.           | O26.4                                  |
| Dmitriev V. V.       | P28.1 O30.4 P30.1 P30.2 P30.7          |
| Dmitriev Yu. A.      | P26.12                                 |
| Doebele V.           | P26.4                                  |
| Dzebisashvili D. M.  | P27.23                                 |
| Edmonds M. J.        | P30.28                                 |
| Eikoku Y.            | P28.38                                 |
| Eltsov V. B.         | P27.29 O28.7 P28.2 O30.7 P30.2 P30.10  |
| Enss C.              | O31.7                                  |
| Eyal A.              | P26.17                                 |
| Fåk B.               | O27.9                                  |
| Fan H. -H.           | P28.27                                 |
| Fefferman A.         | P27.31 P30.38                          |
| Flachi N.            | P26.1                                  |
| Fleischmann A.       | O31.7                                  |
| Flowers-Jacobs N. E. | P28.36 O31.6                           |
| Forstner S.          | P27.27 P28.10                          |
| Fujisawa T.          | P27.24                                 |
| Fukui K.             | P26.28                                 |
| Fukuyama H.          | O27.5 P27.10 P27.32 P28.14             |
| Furukawa S.          | P30.14                                 |
| Galli D. E.          | O27.10                                 |
| Garcia S.            | P28.36 O31.6                           |
| Gazibegovic S.       | O26.4                                  |
| Gazizulin R.         | P27.31 P28.35                          |
| Gneiting C.          | P26.30                                 |
| Godfrin H.           | O27.9                                  |
| Golov A. I.          | O26.11                                 |
| Gong S. H.           | P30.32                                 |
| Gotoh S.             | P26.36                                 |
| Grosman A.           | P26.4                                  |
| Guénault A. M.       | P26.33 P26.34 O28.9 P28.35 O30.2 P30.3 |
| Gunnarsson D.        | P26.33                                 |



Guo W. P28.20 O30.1  
 Guthrie A. P28.35  
 Hagimoto E. P30.35  
 Hakonen P. J. P26.18  
 Halberstadt N. P28.4  
 Haley R. P26.33  
 Haley R. P. O26.3 P26.34 O28.9 P28.11 P28.35 O30.2 P30.3 P30.11  
 Halperin W. P. P30.4 P30.5  
 Hamazaki K. P28.24  
 Han J. P30.13  
 Harada S. P26.36  
 Harris G. I. P27.27 P28.10  
 Harris J. G. E. P28.36 O31.6  
 Hashizume K. P27.1 P27.2 P27.3  
 Hatayama N. P26.24  
 Hatsuda T. O28.4  
 Hayashida H. P28.20  
 He X. P27.27 P28.10  
 Heedt S. O26.4  
 Heguri S. P27.24  
 Heikkinen H. P26.33  
 Heikkinen P. J. O27.6 O28.8 O30.7  
 Helm J. L. P30.28  
 Hieda M. P26.3 P26.5 P27.8  
 Higashikawa S. P30.14  
 Hirashima D. P26.15  
 Hiresaki Y. P26.36  
 Hiroi K. P28.20  
 Hirota K. P28.20  
 Hoch S. W. P28.36  
 Hohmann L. P28.36  
 Holt S. P26.33  
 Hrubcová P. P28.18  
 Hsueh C. H. P30.16  
 Huan C. P26.9  
 Ichida H. P26.6  
 Ienaga K. P27.2 P27.3  
 Iguchi T. P28.20  
 Iida K. O28.5  
 Iida Y. P28.29  
 Ikeda R. O30.6  
 Ikeuchi M. P26.36  
 Inagaki Y. P27.1 P27.2  
 Inotani D. P30.19 P30.20 P30.21 P30.22 P30.23  
 Inouye S. O31.2  
 Inui S. P28.7 P28.8  
 Ishibashi K. P27.13  
 Ishida K. P28.38  
 Ishiguro R. P28.31 P30.35

|                  |  |
|------------------|--|
| Ishikawa O.      | P27.34 P28.22 P28.23 P28.24 P28.25                   |
| Ishizuka H.      | P30.33   |
| Islam S.         | P27.3  |
| Itaka K.         | P27.14   |
| Ito D.           | P28.20   |
| Itoh K.          | P27.30   |
| Iwamoto A.       | P28.38   |
| Iwano K.         | P27.19   |
| Iwasa I.         | P26.14   |
| Jackson M. J.    | P28.5 P28.9 P30.9                                    |
| Jarvinen J.      | P26.12   |
| Jennings A.      | P26.34 O28.9 P30.3                                   |
| Jeong J.         | P26.35 P30.36  |
| Jernigan G.      | P30.38   |
| Jiang W. G.      | P26.32 P28.13  |
| Johansson G.     | P26.31   |
| Jones A.         | P26.33   |
| Kafanov S.       | P26.33 P26.34 O28.9 P28.11 P28.35 O30.2 P30.3 P30.11 |
| Kagamihara D.    | P30.19 P30.20 P30.23                                 |
| Kaiya K.         | P27.30   |
| Kajiwara Y.      | P27.1  |
| Kalyoncu Y.      | P26.33   |
| Kamada M.        | O27.5 P27.10   |
| Kamppinen T.     | P30.10   |
| Kanazawa I.      | P27.18 P28.26  |
| Kang H. K.       | P30.32   |
| Kang S.          | P30.32   |
| Kanoda K.        | O27.3  |
| Kasamatsu K.     | P28.16   |
| Kashkanova A. D. | P28.36 O31.6   |
| Kato K.          | P28.15 O31.2   |
| Kato Y.          | P26.23 P26.28 P26.36                                 |
| Kawade N.        | P27.24   |
| Kawae T.         | P27.1 P27.2 P27.3                                    |
| Kawamura H.      | O27.4 P27.11   |
| Kawasaki I.      | P26.25   |
| Khmelenko V. V.  | P26.12   |
| Khomenko D.      | P28.12   |
| Kim E.           | P26.10 O27.8   |
| Kim J. H.        | P30.32   |
| Kim K.           | P30.36   |
| Kim P. H.        | O31.5  |
| Kim S.           | P26.35 P30.36  |
| Kimura Y.        | P28.23 P28.24  |
| Kirikoshi A.     | P30.29 P30.30  |
| Kita T.          | P30.29 P30.30 P30.34                                 |
| Kitaguchi M.     | P28.20   |
| Kiyanagi Y.      | P28.20   |
| Klimin S. N.     | O28.3  |

Klochkov A. V. P27.15  
 Kobayashi H. P28.19 O30.3  
 Kobayashi M. P27.24 P28.16  
 Kockum A. F. P26.31  
 Koga A. P27.20 P27.21  
 Kohara U. P26.24  
 Kohno W. P30.29 P30.30  
 Kokuryu S. P28.20  
 Konno R. P26.24  
 Kono K. P27.6 P28.7 P28.8 O31.4  
 Konstantinov D. P27.4 P27.5  
 Korovushkin M. M. P27.23 P28.30  
 Kosterlitz J. M. O27.1  
 Kotani T. P26.25  
 Kouwenhoven L. O26.4  
 Krotscheck E. O27.9 P28.27  
 Krstulovic G. P30.12  
 Kubo W. P28.20 P28.37  
 Kubota M. P26.36  
 Kumar S. P30.38  
 Kunimi M. P30.17  
 Kurkjian H. O28.3  
 Kutuzov M. S. O30.4 P30.1  
 Kuwahara K. P26.8  
 Kwon M. S. P30.32  
 La Mantia M. P28.18  
 Lambert N. P28.39  
 Lee D. M. P26.12  
 Lee Y. P26.32 P28.13  
 Leggett A. J. O26.1  
 Lehtonen L. P26.12  
 Leiderer P. P27.6 P28.7 P28.8  
 Levitin L. V. O27.6 O28.8  
 Lewkowitz M. P26.9  
 Lin J. -Y. P27.4 P27.5  
 Liu B. P26.27 P28.32 P28.33  
 Liu X. P30.38  
 Liu Y. P26.27  
 Lotnyk D. P26.17  
 Luck A. P30.38 O31.7  
 Luzuriaga J. P30.9  
 L'vov V. S. P28.12 P28.17 O30.7  
 Maeda R. P27.18 P28.26  
 Maekawa S. P26.19  
 Maillet O. P28.35  
 Maki H. P28.15  
 Mäkinen J. T. P28.2 P30.2 O30.7 P30.10  
 Makiuchi T. O26.5 P26.2 P26.7 P26.8 P27.7  
 Manabe K. P30.20 P30.23

Manske D. O28.10  
Maradan D. P26.33  
Masaki Y. P26.23  
Masaki-Kato A. P26.15  
Masuhara N. P26.9  
Matsui T. O27.5 P27.10 P28.14  
Matsumoto K. P27.16  
Matsumura I. P28.23  
Matsunaga R. P28.29  
Matsushita T. P26.3 P26.5 P27.8 P28.20  
McAuslan D. P28.10  
Melnikovskiy L. A. P30.1  
Metcalf T. P30.38  
Midlik Š. P28.5 P28.9  
Mikheev A. Y. O30.4  
Mineev V. P. O30.5  
Minezaki H. P27.14  
Minoguchi T. P27.12  
Mita Y. P27.30  
Mitskan V. A. P27.23  
Miura H. P30.8  
Miyakawa K. P27.1  
Mizushima T. O28.6  
Möller Th. B. P27.6  
Momose T. O31.1  
Mondal S. P30.22  
Morikawa Y. P28.15  
Morishita M. O26.6  
Moroshkin P. P27.6 P28.7 P28.8  
Morozov V. N. O30.4  
Moskvin A. S. P26.21 P27.22  
Motoyama G. P26.25  
Mukaida M. P26.8  
Mukharsky Yu. M. O26.11  
Murakawa S. P26.20 P27.30 P27.32 P28.15  
Mushiake R. P28.22 P28.25  
Nagamura N. O30.6  
Nagaosa N. P30.33  
Nago Y. O26.5 P26.2 P26.7 P26.8 P27.7 P28.15  
Naidon P. P30.18 P30.27  
Nakajima A. P27.16  
Nakajima M. P27.18 P28.26  
Nakajima S. P27.18  
Nakamori M. P26.24  
Nakamura R. O27.5 P27.10  
Nakamura S. P28.26 P28.29  
Narita T. P28.31  
Narushima Y. P30.24  
Nasu J. P27.20 P27.21

|                   |   |
|-------------------|---|
| Nava M.           | P27.9   |
| Navon N.          | O30.9   |
| Nazarenko S.      | O30.10  |
| Ngampruetikorn V. | O28.11  |
| Nguyen M. D.      | P30.4 P30.5   |
| Nikuni T.         | P30.24 P30.25 P30.31                                |
| Nissinen J.       | P26.29 P28.2  |
| Nitta M.          | P26.1 P28.28  |
| Noble M. T.       | P28.11 O30.2 P30.11                                 |
| Nomura R.         | O27.11 P27.14                                       |
| Nori F.           | P26.30 P26.31 O28.12 P28.34 P28.39                  |
| Nyeki J.          | O27.6   |
| Obara K.          | P27.14 P27.34 P28.22 P28.23 P28.24 P28.25           |
| Ogawa K.          | O27.5 P27.10  |
| Oh B. Y.          | P30.32  |
| Ohashi Y.         | P30.19 P30.20 P30.21 P30.22 P30.23                  |
| Ohuchi M.         | P30.34  |
| Ohya H.           | P30.31  |
| Okamoto R.        | P27.16  |
| Okuda Y.          | O27.11 P27.14                                       |
| Ollivier J.       | O27.9   |
| Onorato M.        | O30.10  |
| op het Veld R.    | O26.4   |
| Ott K.            | P28.36 O31.6  |
| Palma M.          | P26.33  |
| Panov Yu. D.      | P26.21 P27.22                                       |
| Parpia J. M.      | P26.17 O27.6 O28.8                                  |
| Pashkin Yu. A.    | P26.33 P28.35                                       |
| Penttilä J.       | P26.33  |
| Perez C. B.       | P26.32  |
| Pi M.             | P28.4 P28.6   |
| Pickett G. R.     | O26.3 P26.34 O28.9 P28.11 P28.35 O30.2 P30.3 P30.11 |
| Pieri P.          | P30.26 O31.3  |
| Pini M.           | P30.26  |
| Pisani L.         | O31.3   |
| Pomyalov A.       | P28.12 P28.17                                       |
| Poole M.          | O30.2 P30.11  |
| Popovic B.        | P26.32  |
| Prance J.         | P26.33  |
| Procaccia I.      | P28.12  |
| Proment D.        | O30.10 P30.12                                       |
| Prunnila M.       | P26.33  |
| Quintero P. M.    | O26.4   |
| Ramiere A.        | P26.11  |
| Reatto L.         | O27.10 P27.9  |
| Rees D.           | P27.4   |
| Reeves M.         | P28.10  |
| Regan R. C.       | P28.3   |
| Reichel J.        | P28.36 O31.6  |

Reiser A. O31.7  
 Reppy J. D. O27.2  
 Riekki T. S. P27.28 P27.29  
 Rojas X. O27.6 O28.8  
 Rolley E. P26.4  
 Roschier L. P26.33  
 Rybalko A. S. P27.26  
 Rysti J. P27.29 P28.2 P30.2  
 Sachkou Y. P27.27  
 Safin T. R. P27.15  
 Safiullin K. R. P27.15  
 Sahoo G. P28.12  
 Saito Y. P28.20  
 Sarsby M. P26.33  
 Sato K. P28.22 P28.23 P28.24 P28.25  
 Sato R. P30.20  
 Sauls J. A. O26.2 P26.16 O28.11 P28.3  
 Saunders J. O27.6 O28.8  
 Savin A. M. P26.18  
 Sawadsky A. P27.27 P28.10  
 Schanen R. P26.34 O28.9 P30.3 P30.11  
 Scheer E. P27.6  
 Scheller C. P26.33  
 Schmoranz D. P27.31 P28.5 P28.9 P30.9 P30.38  
 Sebedash A. P. P27.28 P27.29 P27.33  
 Sfindla Y. P27.27 P28.10  
 Shammah N. P28.39  
 Sheludiakov S. P26.12  
 Shibuya S. P27.16  
 Shigematsu T. P26.36  
 Shim S. B. P30.36  
 Shimano R. O28.2 P28.29  
 Shimizu H. M. P28.20  
 Shimoda T. P26.8  
 Shin J. O26.9 P26.10  
 Shin Y. O30.8  
 Shinohara T. P28.20  
 Shinzaki R. P27.20  
 Shirahama K. O26.5 P26.2 P26.7 P26.8 P27.7 P27.30 P28.15  
 Shkarin A. B. P28.36 O31.6  
 Shook A. O31.5  
 Silvestrelli P. L. P27.9  
 Sim S. P26.35  
 Skrbek L. P28.5 P28.9 O30.11  
 Skyba P. P30.37  
 Slavov B. D. P30.1  
 Smith E. N. P26.17  
 Smorodin A.V. P27.4 P27.5  
 Soldatov A. A. P26.34 O28.9 P28.1 O30.4 P30.1 P30.7

Song J.D. P30.32  
 Sonnenschein V. P28.20  
 Souris F. P26.4 O31.5  
 Spathis P. P26.4  
 Stockdale O. P28.10  
 Strinati G. C. P30.26 O31.3  
 Strydom A. M. P26.26 P27.25  
 Suh J. P26.35 P30.36  
 Sullivan N. S. P26.9  
 Sumiyama A. P26.25 P27.24  
 Surovtsev E. P30.6  
 Suzuki A. P27.14  
 Suzuki M. O26.6 O26.7 P26.6 P27.13  
 Suzuki S. P28.20  
 Suzushika H. P26.36  
 Švančara P. P28.18  
 Tachiki A. O27.11  
 Tada Y. P26.22  
 Tagai M. O26.5 P26.2 P26.7 P27.7  
 Tagirov M. S. P27.15  
 Taguchi Y. P27.21  
 Tajima H. P30.27  
 Takada S. P26.1  
 Takagi T. P28.15  
 Takahashi D. O26.5 P26.7  
 Takahashi T. P27.14  
 Takata H. P27.1 P27.2 P27.3  
 Takayanagi H. P28.31  
 Takeuchi H. P28.16 P30.15  
 Takimoto S. P27.32  
 Tanabe H. P27.34  
 Tanaka H. P26.25  
 Tanaka Y. P28.15  
 Tani T. P27.30  
 Tanigaki K. P27.24  
 Taniguchi J. O26.6 O26.7 P26.6 P27.13  
 Taniguchi K. O26.7  
 Tempere J. O28.3  
 Terabayashi T. P26.8  
 Terai H. P28.29  
 Terelli M. P26.17  
 Toda R. P26.5 P27.32  
 Tokimoto J. P30.25  
 Tomita H. P28.20  
 Tozaki K. P26.36  
 Trimaille I. P26.4  
 Triqueneaux S. P27.31  
 Tsepelin V. P26.34 O28.9 P28.11 P28.35 O30.2 P30.3 P30.11  
 Tsubota M. P28.7 P28.8 P28.19 O30.3 P30.13 P30.16

Tsuchiura H. P27.21  
 Tsuchiya S. P28.28 P30.25  
 Tsuji Y. P28.20 P28.37 P28.38 P30.8  
 Tsujii H. P27.2  
 Tsumura K. P28.31  
 Tsutsumi Y. P26.19  
 Tuoriniemi J. T. P27.28 P27.29  
 Uccelli E. O26.4  
 Ueda H. P26.36  
 Ueda M. P30.14  
 Ueki H. P30.34  
 Uematsu K. P27.11  
 Ulitko V. V. P27.22  
 Umemoto M. O26.6  
 Usami J. P28.14  
 Val'kov V. V. P27.23 P28.30  
 van Hoogdalem K. O26.4  
 van Wyk P. P30.21  
 Varga E. P28.21 O30.11  
 Vasiliev S. P26.12  
 Vasinovich E. V. P26.21  
 Vavrek F. P30.37  
 Villois A. P30.12  
 Volovik G. E. P26.29 O28.1 P28.2  
 Volz S. P26.11  
 Vorontsov A. O28.8  
 Wada N. P26.3 P26.5 P27.8 P28.20  
 Wada R. P27.30  
 Wang D. P28.32  
 Watabe S. P30.24 P30.31  
 Waterworth A. O27.6  
 Wilcox T. P28.11 O30.2 P30.11  
 Wiman J. J. P26.16 P28.3  
 Wimmer M. O26.4  
 Wolf P. E. P26.4  
 Wu W. C. P30.16  
 Yamada K. P27.30  
 Yamaguchi A. P26.25 P27.24  
 Yamaguchi H. P27.8  
 Yamaguchi T. P27.19  
 Yamamoto D. P28.28  
 Yamamura T. P26.25  
 Yamashita K. O26.5 P26.2 P26.7 P27.7  
 Yamazaki S. P26.20  
 Yan J. P26.8  
 Yano H. P27.34 P28.22 P28.23 P28.24 P28.25  
 Yoshida K. P26.20 P30.8  
 Yoshida T. O27.11  
 Yoshii R. P26.1 P28.28



|                 |   |
|-----------------|---|
| Yoshino T.      | P30.14  |
| Yoshioka T.     | P27.21  |
| Yu X.           | P28.10  |
| Yudin A. N.     | P28.1 O30.4 P30.1 P30.2 P30.7                       |
| Yui S.          | P28.19 O30.3  |
| Yunoki S.       | P26.15  |
| Zadorozhko O.   | O27.8   |
| Zavjalov V. V.  | P26.18 O30.7  |
| Zhang G. M.     | P27.17  |
| Zhang K.        | P28.2   |
| Zhelev N.       | P26.17 O27.6 O28.8                                  |
| Zheng P.        | P28.13  |
| Zimmerman A. M. | P30.4 P30.5   |
| Zmeev D. E.     | O26.3 P26.33 P26.34 O28.9 P28.11 O30.2 P30.3 P30.11 |
| Zumbühl D.      | P26.33  |
| Zuo K.          | O26.4   |

# QFS2018 Program

| Time  | July 25 (Wed)                                | July 26 (Thu)                       | July 27 (Fri)   | July 28 (Sat)                           | July 29 (Sun) | July 30 (Mon)   | July 31 (Tue)                   | Time  |
|-------|--|-------------------------------------|---|---|---------------|---|---------------------------------|-------|
| 8:30  |  | Registration                        | <b>S5</b> KT transition and He films                  | <b>S9</b> quantum matters               |               | <b>S13</b> quantum turbulence 1   | <b>S16</b> cold atoms/molecules | 8:30  |
| 9:00  |  | 8:50 Opening                        | Kosterlitz  | Volovik                                 |               | Guo   | Momose                          | 9:00  |
|       |  | <b>S1</b> Leggett                   | Reppy   | Shimano                                 |               | Tsepelin  | Inouye                          |       |
|       |  |                                     |   | Tempere                                 |               | Yui   | Pieri                           |       |
| 10:00 |  | 10:00–10:30 Break                   | 10:00–10:30 Break                                     | 10:00–10:30 Break                       |               | 10:00–10:30 Break   | 10:00–10:30 Break               | 10:00 |
|       |  | <b>S2</b> topological matters 1     | <b>S6</b> spin liquids                                | <b>S10</b> neutron star                 |               | <b>S14</b> superfluid <sup>3</sup> He 2                                 | <b>S17</b> novel techniques     |       |
| 11:00 |  | Sauls                               | Kanoda  | Hatsuda                                 |               | Dmitriev  | Kono                            | 11:00 |
|       |  | Haley                               | Kawamura  | Iida                                    |               | Mineev  | Davis                           |       |
|       |  | Zuo                                 | Kamada  | Mizushima                               |               | Ikeda   | Shkarin                         |       |
| 12:00 |  | 12:00–13:30 Lunch                   | 12:00–13:30 Lunch                                     | 12:00–13:30 Lunch                       |               | 12:00–13:30 Lunch   | Halperin                        | 12:00 |
|       |  |                                     |   |   |               |   | 12:20 Closing                   |       |
| 13:00 |  |                                     |   |   |               |   |                                 | 13:00 |
|       |  | <b>S3</b> low-D Shirahama           | <b>S7</b> 2D helium                                   | <b>S11</b> superfluid <sup>3</sup> He 1 |               | <b>S15</b> quantum turbulence 2   |                                 |       |
|       |  | Morishita                           | Saunders  | Eltsov                                  |               | Yong-il Shin  |                                 | 14:00 |
| 14:00 |  | Taniguchi                           | Beekman   | Heikkinen                               |               | Navon   |                                 |       |
|       |  | Bunkov                              | Kim   | Zmeev                                   |               | Proment   |                                 |       |
| 15:00 |  | 14:50–15:20 Break                   | 14:50–15:20 Break                                     | 14:50–15:20 Break                       |               | Varga   |                                 | 15:00 |
|       |  | <b>S4</b> quantum solids Jaeho Shin | <b>S8</b> liquid and solid <sup>4</sup> He Krotscheck | <b>S12</b> topological matters 2 Manske |               | 15:20–17:20 Poster Session 4  |                                 |       |
| 16:00 | 16:00–19:00 Registration                     | Cheng                               | Reatto  | Ngampruetikorn                          |               |   |                                 | 16:00 |
|       |  | Golov                               | Nomura  | Nori                                    |               |   |                                 |       |
| 17:00 |  | 16:30–18:30 Poster Session 1        | 16:30–18:30 Poster Session 2                          | 16:30–18:30 Poster Session 3            |               |   |                                 | 17:00 |
|       |  |                                     |   |   |               |   |                                 |       |
| 18:00 | 17:30–19:00 Oxford Instruments Welcome party |                                     | 18:40–19:00 musical                                   |   |               | 17:40 Bus-1 departure<br>17:50 Bus-2 departure<br>18:00 Bus-3 departure |                                 | 18:00 |
|       |  |                                     |   |   |               | 18:30–19:00 Welcome drink   |                                 |       |
| 19:00 |  |                                     |   |   |               | 19:00–21:00 Banquet @Hotel New Ohtani                                   |                                 | 19:00 |

Excursion A (mountain hiking)

Excursion B (Tokyo half-day sightseeing)

Quantum Turbulence Workshop

20:00

20:00



**BUSINESS EVENTS  
TOKYO**



**iTHEM<sup>®</sup>**  
RIKEN interdisciplinary Theoretical & Mathematical Sciences



**ROCKGATE**  
ロックゲート株式会社

